UNIVERSITY OF CATANIA
FACULTY OF MATH AND PHYSICS

PhD – MATERIAL SCIENCE AND TECHNOLOGY – XXVII C.

SIMONE MAENZA

Integration and Optimization of New Technology for Building Integrated PV Systems

PhD thesis

Supervisor: Prof. Ing. Rosario Lanzafame
Faculty of Engineering

YEARS 2011 – 2014

ABSTRACT

The following thesis deals with the energy generation comparison between two different conversion technologies for photovoltaic systems: central-inverter conversion versus micro-inverter conversion.

After an analysis over the many energy generation technologies, the thesis focuses on photovoltaic energy systems.

The study of cell, module and system efficiencies will explain all causes of energy losses that can affect the photovoltaic energy generation.

The second part of the thesis is focused on the micro-inverter technology and the differences with the central-inverter systems.

Data analyses have been made on many systems in different locations (with almost the same sun radiation received), different azimuth and tilt angles, and different shading percentage.

The analyses will show how micro-inverter systems can improve energy production not only during shaded but also in not-shaded conditions.

At the end an economic comparison between the two different technologies will try to justify the use of micro-inverter systems not only for energy production efficiency but even for economic affordability.

Key words: micro-inverter; PV systems; shading; renewable energy.

摘要

这篇论文将会处理并对比光伏发电系统的两种不同转换技术：中央逆变器转换和微型逆变器转换。

透过对不同种类的转换技术的分析，
这篇论文将集中研究光伏发电系统。光伏发电能量损失的各种原因会从太阳能电池，模板和系统效率来解释。

这篇论文的第二部份主要处理微型逆变器的转换和其与中央逆变器系统的差异。从不同的地点（相同太阳辐射），方位，倾角，以及遮光率所得出的数据都能够证明微型逆变器系统可以改善于遮阴情况甚至非遮阴情况下的能源生产。

最后，经过对这两种转换技术进行经济效益上的比较，这篇文章将会证明微型逆变器不但有更高的生产效率，而且更经济实惠。

关键词：微型逆变器，光伏矩列，阴影遮挡，可再生能源

Zhāiyào (jiǎntǐ)

zhè piān lùnwén jiāng huì chǔlǐ bìng duìbǐ guāngfú fādiàn xìtǒng de liǎng zhǒng bùtóng zhuǎnhuàn jìshù: Zhōngyāng nì biàn qì zhuǎnhuàn hé wéixíng nì biàn qì zhuǎnhuàn.

Tòuguò duì bùtóng zhǒnglèi de zhuǎnhuàn jìshù de fēnxī, zhè piān lùnwén jiāng jízhōng yánjiū guāngfú fādiàn xìtǒng. Guāngfú fādiàn néngliàng sǔnshī de gè zhǒng yuányīn huì cóng tàiyángnéng diànchí, múbǎn hé xìtǒng xiàolǜ lái jiěshì.

Zhè piān lùnwén de dì èr bùfèn zhǔyào chǔlǐ wéixíng nì biàn qì de zhuǎnhuàn hé qí yǔ zhōngyāng nì biàn qì xìtǒng de chāyì. Cóng bùtóng dì dìdiǎn (xiāngtóng tàiyáng fúshè), fāngwèi, qīngjiǎo, yǐjí zhēguāng lǜ suǒdé chū de shùjù dōu nénggòu zhèngmíng wéixíng nì biàn qì xìtǒng kěyǐ gǎishàn yú zhē yīn qíngkuàng shènzhì fēi zhē yīn qíngkuàng xià de néngyuán shēngchǎn.

Zuìhòu, jīngguò duì zhè liǎng zhǒng zhuǎnhuàn jìshù jìnxíng jīngjì xiàoyì shàng de bǐjiào, zhè piān wénzhāng jiāng huì zhèngmíng wéixíng nì biàn qì bùdàn yǒu gèng gāo de shēngchǎn xiàolǜ, érqiě gèng jīngjì shíhuì.

Guānjiàn cí: Wéixíng nì biàn qì; guāngfú zhènliè; yīnyǐng zhēdǎng; kě zàishēng néngyuán

SOMMARIO

La seguente tesi ha come argomento l'analisi energetica comparativa di due differenti sistemi di conversione energetica per impianti fotovoltaici: inverter di stringa e micro-inverter.

Dopo un'analisi riguardante le diverse tecnologie di generazione dell'energia elettrica, la tesi si focalizza sui sistemi fotovoltaici.

Lo studio dell'efficienza energetica di cella, modulo e sistema esporrá le varie cause di perdita di energia che possono affliggere un sistema fotovoltaico.

La seconda parte della tesi si focalizza sulla tecnologia dei micro-inverter e le differenze con gli inverter di stringa.

Un'accurata analisi é stata svolta nel corso di un anno su 6 diversi sistemi fotovoltaici con una simile latitudine (tutti i siti sono in Sicilia), con differente angolo azimutale ed inclinazione, con differenti percentuali di ombreggiamento.

L'analisi mostrerá come i sistemi con micro-inverter sono in grado di incrementare la produzione di energia non soltanto nei casi di ombreggiamento sul sistema, ma anche in condizioni di non ombreggiamento.

Infine un'analisi economica confronterá le due differenti tecnologie cercando di giustificare la convenienza dei sistemi dotati di micro-inverter non soltanto per ragioni di generazione energetica, ma soprattutto per una convenienza a livello economico.

Parole chiave: micro-inverter; sistemi fotovoltaici; ombreggiamento; energia rinnovabile.

INDEX

ABSTRACT **1**

SOMMARIO **3**

INTRODUCTION **6**

CHAPTER 1 ..... **7**

ENERGY SOURCES **7**

1.1 RENEWABLE ENERGY SOURCES 7
1.1.1 New frontiers in renewable energy production *12*
1.2 ENERGY PRODUCTION IN ITALY 17

CHAPTER 2 SOLAR ENERGY **22**

2.1 PHOTOVOLTAIC EFFECT 23
2.2 ELECTRICAL MODEL OF A PV-CELL 28
2.3 EFFICIENCY AND LOSSES OF A PV-MODULE 36
2.4 REFERENCE INDEXES AND LOSSES OF A PV SYSTEM 37
2.4.1 The Reference Yield - Y_R *38*
2.4.2 The Array Yield - Y_f *38*
2.4.3 The PERFORMANCE RATIO - PR *38*
2.4.4 Efficiency of the system DC η_{sist_DC} *40*
2.4.4.1 MISMATCH 40
2.4.4.2 SHADOWING OR SHADING 42
2.4.4.3 SOILING 44
2.4.4.4 CONDENSATION 44
2.4.4.5 SUN-TRACKING 45
2.4.4.6 DC WIRES 45
2.4.4.7 AGING 45
2.4.5 Efficiency of the system AC η_{sist_AC} *46*
2.4.5.1 INVERTER AND TRANSFORMATION LOSSES 46
2.4.5.2 AC WIRES, DIODES AND CONNECTIONS 47
2.4.6 Final efficiency *47*
2.4.6.1 SYSTEM AVAILABILITY 48

CHAPTER 3 EVOLUTION OF PHOTOVOLTAIC **49**

3.1 DIFFERENT KIND OF CELLS AND MANUFACTURING 49
3.1.1 Silicon cells *51*

3.1.2 Thin film cells *56*
3.1.3 Multi junction cells *59*
3.1.4 Emerging PV cells *60*
3.2 CONCENTRATED PV SYSTEMS 63
3.2.1 Optic systems *64*
3.2.2 Tracking systems *66*
3.3 CONVERSION SYSTEMS 66
3.4 THE PHOTOVOLTAIC MARKET 69
3.4.1 World market *72*
3.4.2 Italian market *73*

CHAPTER 4 EXPERIMENTAL EVALUATION OF THE TESTED PV SYSTEMS 75

4.1 SYSTEMS DESCRIPTIONS 75
4.2 CENTRAL INVERTER SYSTEMS 76
4.2.1 Central inverter system -1 ..... *76*
4.2.2 Central inverter system-2 ..... *79*
4.3 MICRO INVERTER SYSTEMS 81
4.3.1 Micro-inverter system - 1 ..... *81*
4.3.2 Micro-inverter system - 2 ..... *83*
4.3.3 Micro-inverter system - 3 ..... *85*
4.3.4 Micro-inverter system - 4 ..... *87*

CHAPTER 5 DATA ANALYSIS 90

CHAPTER 6 CONCLUSIONS 95

NOMENCLATURE 99

BIBLIOGRAPHY 102

SPECIAL THANKS 104

INTRODUCTION

The world energy request is nowadays as important as the needs of water or food. Analyses say that during the next 50 years the population will keep growing and so the need of energy will grow even more than 50% than today: the human society is pushing to a more technological standard of living, increasing so the energy consumption per person. This means that to maintain the same technological level new power plants for energy generation will have to be built.

Most of the power plants currently in function are thermoelectric power plants, i.e. that a combustion reaction is needed to generate the heat for generating vapor steams usefully for the rotation of turbines and so of the electric generators.

Every combustion reaction generates gasses that contribute to raise the greenhouse effect on the planet, causing temperature rising and climate alterations.

Moreover the supply of fossil fuels is coming to a shortage, that means that the prices of the fuels will increase and the cost of energy production will get higher and higher.

The solution obviously cannot be searched in installing more thermoelectric power plants, that will cause more pollution and an energy cost raises.

The only way to keep growing in energy generation without affecting on the climate or on the policies of many countries (often in contrast for energy fuel stocks control) is by using distribute and renewable energy sources, i.e. a source of energy that has a regeneration time faster than its consumption.

This thesis deals with the photovoltaic energy generation with micro-inverter conversion systems for building integrated installations; the aim is to show how photovoltaic generation with micro-inverter systems could be a way for reducing the energy losses and so increasing energy generation compared to the traditional photovoltaic systems.

CHAPTER 1

ENERGY SOURCES

Energy sources are mainly separated in traditional and alternative energy sources.

The traditional energy sources are most of all the fossil fuels utilized starting from the first industrial revolution until today to generate heat by combustion reactions.

All the other sources have to be considerate as alternative.

The most common traditional sources are so the fuels generated from petroleum refining, (such as gasoline, diesel fuel, heavy fuels), methane, coal, et cetera.

Bio-gas from the waste or bio-fuels from the refining of agricultural products, even if are quite similar to the traditional fuels (for example bio-ethanol), are considered as an "alternative" to the traditional sources.

The use of nuclear energy or the combustion of waste directly in the furnaces could be considered as an alternative to the traditional sources of energy.

Among the alternative sources of energy there is another subclass: the renewable energy sources. An energy source is considered renewable if its consumption is slower than its regeneration.

It obviously depends on the policies of each country how to describe a source of energy in order to set which kind of economical action should be taken for that specific energy source (for many years also nuclear energy has been considered as renewable).

1.1 RENEWABLE ENERGY SOURCES

The renewable sources are most commonly identified in geothermal, sun, wind and water (rivers, falls, sea shores) energy.

Most of the power plants that use renewable sources of energy do not usually have electricity generation costs comparable to the traditional power plants, exception made for hydroelectric power plants (that have been the first power plants ever used for energy generation).

Renewable sources have been given a market pull from the governments of different countries thanks to the policies against pollution that started from the international protocol agreed in Kyoto in 1997 (it actually started only in 2005 after the approval of the Russian government).

New environmental policies in Europe have been given for 2020 giving another push to the renewable sources, thanks to the deal "*20-20-20*":

- 20% reduction in EU greenhouse gas emissions from 1990 levels
- 20% raising of electricity used from renewable sources production
- 20% improvement in the EU's energy efficiency

The most used renewable source of energy is undoubtedly *hydraulic energy*, historically used even before the fossil fuels as source for electric generation.

These power plants have a huge territorial impact due to the landscape alteration that has to be made: to create dams and reservoirs for the water, to deviate rivers or to intercept falls for letting the water flow through the turbines.

Fig. 1.1 – *Hydroelectric power plant*

It is possible to use many hydroelectric generators also as pumps: by using basins at different heights connected one each other is it possible to "store" energy in case of energy overproduction by the traditional power plants on grid.

Geothermal power plants work with the same processes of the traditional power plants, by using a Rankine cycle for the generation of steam for the turbines. The main difference is the source of the heat or the steam: instead of having a boiler where a combustion reaction is needed to generate the heat, in geothermal power plants the heat is collected by the ground where particular condition permits the generation of steam. Depending on the quality of the vapor there could be a direct or an indirect cycle.

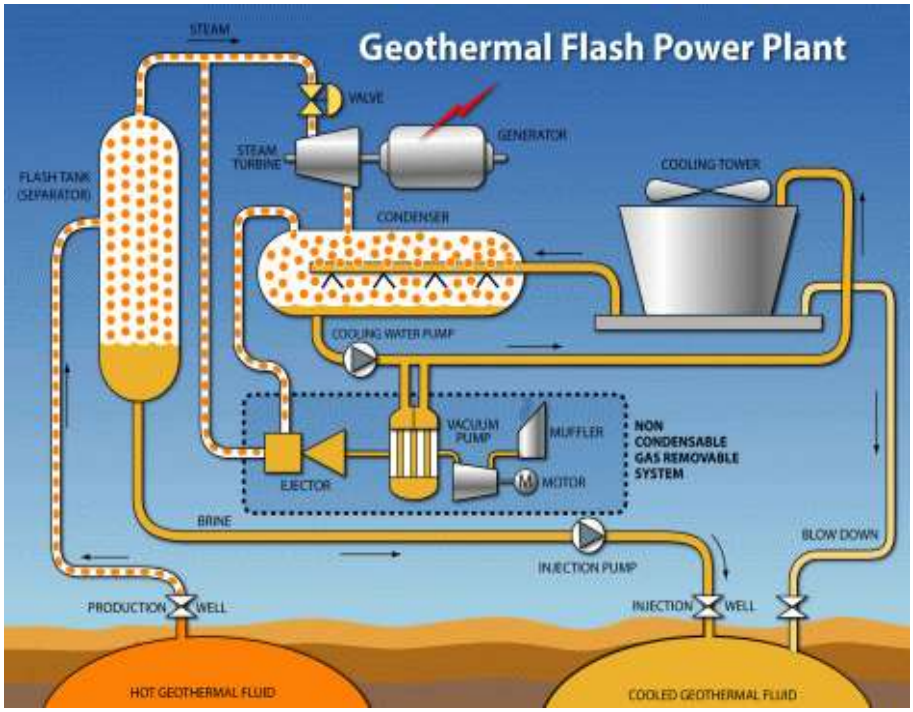

Fig. 1.2-a – *Geothermal power plant scheme*

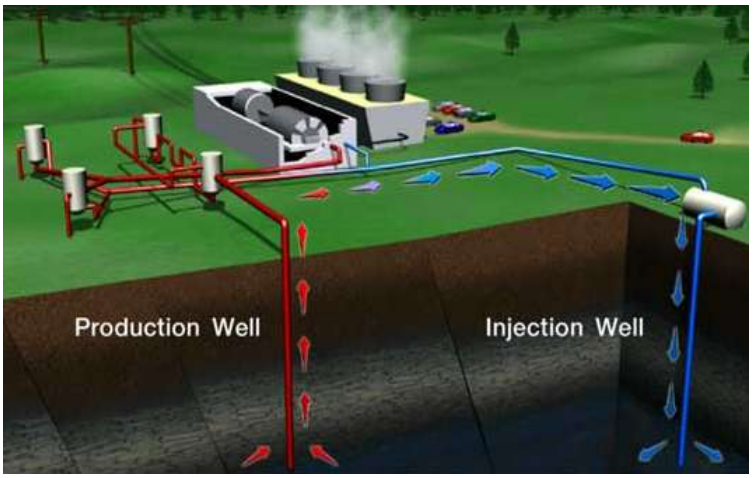

Fig. 1.2-b – *Geothermal power plant scheme*

The most promising renewable sources for the future are surely *wind* and *solar* energy.

In the *wind power plants* (on-shore or off-shore) the air flows through the turbines causing a rotation that so generates electricity in the generators. Wind turbines can be with a vertical axis of rotation (VAWT) or a horizontal axis of rotation (HAWT). [1]

There's a growing interest in putting them off-shore where the wind velocity is more constant and less affected by the landscape, even if there are much more electric energy losses due to the cables to reach the shore.

At the present time energy cost production are similar to the fossil fuels power plants, but the need of constant breezes does not permit a constant energy production.

Fig. 1.3 – *Horizontal axis wind turbines (HAWT)*

Solar energy can be used in two main different ways: using the heat generated by the sun or using the energy power of the photons to directly generate energy.

Thermodynamic solar power plants are getting more and more importance in energy production. The use of "molten salts" permits to store the heat received from the daily sun irradiation and to use it to generate steam for a Rankine cycle in order to generate electricity.

The main goal behind the energy storage systems in solar power is to consent the utilization of the energy generated by the sun beams also during the night time or during days of bad weather conditions, when the sun radiation cannot reach the ground.

Spain already uses this kind of power plants; at the beginning of 1980's the "SEGS" project started the developing of thermodynamic solar power plants in the USA.

In Italy the "Archimede" project is developing a thermodynamic solar power plant that can store the heat also during night time and have a 24 hours energy production.

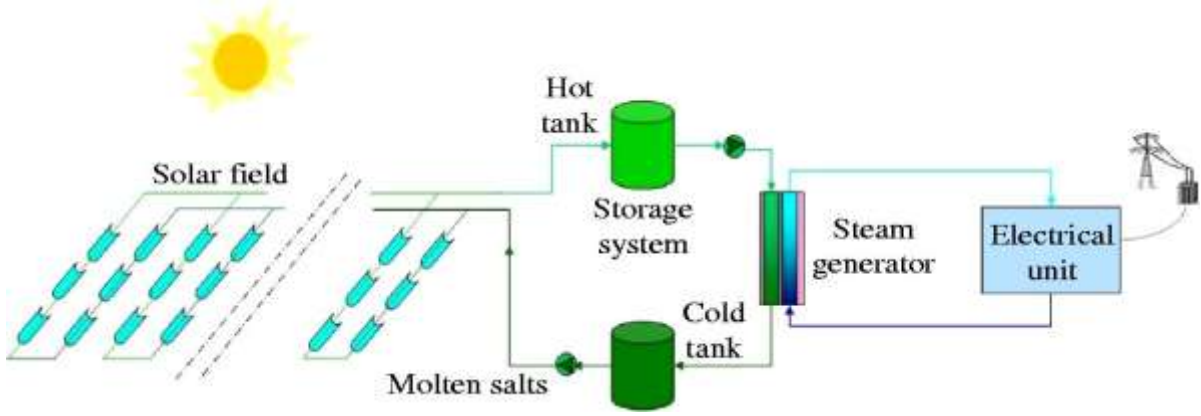

Fig. 1.4 – *Thermodynamic solar power plant scheme*

Photovoltaic systems are the most used technology to generate electricity from the sun.

The direct transformation in electric energy of the solar beams is the basis of the photovoltaic effect.

The energy received from the sun permits the electrons in the valence band to jump to the conduction band. If not "collected" the electrons would come back to the original position heating the material by releasing energy; by modifying the semiconductor that receives the irradiation it is possible to create an electric potential and use the "free electrons" generated by the sun beams to have an electric current.

Thanks to the policies for renewable energy power plants, photovoltaic generation has had a great expansion during the last years; the goal is to reach a power production percentage higher than the traditional power plants, and surely thanks to the new opportunities given by new battery systems or hydrogen generation to store energy during the overproduction times in daytime (to use hydrogen in fuel cells during the underproduction or the night-time) it is going to gain more weight in the next decades, also forecasting a greater efficiency and a reduction of cost production.

PV energy will be analyzed better in the next chapter.

1.1.1 *New frontiers in renewable energy production*

There are some more ways to use renewable energy sources, but are still in a starting phase of development, and not yet commercialized.

Many ways to generate energy from *oceans* have been developed.

Tidal barrage power plants utilize the different heights of the sea level on the coast to fill and vent some basins behind a dam, as for the re-pump hydro power stations (but in this case the higher basin is filled with the high tide of the sea).

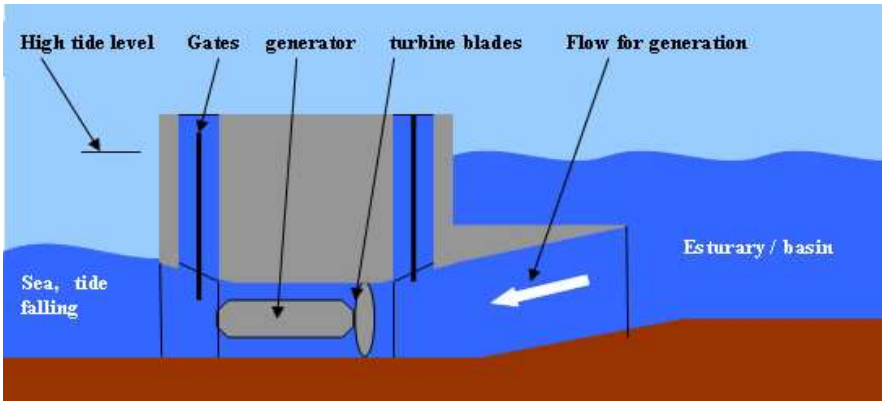

Fig. 1.5 – *Tidal barrage power plant*

The ocean waves can be used to compress or expand rhythmically the pieces of the *Pelamis power plant*, snake shaped that contains hydraulic pistons connected to generators.

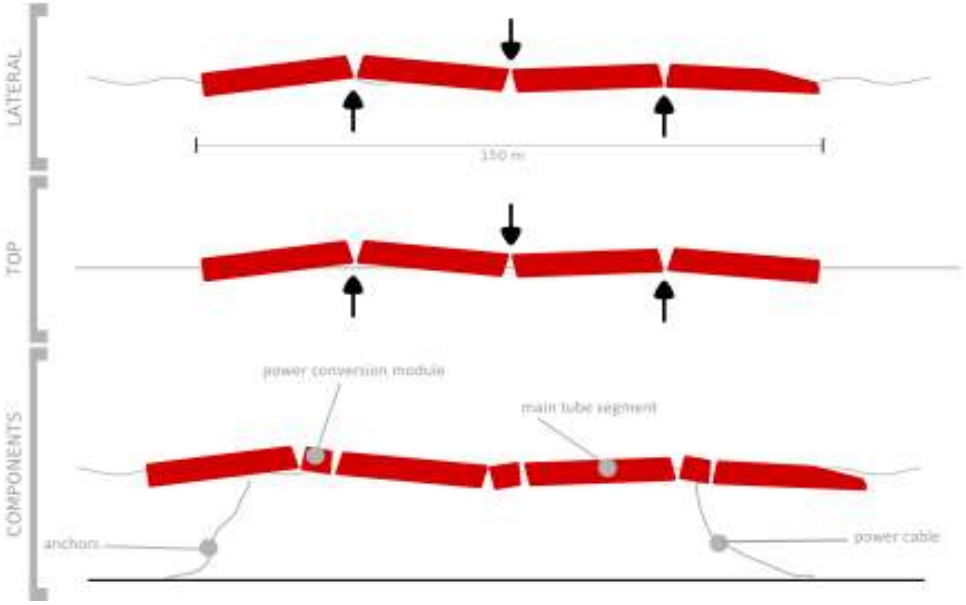

Fig. 1.6 – *Pelamis generator*

The ocean waves can be also used to create wind for *micro wind turbines* by the compression and expansion of the air in some chambers semi-submersed.

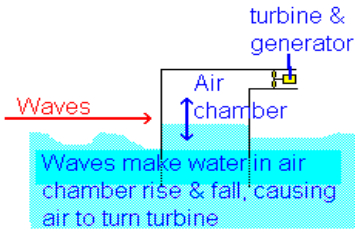

Fig. 1.7 – *Micro wind generator*

The tides can be used also alternatively for the *tidal stream generators*: similar to undersea wind power plants they have the advantage of using a density 1000 times higher than the air.

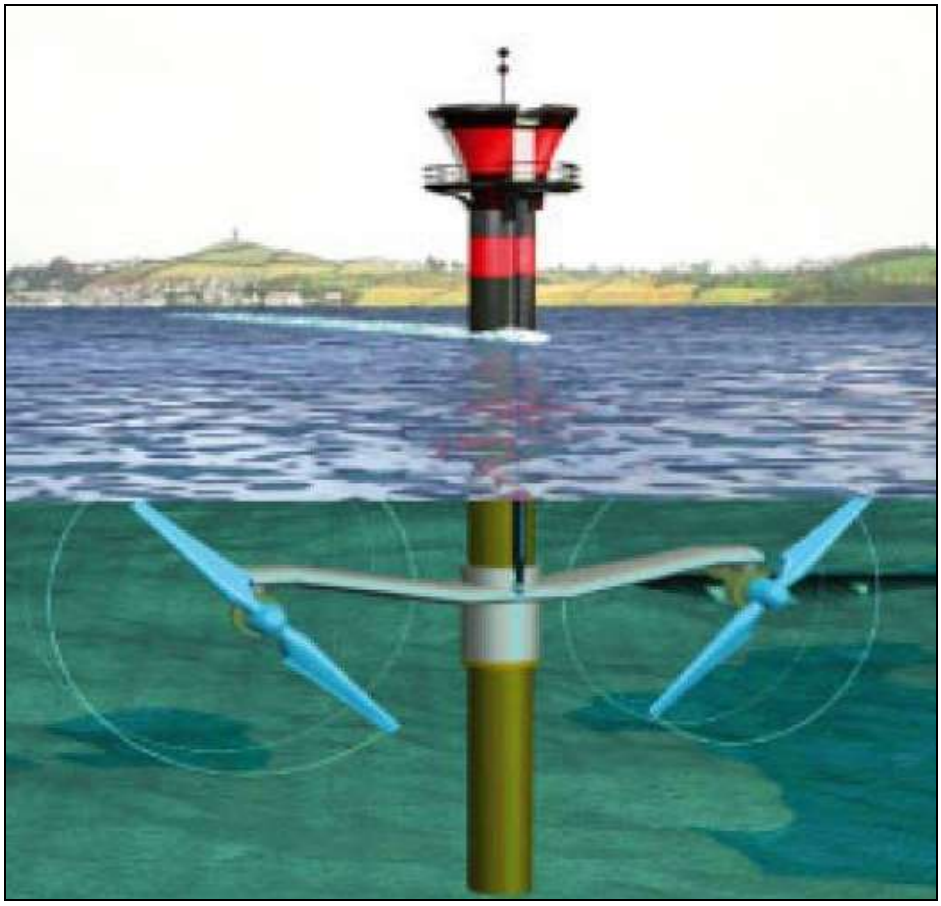

Fig. 1.8 – *Tidal stream generator*

Ocean thermal energy conversion (OTEC) uses the temperature difference between warm surface water and cold deep water. It's a Rankine cycle using working fluids such as ammonia or R-134a. The small temperature difference permits a small quantity of energy generation, but it is very useful for desalination of water from the sea water.

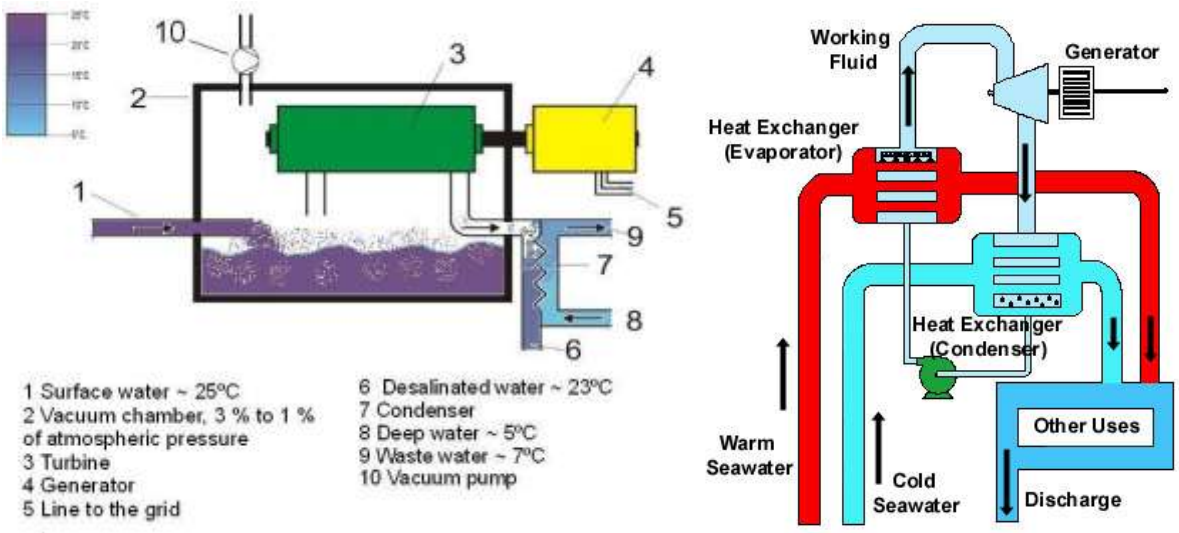

Fig. 1.9 – *OTEC power plant scheme*

Osmotic power plants use the difference in salt concentration between the water of two different basins.

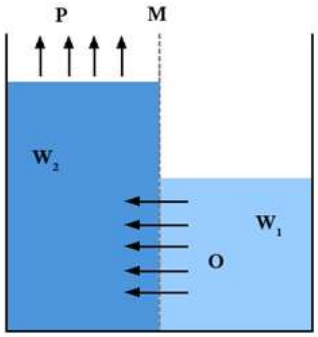

W1	Fresh water
W2	Salt water
M	Membrane
O	Osmosis
P	Pressure

Fig. 1.10 – *Osmotic process*

Saltwater is pumped into a pressure chamber. Fresh water, separated through a membrane is so introduced. The osmosis process makes the two levels flow till a balance is reached. By using the different height a turbine is used to let the levels back at the starting point.

A way of storing the heat of solar beams and generate electricity through a Rankine cycle are the *solar ponds power plants*: a pond is filled with salt in order to use the salinity differences to avoid convection inside the basin generated by the temperature differences that the heating from the sun causes at different heights inside the basin. By doing these the bottom of the basin reaches temperature higher also over 25 degrees more than the surface. A heat exchanger at the bottom can be used to operate an organic Rankine cycle.

It is more or less like a revers OTEC cycle, where the hot water is at the bottom of the basin. To maintain the temperature difference is necessary to control the salinity gradient of the basin for blocking the heat transfers due to convection. [2]

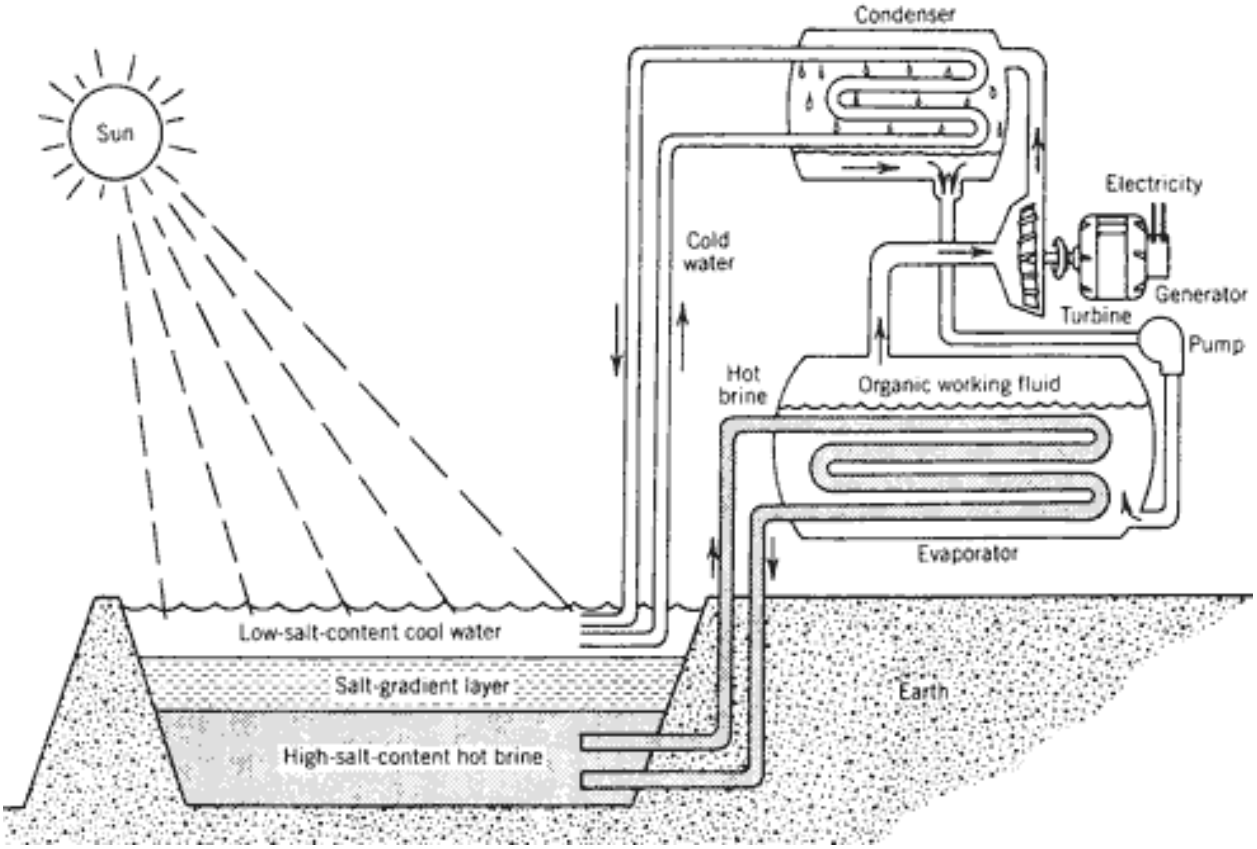

Fig. 1.11 – *Solar pond power generator*

The common issues with ocean power plants are the fouling and the corrosion of the systems that can affect the use of the power plants.

New generation wind power plants are under testing in these years.

The *kite wind generator* uses kites at high heights (almost 800 *meters*) to have more wind for the generation of electricity by using a turbine of 1600 *meters* of diameter rotating at 15 *rounds per hours*. The regulation is permitted by the change of heights of the kites (and so of the wind received).

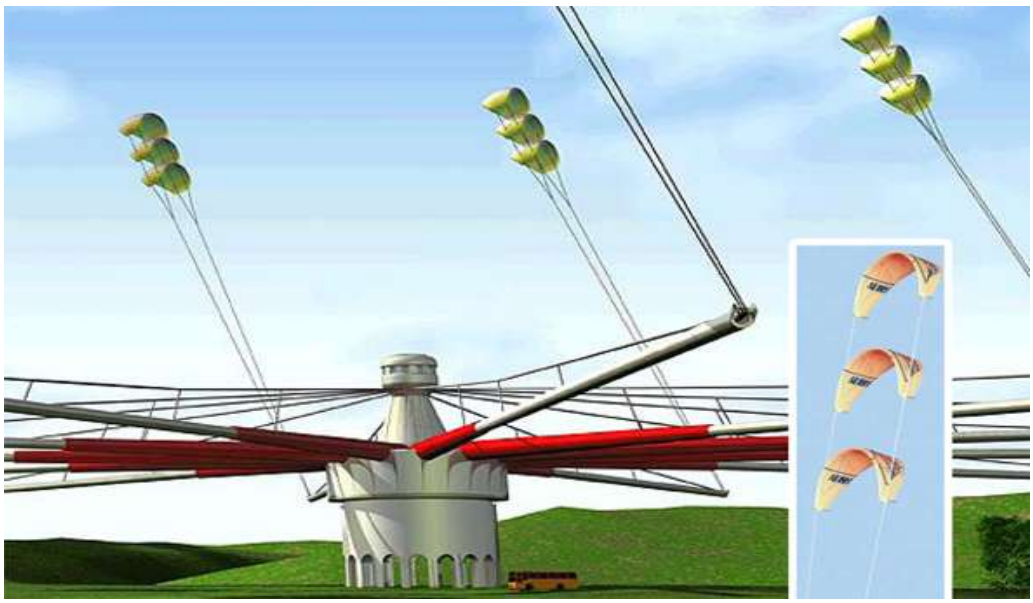

Fig. 1.12 – *Kite wind generator*

The *solar-wind towers* are going to use evaporative towers to generate air flows that can be used for electric generation.

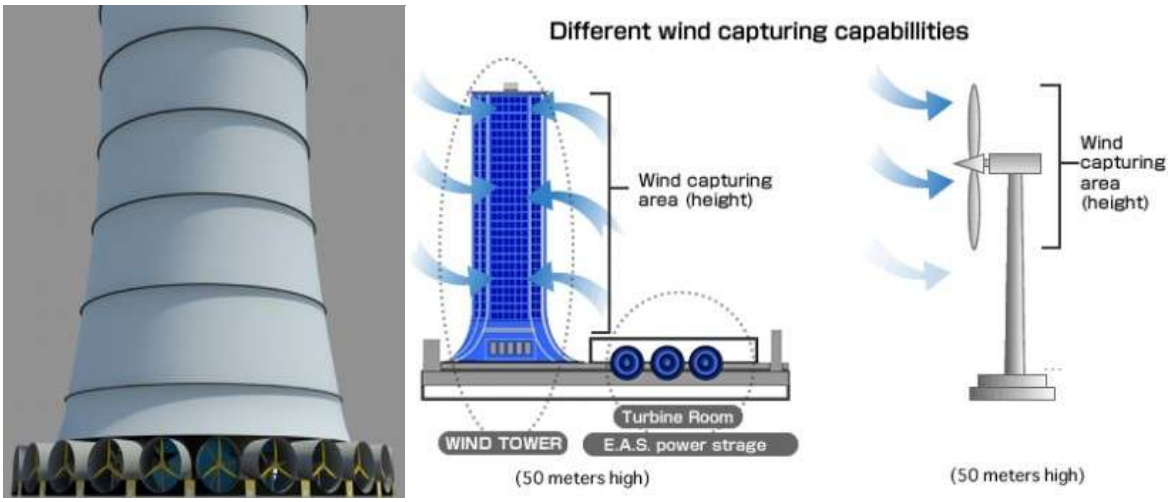

Fig. 1.13 – *Solar-Wind towers*

The future for sure is going also to ***nano electric generation***.

An example could be *piezoelectric flooring*, a technology with a wide range of applications that is slowly being adopted in the race to develop alternative energy sources. The weight of the people walking (as in subways, stations or dance floors) or of the cars passing over a piezoelectric floor can generate electricity that, even if in small quantity, in places where there is a great number of cars or persons it could be considered a useful renewable energy source.

1.2 ENERGY PRODUCTION IN ITALY

Analyzing the reports released from the GSE (Gestore dei Servizi Energetici - Manager of Energy Services) and from TERNA (Trasmissione Elettrica Rete NAzionale - National Grid Electricity Transmission) (the official authorities on energy control in Italy), it is possible to have some ideas about the energy production in Italy.

The total amount of energy production in Italy is about 277,4 *TWh*.

Italy imports about the 13,3% of the energy needed.

In the year 2013 the 16,6% of energy was generated by hydroelectric power plants, 13,3% by other renewable systems (photovoltaic, wind and geothermal) for a total of 30% of energy in 2013 generated by renewable sources.

Obviously these levels of energy production through the renewable sources of energy depend on the weather condition during the whole year above the country: the amount of rainfalls could assure an higher production from hydroelectric power plants though could affect negatively the energy production of photovoltaic systems that may miss an quantity of solar irradiation during the year. Only geothermal energy can keep constant levels during the years, due to a more stable source of energy for the electric generation.

The last 56,8% is so generated by traditional power plants. Italy has got more than everything turbo-gas and dense-oil power plants.

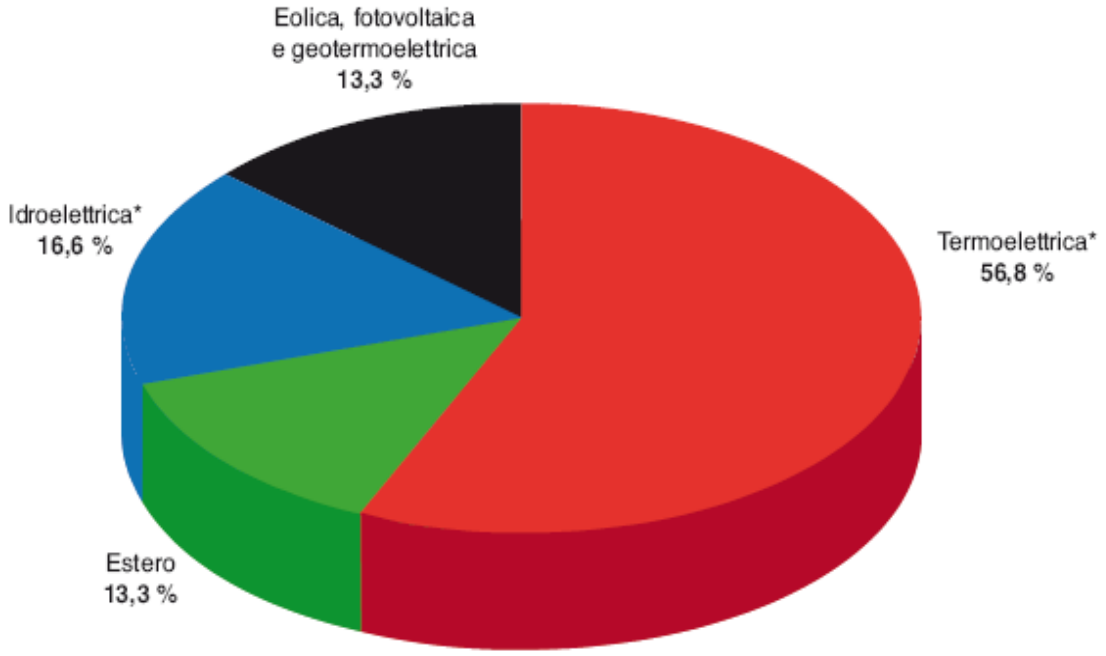

Fig. 1.14 – *Energy production in Italy in 2013*

Looking at the historic tables it is possible to notice that renewable energy (wind and photovoltaic) in Italy started its production about 22 years ago, in 1992.

	Produzione lorda						Energia destinata a		Saldo scambi con l'estero	Energia elettrica richiesta	Variazione della richiesta rispetto anno precedente
	Idroelettrica	Termoelettrica tradizionale	Geotermo-elettrica	Nucleoter-moelettrica	Eolico e fotovoltaico	Totale	Servizi ausiliari	Pompaggi			
GWh											
1982	44.080	130.823	2.737	6.804		184.444	9.158	3.736	+7.151	178.701	+0,2%
1983	44.216	130.167	2.714	5.783		182.880	9.083	3.909	+11.082	180.970	+1,3%
1984	45.434	127.508	2.840	6.887		182.669	9.229	4.278	+20.890	190.052	+5,0%
1985	44.595	131.440	2.681	7.024		185.740	9.486	4.950	+23.669	194.973	+2,6%
1986	44.531	136.281	2.760	8.758		192.330	9.724	4.786	+22.114	199.934	+2,5%
1987	42.585	155.627	2.986	174		201.372	10.476	4.216	+23.146	209.826	+4,9%
1988	43.547	156.932	3.082	-		203.561	10.385	3.902	+31.256	220.530	+5,1%
1989	37.484	170.111	3.155	-		210.750	11.046	4.714	+33.729	228.719	+3,7%
1990	35.079	178.590	3.222	-	..	216.891	11.640	4.782	+34.655	235.124	+2,8%
1991	45.606	173.253	3.182	-	..	222.041	11.577	4.577	+35.082	240.969	+2,5%
1992	45.786	176.995	3.459	-	3	226.243	11.810	4.946	+35.300	244.787	+1,6%
1993	44.482	174.634	3.667	-	5	222.788	11.431	4.189	+39.432	246.600	+0,7%
1994	47.731	180.648	3.417	-	8	231.804	11.642	4.150	+37.599	253.611	+2,8%
1995	41.907	196.123	3.436	-	14	241.480	12.272	5.626	+37.427	261.009	+2,9%
1996	47.072	193.551	3.762	-	39	244.424	12.058	6.882	+37.389	262.873	+0,7%
1997	46.552	200.881	3.905	-	124	251.462	12.174	6.728	+38.832	271.392	+3,2%
1998	47.365	207.970	4.214	-	237	259.786	12.843	8.358	+40.732	279.317	+2,9%
1999	51.777	209.068	4.403	-	409	265.657	12.920	8.903	+42.010	285.844	+2,3%
2000	50.900	220.455	4.705	-	569	276.629	13.336	9.129	+44.347	298.510	+4,4%
2001	53.926	219.379	4.507	-	1.183	278.995	13.029	9.511	+48.377	304.832	+2,1%
2002	47.262	231.069	4.662	-	1.408	284.401	13.619	10.654	+50.597	310.726	+1,9%
2003	44.277	242.784	5.340	-	1.463	293.865	13.682	10.492	+50.968	320.658	+3,2%
2004	49.908	246.125	5.437	-	1.851	303.321	13.299	10.300	+45.635	325.357	+1,5%
2005	42.927	253.073	5.324	-	2.347	303.672	13.064	9.319	+49.155	330.443	+1,6%
2006	43.425	262.165	5.527	-	2.973	314.090	12.864	8.752	+44.985	337.459	+2,1%
2007	38.481	265.764	5.569	-	4.073	313.888	12.589	7.654	+46.283	339.928	+0,7%
2008	47.227	261.328	5.520	-	5.054	319.130	12.065	7.618	+40.034	339.481	-0,1%
2009	53.443	226.638	5.342	-	7.219	292.642	11.534	5.798	+44.959	320.268	-5,7%
2010	54.407	231.248	5.376	-	11.032	302.062	11.314	4.454	+44.160	330.455	+3,2%
2011	47.757	228.507	5.654	-	20.652	302.570	11.124	2.539	+45.732	334.640	+1,3%
2012	43.854	217.561	5.592	-	32.269	299.276	11.470	2.689	+43.103	328.220	-1,9%

Fig. 1.15 – *Energy production in Italy from 1982*

The growth on power installed and energy production in the last four years has been enormous.

For the first time on June 16th 2013 for a couple hours during the morning all the electricity needs were covered totally by renewable power plants.

This result, even if obtained in a sunny and windy day all over the nation that raised the production of wind and PV systems, shows the huge importance of renewable power plants in Italian energy production that have been capable of covering the 100% of the grid energy request.

Potenza Efficiente Lorda (MW)	2008	2009	2010	2011	2012
Idraulica	17.623	17.721	17.876	18.092	18.232
Eolica	3.538	4.898	5.814	6.936	8.119
Solare	432	1.144	3.470	12.773	16.420
Geotermica	711	737	772	772	772
Bioenergie[1]	1.555	2.019	2.352	2.825	3.802
Totale FER	**23.859**	**26.519**	**30.284**	**41.399**	**47.345**

Produzione Lorda (GWh)	2008	2009	2010	2011	2012
Idraulica	41.623	49.137	51.117	45.823	41.875
Eolica	4.861	6.543	9.126	9.856	13.407
Solare	193	676	1.906	10.796	18.862
Geotermica	5.520	5.342	5.376	5.654	5.592
Bioenergie[1]	5.966	7.557	9.440	10.832	12.487
Totale FER	**58.164**	**69.255**	**76.964**	**82.961**	**92.222**

Fig. 1.16 – *Renewable energy production in Italy*

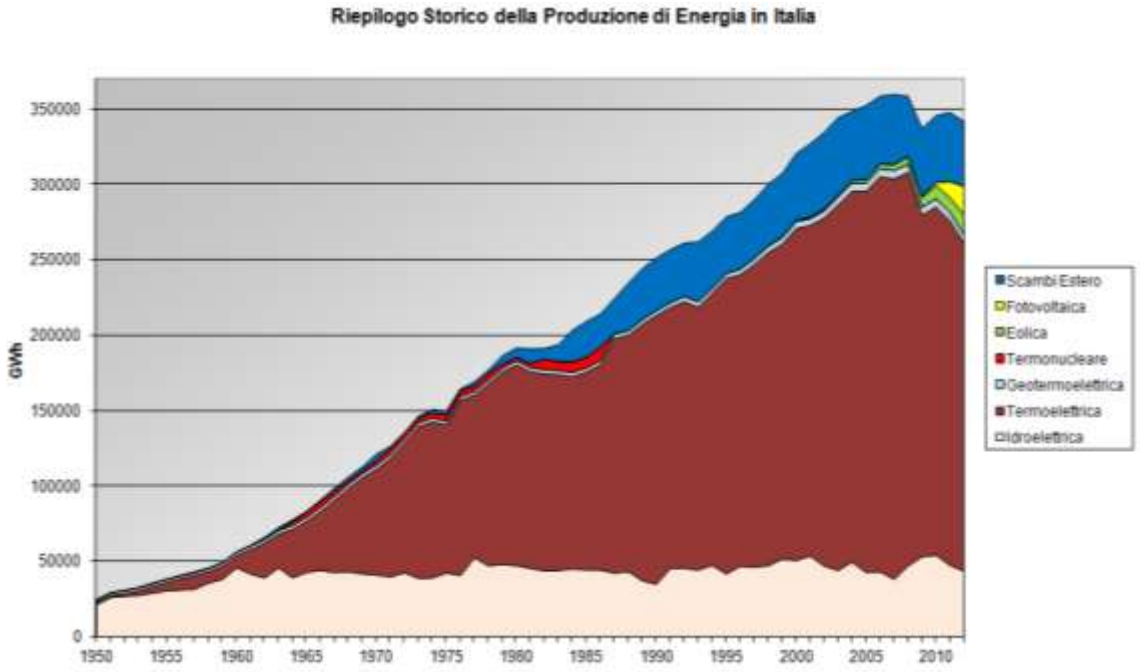

Fig. 1.17 – *Historical energy production in Italy*

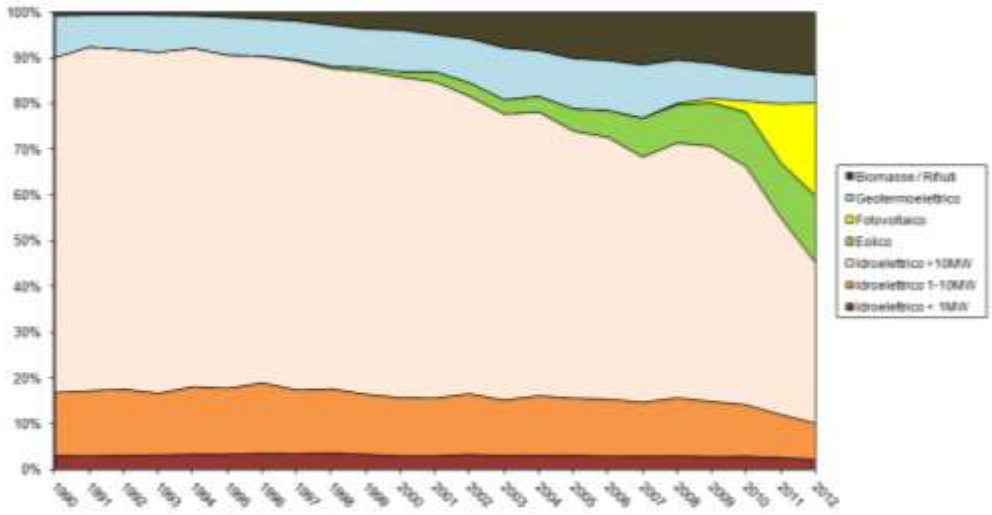

Fig. 1.18 – *Renewable percentage in Italy*

The policy of financing renewable energy systems produced the enormous growth and proliferation of these power plants in the energy production market.

The "grid parity" is the point in which the cost of electricity generated with a power reaches the mean market price. The cheapest generation costs are actually the ones obtained with the traditional fossil-fuels power plants. The renewable power plants reached the same value thanks to economical incentives.

Reaching the grid parity means that (even without economical incentives) generating electricity via renewable power plants is as affordable as traditional systems. The grid parity has been already reached as shown in the figure below.

This means that photovoltaic systems can be competitive with the traditional power plants without the need of economic helps from the government.

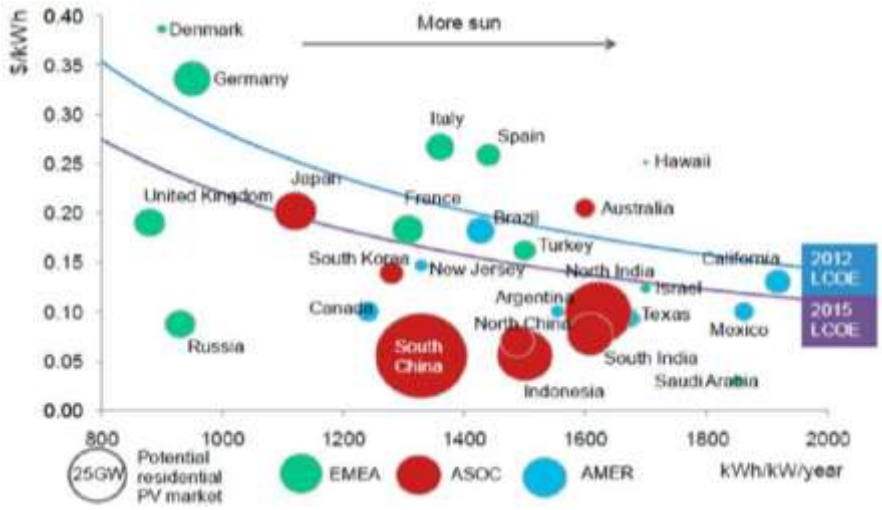

Fig. 1.19 – *Grid parity in Italy*

The installation and energy production in the last years is shown below. The growth of the photovoltaic energy production has been massive thanks to the policies applied during the last 10 years in Italy to help the PV market to increase.[3]

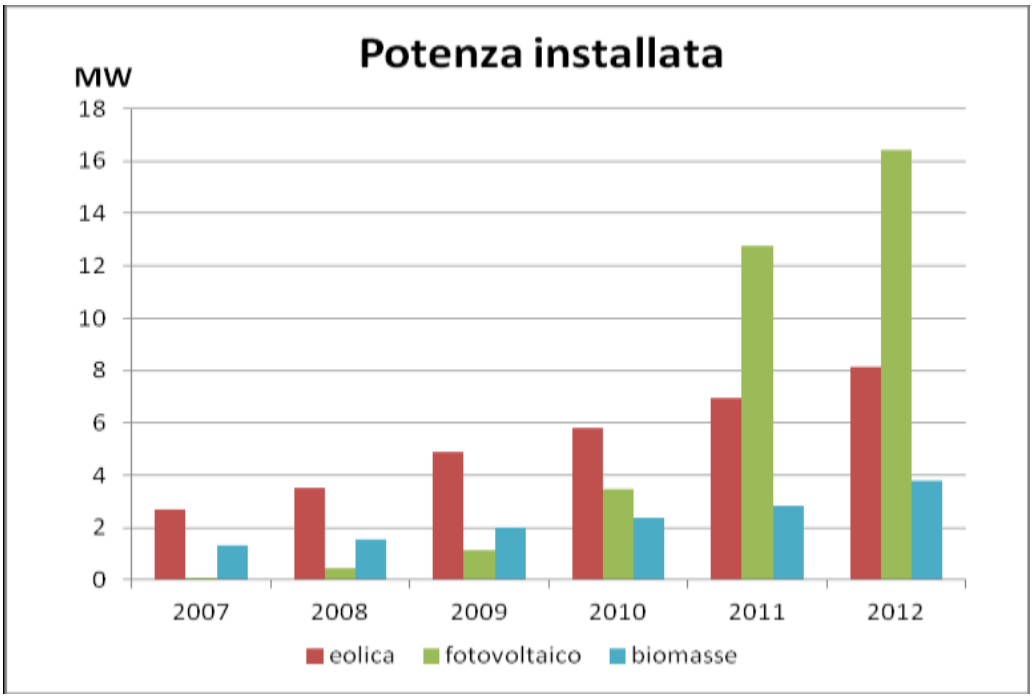

Fig. 1.20 – *Renewable power installed in Italy at 2012.*

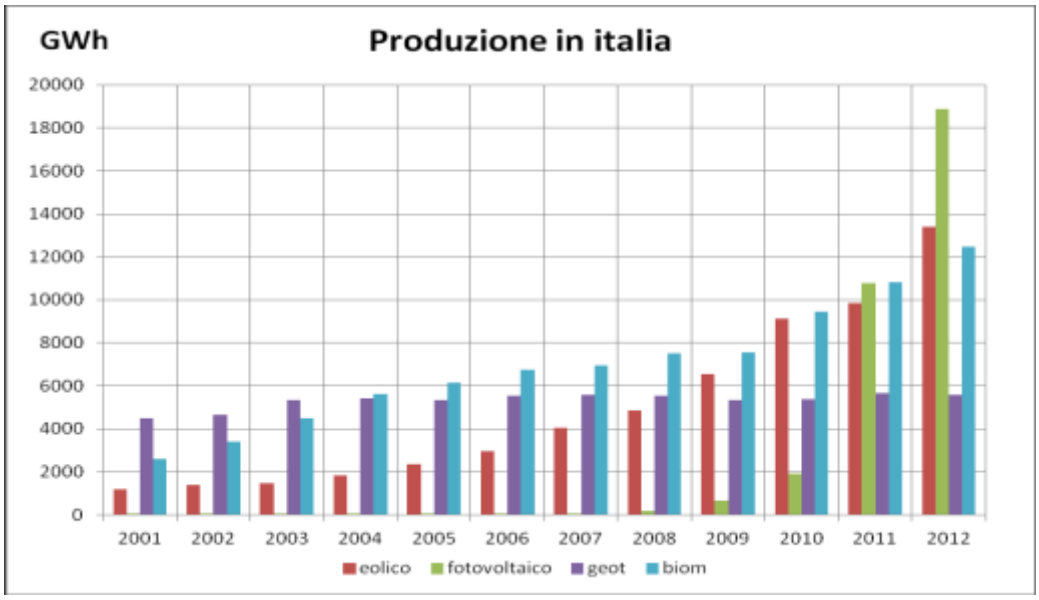

Fig. 1.21 – *Energy produced by renewable power plants at 2012*

CHAPTER 2

SOLAR ENERGY

Every second 600.000.000 *tons* of Hydrogen are converted in 595.740.000 *tons* of Helium through the nuclear fusion reaction inside the Sun nucleus. After this process 4.260.000 *tons* of Hydrogen seems to have disappeared: the loss of mass has become energy following the Einstein relation $\mathbf{E = mc^2}$.

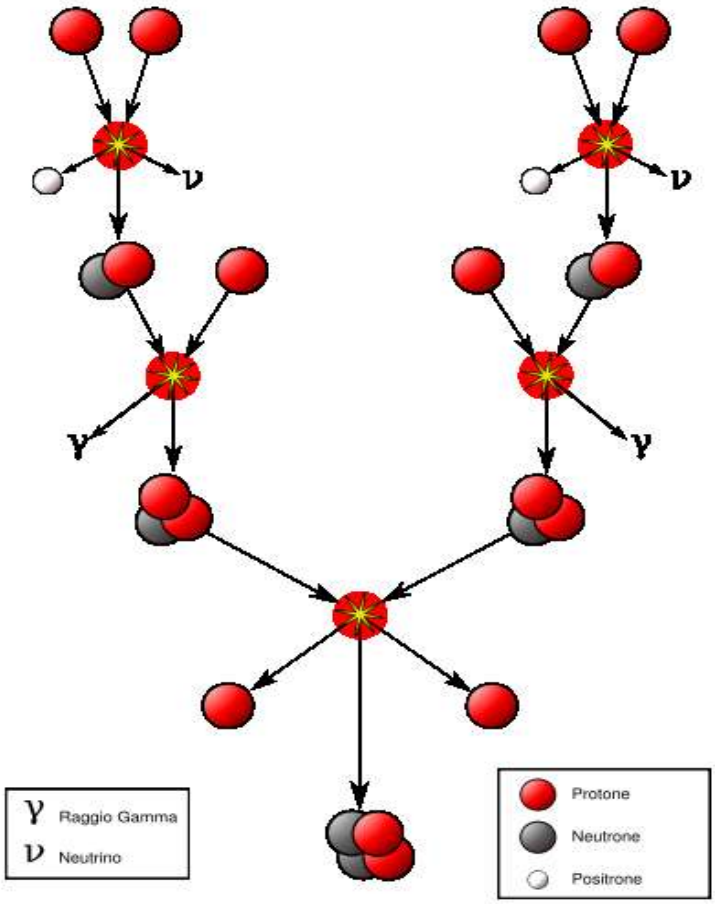

Fig. 2.1 – *Nuclear fusion reaction scheme*

The fusion reaction is:

$$4\ {}^{1}\mathrm{H} \rightarrow {}^{4}\mathrm{He} + 2\ e^{+} + 2\ \nu_e + 2\ \gamma\ (26{,}7\ \mathrm{MeV})$$

where: $\mathbf{e^+}$ is a positron; $\boldsymbol{\gamma}$ is a photon;

$\boldsymbol{\nu_e}$ is a neutrino; **H** and **He** are hydrogen and helium.

The energy generated every second is $3{,}83 \times 10^{26}$ *J* , almost 112.500.000.000 *TWh*: the world consumption of electric energy in 2013 was about 25.000 *TWh*. In a second the sun produces enough energy to cover electric energy need on Earth for about 4.500.000 years.

The energy that reaches the Earth outside the atmosphere is about 1.370 W/m^2. The atmosphere attenuates this value by absorbing o reflecting part of this radiation: on the surface of the earth it is considered a value of 1.000 W/m^2, that is the value of the GNI (Global Normal Irradiation) used.

2.1 PHOTOVOLTAIC EFFECT

The emission of electrons by a surface irradiated with an electromagnetic radiation of a certain wavelength is called *photovoltaic effect*.

The electronic band structure theory describes the ranges of energy "allowed" to the electrons on atomic orbitals. The electrons fill the bands starting from the lowest energy required; the last band filled is the valence band, the first free band is the conduction band. The range between these two bands is known as band gap.

Different chances may occur depending on the nature of the material analyzed:

- the last band is partially filled with electrons that may flow with high mobility through the last couple of similar energy bands (thus means that valence and conduction bands are overlapped): the material is **conductive**;
- the last band is totally filled with electrons and there is an high band gap before the next energy level (about 5 *eV*): these are the **non-conducting** materials;
- the last band gap is low enough to permit to the electrons of the last level to "jump" to the next energy level: the material is **semi-conductive**.

The photovoltaic effect happens on semi-conductive materials irradiated by an electromagnetic radiation with enough energy to permit the "jump" of the electrons and the creation of electrons-holes couples:

$$E_{photon} = E_\lambda \geq E_{gap} \qquad E_\lambda = \frac{hc}{\lambda}$$

where λ is the wavelength, **h** is the Planck constant, **c** is the speed of light.

The most common semi-conductor used in photovoltaic energy production is the Silicon, that has an $E_{gap} = 1{,}12\ eV$.

Considering:

- speed of light $c = 3 \times 10^9\ m/s$;
- Planck's constant $h = 6{,}6 \times 10^{-34}\ Js$

that means a wavelength $\lambda_{max} = 1{,}1\ \mu m$.

The mismatch losses consider the different sensibility of the solar cell at different wavelength (for silicon the sensibility range is between $0{,}35 \div 1{,}1\ \mu m$).

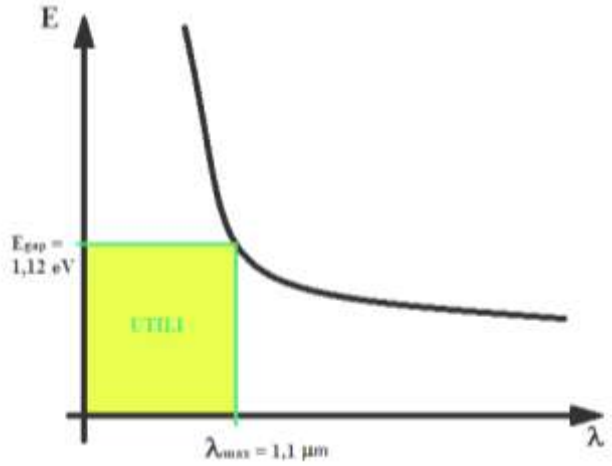

Fig. 2.2 – *Photons with energy higher than 1,12 eV (i.e. with wavelength less than 1,1 μm) are all useful for the electrons to jump the semiconductor gap*

When a radiation with enough energy reaches the semiconductor a certain number of electrons transit from a band to the other. To use these electrons it's necessary to create an electric field in order to canalize the electrons and so have a current: in order to have this electric field the semiconductor is doped.

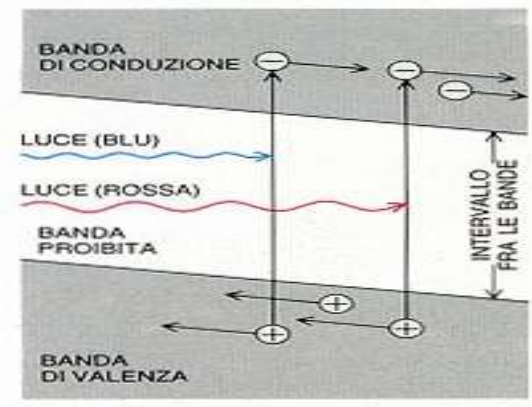

Fig. 2.3 – *Band structure example: the blue light can excite with more energy (so an electron deeper in the valence band) than the red light to permit the jump of the gap*

For each electron that jumps from the valence to the conductive band a hole is created. There is so the presence of two different carriers that leads the charge and so the current.

Most of the semiconductor materials have tetravalent bonds, due to the four electrons in the valence band. Doping the material means to add small percentages of different atoms in order to change the properties of the material:

- ✓ adding atoms of the fifth group (thus means with five electrons on the last band, such as phosphorus, antimony, arsenic) there is an increment in conduction electrons: this is the n-type doping;
- ✓ adding atoms of the third group (thus means with three electrons on the last band, such as boron, indium, gallium) there is an increment in holes: this is the p-type doping.

I	II	III	IV	V	VI
		B	C	N	O
		Al	Si	P	S
Cu	Zn	Ga	Ge	As	Se
Ag	Cd	In	Sn	Sb	Te

Tab. 2.1 – *Periodic table of elements extract*

The material is globally electrically neutral, but there is a change in the number of free electrons. By contacting different doped materials there is a flux of electrons from the n to the p zone to reach the electric equilibrium: there is so the creation depletion region totally neutral and a built-in electric field at the boundary of this region.

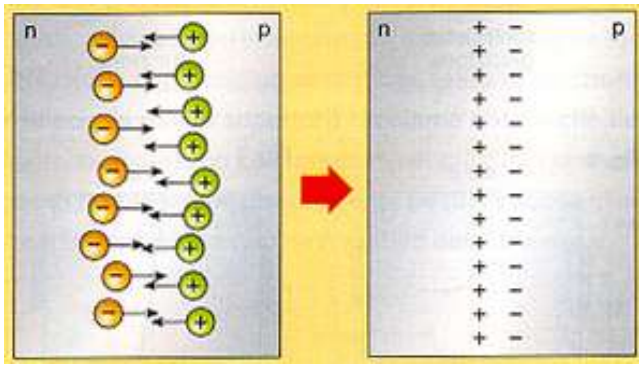

Fig. 2.4 – *Electric field obtained through the doping of the materials*

When the photons hit the semiconductor there are three chances: being reflected, transmitted or absorbed.

These last are the useful ones, because these are the photons that can give the energy to the electrons to jump over the band gap.

Following the equation

$$R = T - A$$

(where ***R*** is the radiation reflected, ***T*** transmitted and ***A*** absorbed) it is possible to understand, by measuring the amount of radiation that passes through the layers of the solar cell, how much Irradiation can be used to generate the band transition.[4]

One of the most important goals of photovoltaic researches is to enhance the amount of absorbed radiation in the wavelength range useful to the permit jump and reflect or transmit all the other wavelengths that have too less or too much energy for our purpose.

By modifying the thickness of each layer or by the use of nanoparticles or nanowires or nanodots to change the properties of the different reflective or adsorption indexes it is possible to generate new materials with the aptitude needed in order to use as much as possible all the radiation received from the sun beams. [6] [7]

In this particular part of the photovoltaic research field there are two new promising kinds of solar cell: the up-converter and the down-converter (see next chapter).

There are so two different charge carriers: the electron on the conduction band, the hole on the valence band.

By connecting with a conductor the two zones is so created a closed circuit with a flux of electrons (generated by the lighting of the n-zone and orientated by the electric field) from the n-zone (at higher electric potential) to the p-zone: there is so the generation of a current.

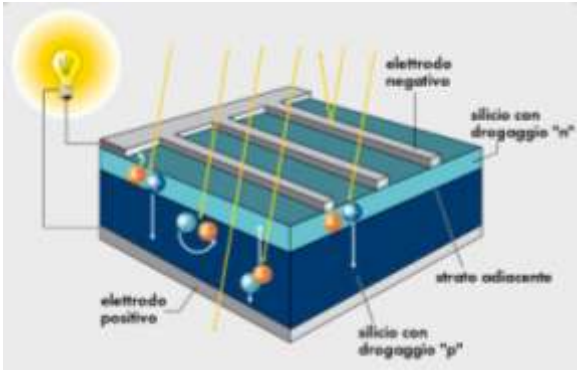

Fig. 2.5 – *Scheme of the layers and the movements of the carrier inside a photovoltaic cell.*

The band gap of a semiconductor can be direct or indirect: the crystal momentum of the valence and the conduction band can be same, so that the photon can directly generate an electron without passing through an intermediate state where the momentum is transferred to the crystal and then the electron receives the energy to jump the gap.

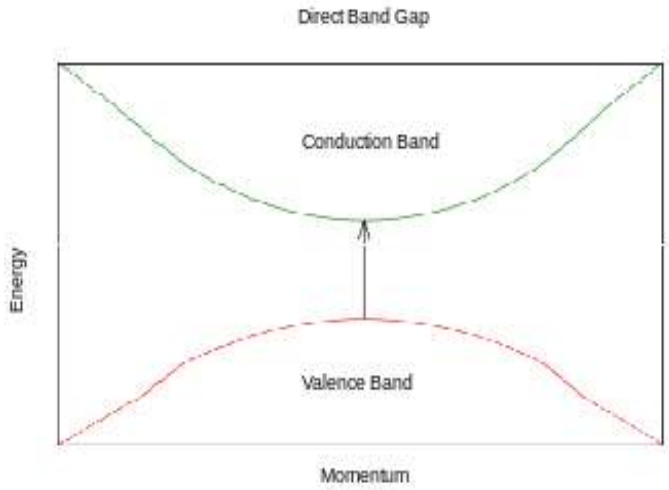

Fig. 2.6a – *Direct band gap sample.*

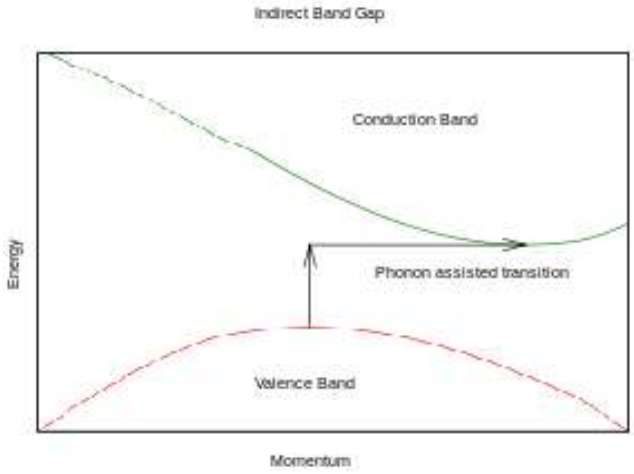

Fig. 2.6b – *Indirect band gap sample.*

The adsorption of the photons is strictly bond to the kind of gap: the thickness of a PV cell can be much more thin for direct gap semiconductor as all the photons received can generate electrons without many losses in phonons or other energy losses due recombination on the grain boundaries or the defects of the material.

2.2 ELECTRICAL MODEL OF A PV-CELL

An equivalent electrical representation of the physics phenomenal that happens inside the photovoltaic cell is useful to better understand the effects of the different components.

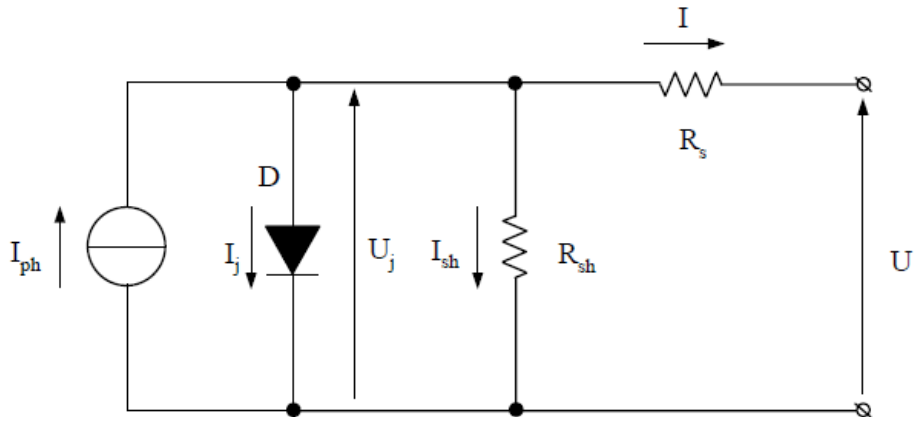

Fig. 2.7 – *Electrical model of a PV-cell.*

The photovoltaic effect can be described with a current source I_{ph} proportional to the cell surface ***A***, radiation received ***G***, kind of cell used ***k***:

$$I_{ph} = k\,A\,G$$

The recombination electron-hole at the p-n junction interface can be represented by a diode **D** with its current I_j:

$$I_j = I_0\left(e^{\frac{U_j\,q}{m\,k\,T}} - 1\right)$$

with:

- I_0 is the current with inverse voltage on the junction;
- U_j tension on the junction;
- ***q*** electron charge;
- ***K*** Boltzmann constant;
- ***T*** temperature of the junction;
- ***m*** coefficient of the junction.

The variation caused on the **I-V** curve by the I_j is shown in the picture below [5]:

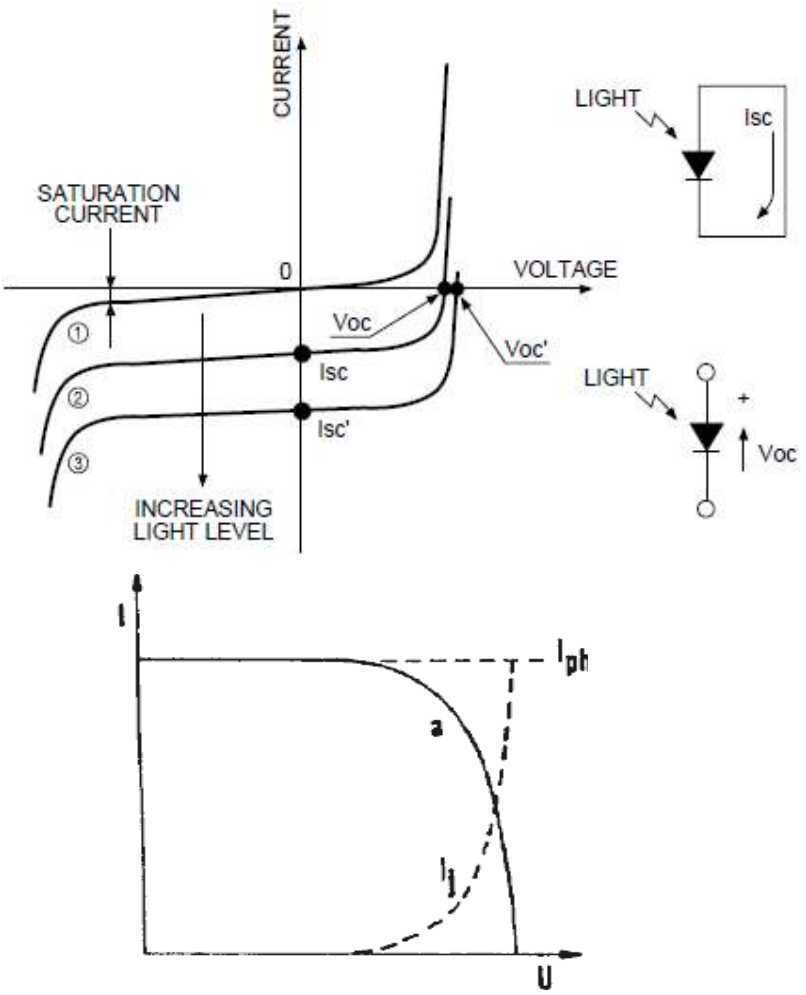

Fig. 2.8 – *I-V curve variation through illumination.*

In the electrical model there are two resistances: the shunt resistance R_{sh} and the series resistance R_s.

The shunt resistance represents the surface dispersions.

It can be considered a current $I_{sh} = U_j / R_{sh}$.

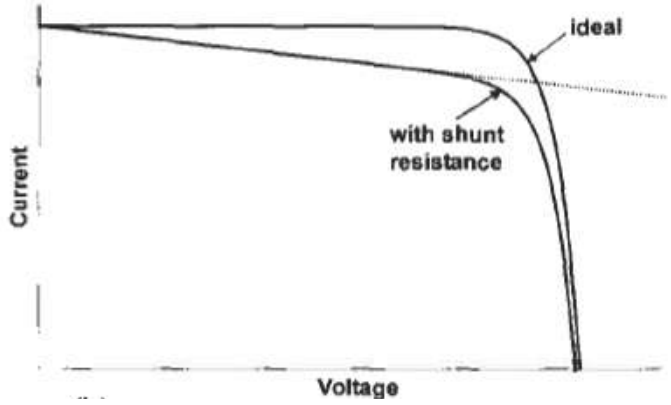

Fig. 2.9 – *I-V curve variation caused by shunt resistance.*

The series resistance is the sum of many internal resistance:

Component of resistance	Notation	Expression
Emitter resistance	R_e	$R_e = \frac{R_{sp} d_f}{7 \ell_f}$
Resistance of the base	R_b	$R_b = A W_b \rho_b$
Contact resistance: front contact	R_{fc}	$R_{fc} = \frac{\sqrt{R_{sp}\rho_{cf}}}{\ell_f} coth\left(W_f \sqrt{\frac{R_{sp}}{\rho_{cf}}}\right)$
Contact resistance: rear contact	R_{bc}	$R_{bc} = A \rho_{cr}$
Resistance of the finger contact	R_f	$R_f = \frac{\ell_f \rho_m}{3 t_f W_f}$
Resistance of the collecting busbar (per unit length)	R_{bb}	$R_{bb} = \frac{\rho_m}{3 t_f W_{bb}}$

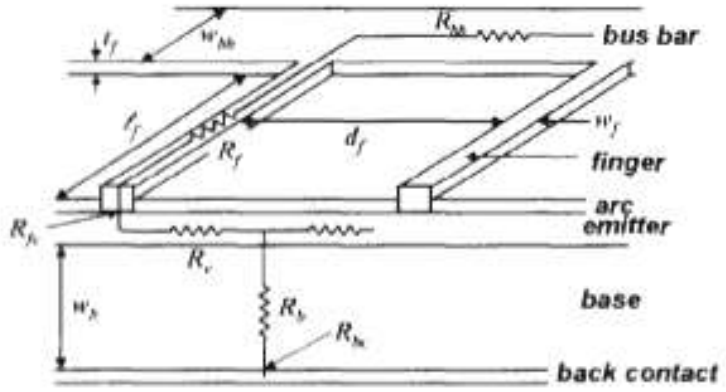

Fig. 2.10 – *Series resistance electrical scheme.*

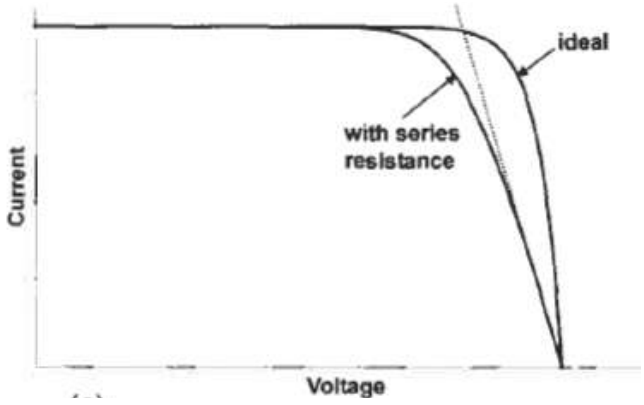

Fig. 2.11 – *I-V curve variation caused by series resistance.*

With the resistances introduced the final current is so:

$$I = I_{ph} - I_j - U_j R_{sh}$$

and the tension becomes:

$$U = U_j - R_s I$$

Making the substitutions:

$$U = \frac{k\,T}{q} \ln \frac{I_{ph} - \left(1 + {R_s}/{R_{sh}}\right) I - {U}/{R_{sh}} + I_0}{I_0} - R_s I$$

considering $R_{sh} >> R_s$:

$$U = \frac{k\,T}{q} \ln \frac{I_{ph} - I + I_0}{I_0} - R_s I$$

The open circuit tension is:

$$U_{oc} = \frac{k\,T}{q} \ln\left(1 + \frac{I_{ph}}{I_0}\right) \approx \frac{k\,T}{q} \ln\left(\frac{I_{ph}}{I_0}\right)$$

with $I_{ph} >> I_o$.

It is possible to obtain the current as:

$$I = I_{ph} - I_0 \left[e^{{q}/{kT}(U + R_s I)} - 1\right]$$

considering **U=o** the value of the short circuit current is:

$$I_{sc} = I_{ph} - I_0 \left[e^{{q}/{kT} R_s I} - 1\right]$$

equal to $I_{ph} = k\,A\,G$ for $R_s = o$.

In the graph current-tension it is possible to find the value of the maximum power point by intercepting the I_{sc} and the V_{oc}. The real curve considers I_j , R_{sh} and R_s .

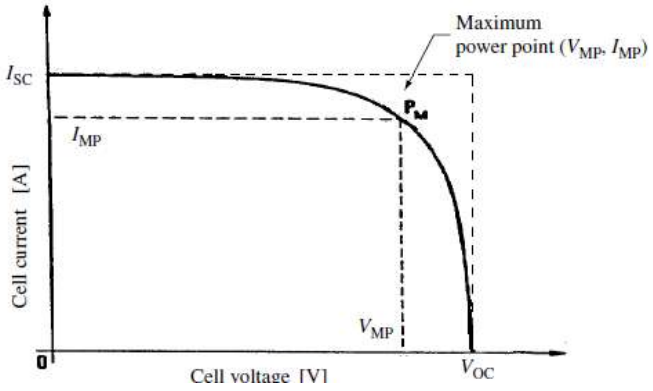

Fig. 2.12 – *I-V curve confrontation with the ideal rectangle* I_{sc} *e* V_{oc} .
The missing area represents the ***Fill Factor.***

The ratio between the ideal maximum power and the real maximum power is known as Fill Factor:

$$FF = \frac{I_m V_m}{I_{sc} V_{oc}} = \frac{P_{max}}{I_{sc} V_{oc}} \qquad \text{or} \qquad FF = \frac{V_{OC} - \frac{kT}{q} \ln[q V_{OC}/kT + 0.72]}{V_{OC} + kT/q}$$

There are three major causes on the losses of photons received by the PV cell:

- photons with energy lower than the band gap ($hc/\lambda < E_{gap}$);
- thermalization losses due to photons with energy too much higher than the band gap ($hc/\lambda > E_{gap}$);
- internal losses represented by the *Fill Factor*.

In the picture below there is an example of a monocrystalline Silicon cell with $E_{gap}=1{,}12\ eV$. The white rectangle is the maximum efficiency that can be reached by the cell.

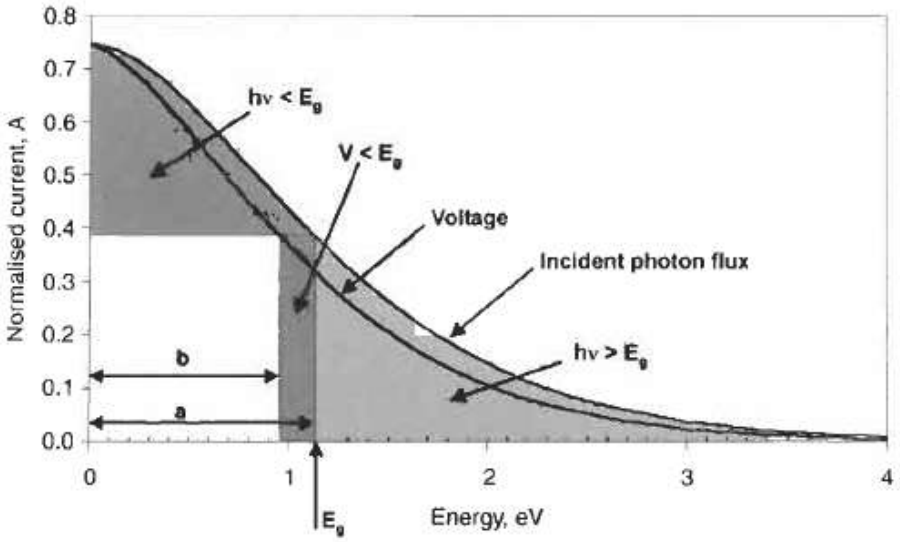

Fig. 2.13 – *Henry scheme of Si-mono losses.*

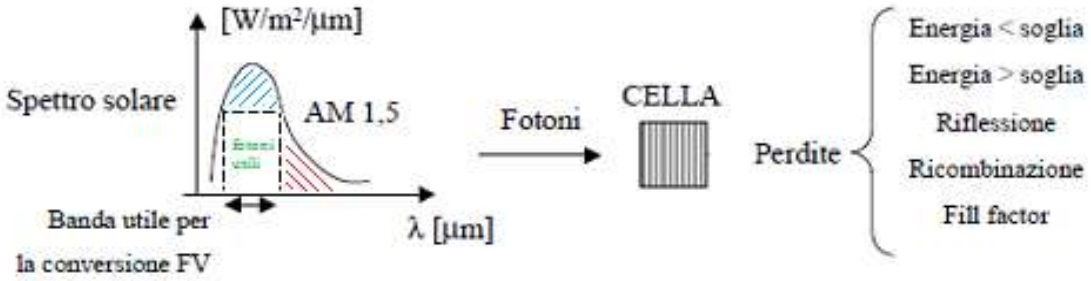

Fig. 2.14 – *PV cell losses analysis.*

The **efficiency** η of the cell can be so defined as:

$$\eta = \frac{P_{MP}}{P_{in}} = \frac{FFV_{OC}I_{SC}}{P_{in}}$$

where $P_{in} = P_{sun}$ is the power of the photons on the cell.

In the tab below there are the typical values for different PV cell technologies.

	Efficiency (%)	J_{sc} (mA/cm²)	V_{oc} (V)	FF (%)
Crystalline: single junction				
c-Si	24.7	42.2	0.706	82.8
GaAs	25.1	28.2	1.022	87.1
InP	21.9	29.3	0.878	85.4
Crystalline: multijunction				
GaInP/GaAs/Ge tandem	31.0	14.11	2.548	86.2
Thin-film: single junction				
CdTe	16.5	25.9	0.845	75.5
CIGS	18.9	34.8	0.696	78.0
Thin-film: multijunction				
a-Si/a-SiGe tandem	13.5	7.72	2.375	74.4
Photoelectrochemical				
Dye-sensitised TiO_2	11.0	19.4	0.795	71.0

Tab. 2.2 – *Values of* η_g , I_{SC} , V_{OC} *e* ***Fill Factor*** *for different kinds of PV cells.*

The short circuit current and the open circuit tension are linked to the radiation ***G*** as shown:

$$I_{sc} = I_{ph} - I_0 \left[e^{q/kT R_s I} - 1 \right]$$

where $I_{ph} = k\,A\,G$ for $R_s = o$.

$$U_{oc} = \frac{k\,T}{q} \ln\left(1 + \frac{I_{ph}}{I_0}\right) \approx \frac{k\,T}{q} \ln\left(\frac{I_{ph}}{I_0}\right)$$

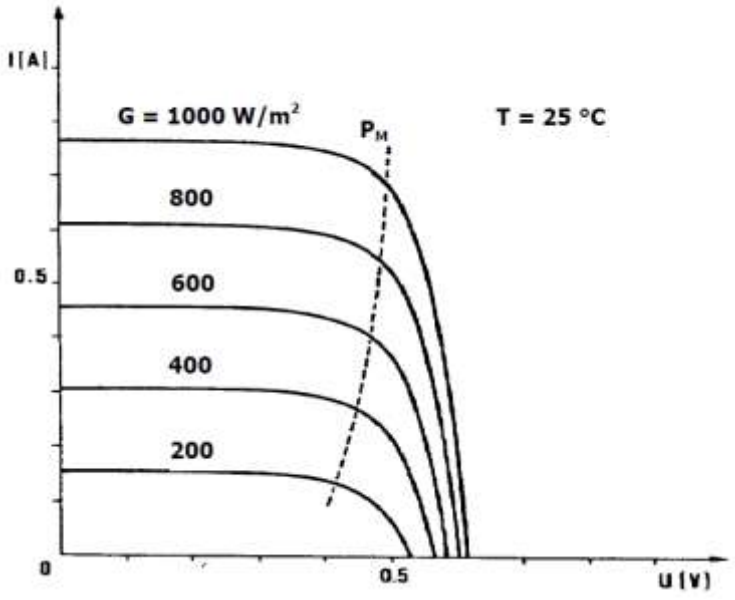

Fig. 2.15 – *I-V curve variation caused by the variation of radiation G.*

The temperature affects also the I-V curve with a raising of the current I_{ph} and I_{sc} with the temperature; also the current of the diode raises up, reducing so the open circuit tension U_{OC} (for the crystalline silicon it reduces of about 4 % every 10 °C).

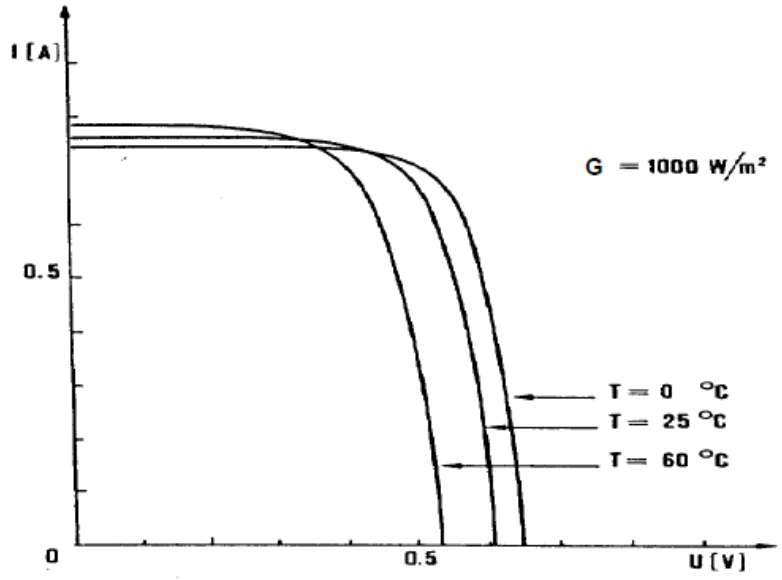

Fig. 2.16 – *I-V curve variation caused by the variation of temperature T.*

The curves of power and of efficiency are showed below: the point of maximum power point is also the point of maximum efficiency.

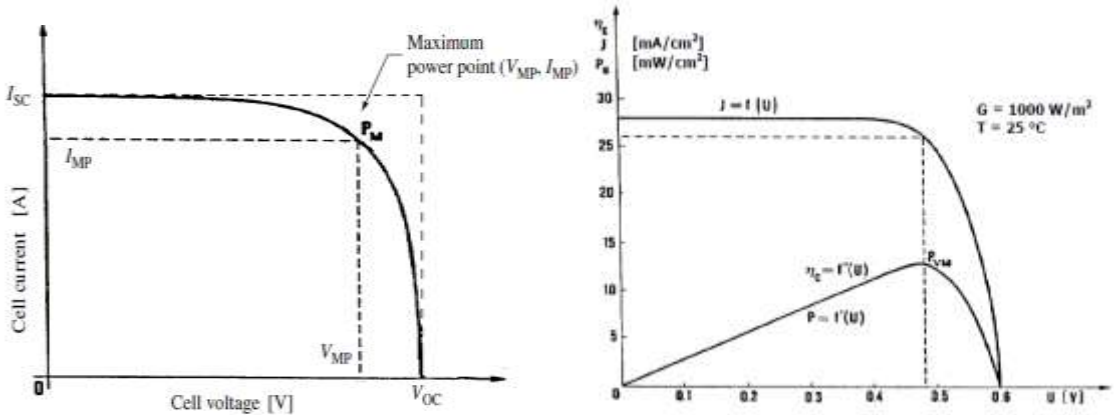

Fig. 2.17 – *I-V curve and efficiency curve samples.*

A maximum power point tracker ***MPPT*** is a resistor bank that optimizes the load to optimize the generation of energy.

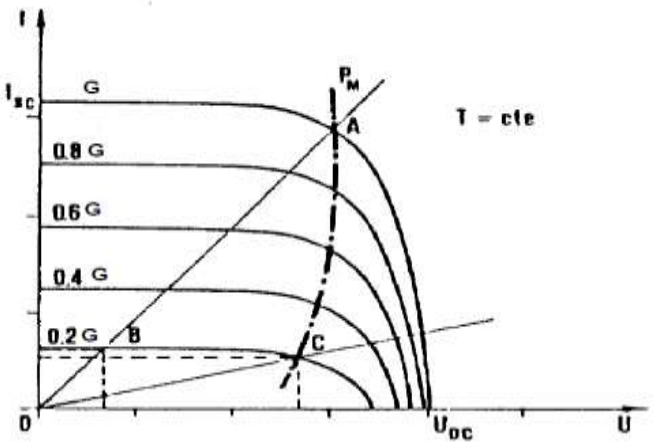

Fig. 2.18 – *MPPT curve. When the radiation becomes 0,2G the operating point goes from A to B. To optimize the system the MPPT creates a resistance to let the cell work in the point C at higher efficiency.*

The nominal operating cell temperature ***NOCT*** indicates the temperature of the module while functioning at open circuit, with an Irradiance ***I*** of 800 W/m^2 and a wind speed ***v*** of 1 *m/s*, atmosphere temperature T_a of 20 °C and ***Air Mass*** 1,5.

The value of the NOCT is useful to find the value of the cell temperature T_c in real irradiance and atmosphere temperature conditions:

$$T_C = T_a + \frac{NOCT - 20}{0.8} \cdot G\left[kW/m^2\right]$$

The thermal losses are a function of the T_c given by:

$$P_{tpv} = (T_{ce}I - 25) * \gamma / 100 \qquad P_{tpv} = [T_{amb} - 25 + (NOCT - 20) * I / 800] * \gamma / 100$$

with: γ as the temperature coefficient (for monocrystalline Silicon modules 0,45 %/°C).

The efficiency loss of the cell can be so reduced as following:

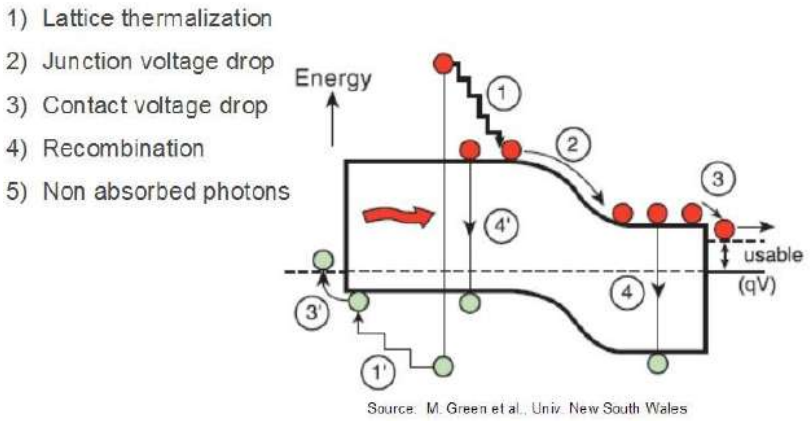

Fig. 2.19 – *Sources of standard PV cell efficiency loss.*

2.3 EFFICIENCY AND LOSSES OF A PV-MODULE

The PV module has many components that may cause efficiency losses that reduce the energy production of the system.

Each cell is connected with conductive material for collecting the electrons with ribbons connection with the other cells in order to have series or parallel connection.

The up surface is a low thermal dilatation material (such as glasses or plastic polymers) and a layer of EVA (ethylene-vinyl acetate) to grant mechanical and thermal resistance. The back surface is usually aluminum, usefully for the fixing system for the roofs or trackers.

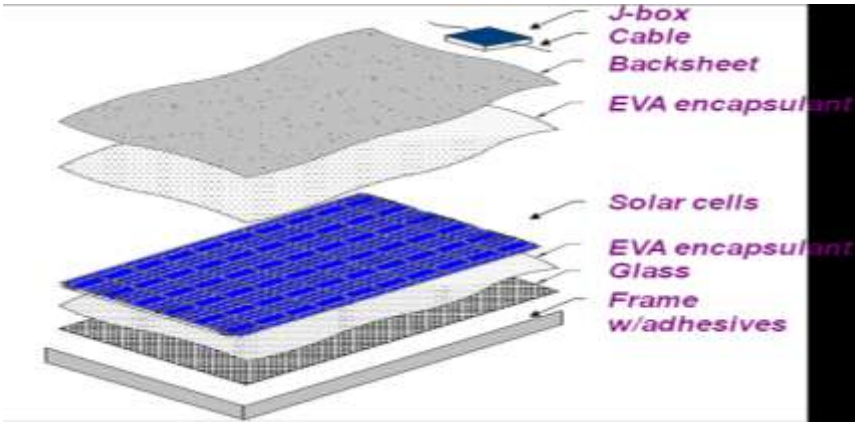

Fig. 2.20 – *PV module components.*

The global module efficiency η_{glob} can be defined as following:

$$\eta_{glob} = P_{max} / P_{sun}$$

where $P_{sun} = G\,S$ (global irradiation and cell surface respectively), $P_{max} = I_m\,V_m$.

It can be considered as the product of different efficiencies:

$$\eta_{glob} = \eta_{filling}\,\eta_{encap}\,\eta_{irr}$$

- ***filling efficiency***: it considers that only the active part of the module (the cells) generates electricity, while the rest of the module receives the radiation in not generating parts. It is defined as the ratio between the surfaces of the cell respect the surface of the (S_{cell} / S_{mod}) ;

➢ ***encapsulation efficiency***: is given by three more efficiencies:

$$\eta_{incap} = \eta_C \, \eta_{TR} \, \eta_{MIS}$$

• η_C is the *conversion efficiency* of the "naked cell", without the glass on it;

• η_{TR} is the *optical transmission efficiency* that indicates the adsorption of the materials interposed between the naked cell and the atmosphere;

• η_{MIS} is the *mismatch efficiency*, it considers the differences of the cells one with each other at receiving the radiation.

➢ ***uneven irradiation efficiency***: it considers the not even radiation received by the cells of the module.

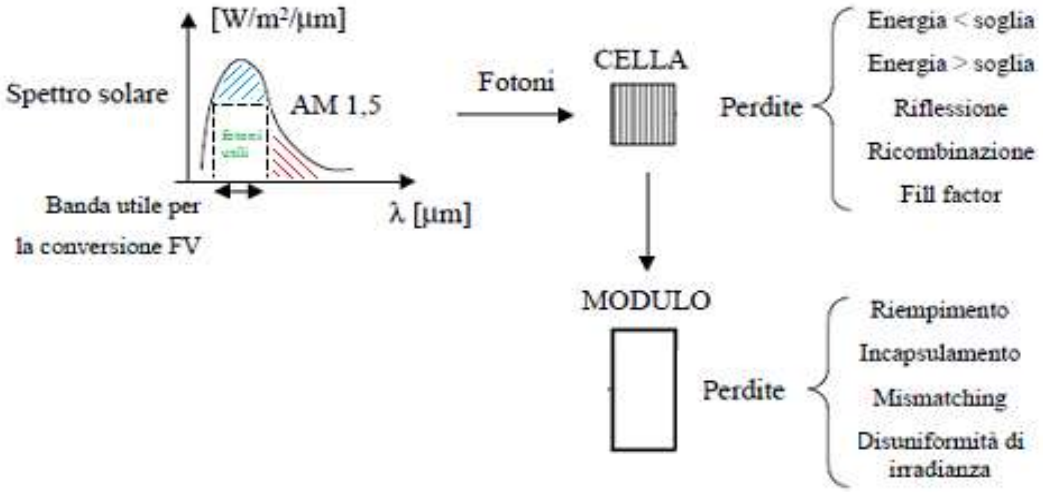

Fig. 2.21 – *PV cell and module losses analysis.*

2.4 REFERENCE INDEXES AND LOSSES OF A PV SYSTEM

For the evaluation of the performances of the system it is useful to introduce some reference indexes that may give further more information than the efficiency.

These parameters can help to compare the performances of different PV systems in different location, with different technologies.

With the introduction of the Performance Ratio ***PR*** it is possible to evaluate the performance of the systems normalized on the radiation received and the power installed of the systems.

2.4.1 *The Reference Yield - Y_R*

For the evaluation of the PR two more indexes have to be introduced.

The first one is the *Reference Yield* (***Y_R***). It is the ratio between the Irradiation received (direct or global, respectively E_{DNI} or E_{GNI} *[kWh/m²]*) and the reference irradiance DNI or GNI (equal to 850 *W/m²* for concentrating system or 1000 W/m² for diffusion PV systems).

It's a representation of the working hours at the reference irradiance and it is so measured in hours *[h]*:

$$Y_R = \frac{E_{DNI}}{DNI_{ref}} \ [h]$$

The *Reference Yield* (Y_R) is a function of location (irradiation received at a precise latitude), orientation (i.e. azimuth angle), inclination of the array (tilt angle), weather condition during the year (shadowing and temperature condition).

2.4.2 *The Array Yield - Y_f*

The second index is the *Array Yield (**Yf**)*. It is the ratio between the Energy Production **E** *[kWh]* of the system and the Power of the system $\mathbf{P_o}$ *[kW_p]* measured in hours **h** = *[kWh/kW_p].*

It can be defined before or after the inverter in order to have the DC or the AC Array Yield:

$$Y_{f\_DC} = \frac{E_{DC}}{P_o} \left[kWh/kWp \right] \qquad \text{or} \qquad Y_{f\_AC} = \frac{E_{AC}}{P_o} \left[kWh/kWp \right]$$

The *Array Yield* normalizes the energy production to the system dimensions and power.

2.4.3 *The PERFORMANCE RATIO - PR*

With the indexes introduced before the *Performance Ratio **PR*** is so defined as:

$$PR = \frac{Y_f}{Y_R}$$

It can be evaluated before or after the energy conversion:

$$PR_{DC} = \frac{Y_{f\_DC}}{Y_R} \ [a\,\mathrm{dim}] \qquad \text{or} \qquad PR_{AC} = \frac{Y_{f\_AC}}{Y_R} \ [a\,\mathrm{dim}]$$

It is dimensionless : $\frac{kWh/kW}{h}$

The performance ratio can so be used to define the different causes of losses of the PV systems:

- mismatch;
- back module temperature;
- imperfect reception of the radiation;
- inverter inefficiencies;
- DC and AC transmission losses;
- system malfunctions;

(the PR represents the ratio between the real and the expected production of the system).

The evaluation of the *energy losses* L_C is so found using the relation:

$$L_c = Y_R - Y_{DC} \left[kWh/kWp \right]$$

In this index are included the thermal losses for cell temperature higher than the NOCT, wiring, diodes, soiling, mismatch, MPPT faults, spectral losses.

The *system losses* L_S as the difference of Y_R and Y_{AC}:

$$L_s = Y_R - Y_{AC} \left[kWh/kWp \right]$$

In this index are included all the other losses after the inverter.

Loss factors	*mean value*	*Range*
PV module nameplate DC rating	0,95	0,8 - 1,05
Mismatch	0,98	0,97 - 0,995
Shading	1	0,00 - 1,00
Soiling	0,95	0,3 - 0,995
Sun-tracking	1	0,95 - 1,00
DC wiring	0,98	0,97 - 0,99
Age	1	0,7 - 1,00
Diodes and connections	0,995	0,99 - 0,997
Inverter and Transformer	0,92	0,88 - 0,96
AC wiring	0,99	0,98 - 0,993
System availability	0,98	0,00 - 0,995
Overall DC-to-AC derate factor	0,77	

Tab. 2.3 – *PV system mean efficiencies. For concentrating systems the performances of the tracking system must also be considered.*

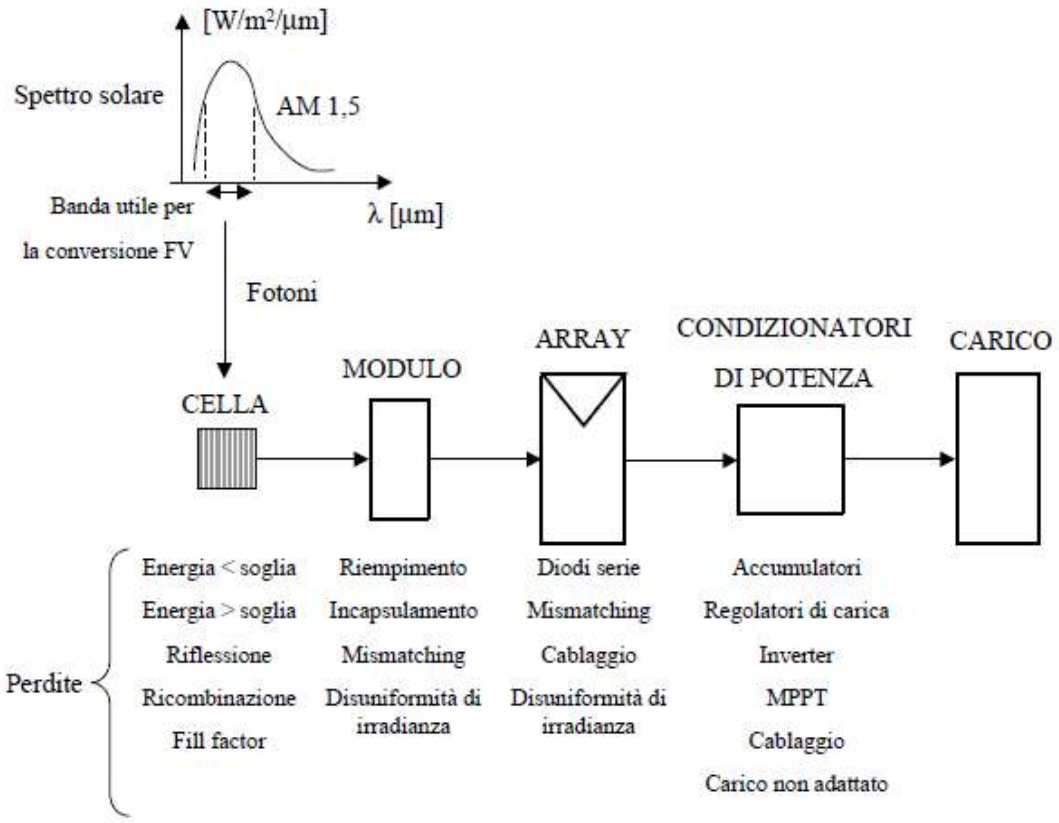

Fig. 2.22 – *PV cell, module and system losses analysis.*

2.4.4 *Efficiency of the system DC* η_{sist_DC}

2.4.4.1 MISMATCH

The solar radiation is composed by photons that have different energy levels in function of the wavelength:

$$E_\lambda = \frac{hc}{\lambda}$$

where λ is the wavelength, h Planck's constant, c is the speed of light.

Only for E_λ higher than E_G (energy gap) of the semiconductor it is possible the generation of the couples electron-holes.

The design of the photovoltaic cells aims to use the most part of the radiation received to permit the electrons band jump, to create the conduction couples.

The radiation on the Earth surface is different by the complete spectrum of the Sun, considered as a black body with a mean temperature of $5762\ K$: outside the atmosphere (*air mass zero* ***AM 0***) there is no absorption of the radiation, so the energy received is about $1{,}353\ kW/m^2$; inside the atmosphere the value of air mass considered is *AM 1,5* and a radiation received of *1* kW/m^2 after the absorption and reflection of the gasses in the atmosphere.

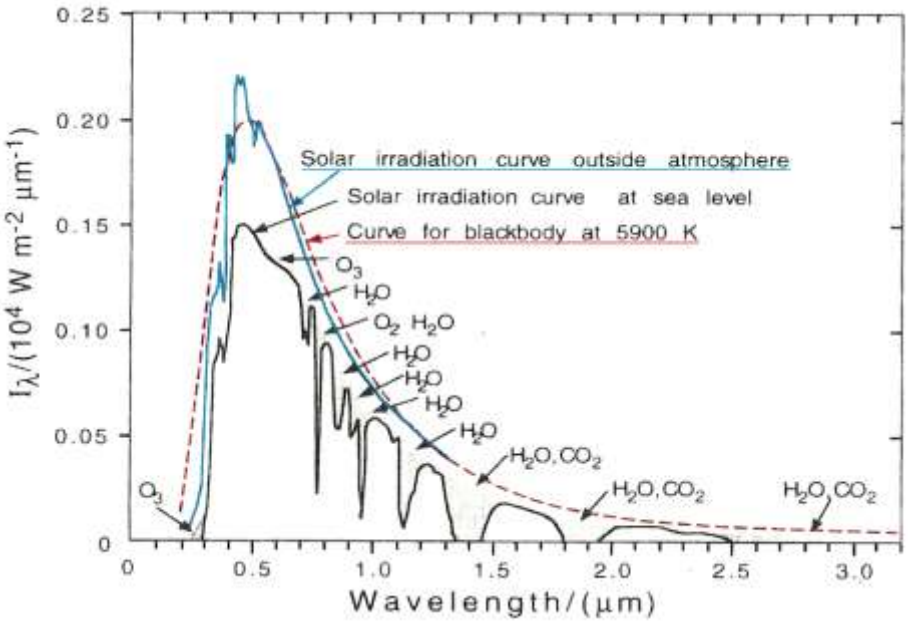

Fig. 2.23 – *Black body radiation at the mean temperature of the Sun surface of 5900 K, AM-o radiation, AM-1,5 (Earth surface) radiation (in these last curve it is possible to notice the different molecules adsorption at different wavelength)*

The air mass is a function of the incidence angle θ (it is the reason of the red light during the sunsets):

$$\text{Air Mass} = \frac{1}{\cos\theta}$$

The real irradiation is different from the indoor tests, because of the adsorption of different wavelengths radiation due to gasses in the atmosphere, and so will be the response of the PV cell.

The multi junction cells are the more influenced by spectral mismatch, due to the fact that these cells are optimized at a specific wavelength that could be modified (adsorbed or reflected) by the atmospheric gasses.

Even to cells of the same kind could response differently at the same radiation due to differences in fabrication.

The spectral mismatch usually causes losses around 2% of the total efficiency.

2.4.4.2 *SHADOWING OR SHADING*

A monocrystalline silicon solar cell generates usually a tension of 0,5 V and a current of 0,25 mA/mm^2 (a cell of 100 mm of diameter gives a current of 2,5 A).

The loads need much higher tension. In order to reach the tension needed by the load it necessary to make series and parallel of solar cells to raise tension and current.

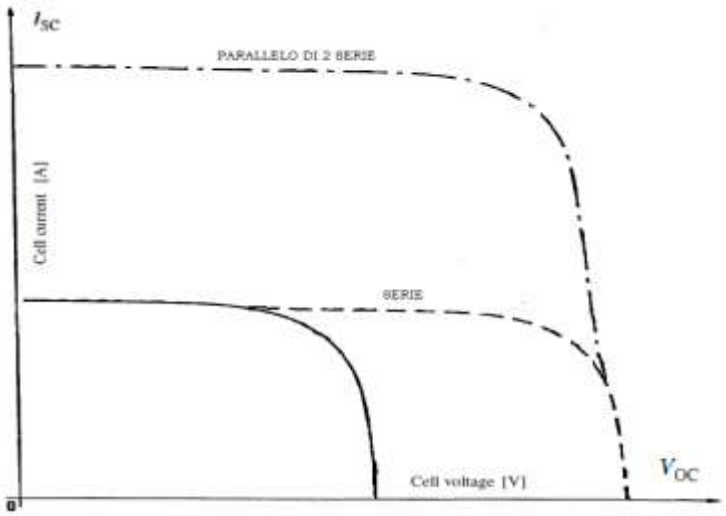

Fig. 2.24 – *Series and parallel connection of the modules.*

As seen before at different radiation the cell changes the response in the I-V curve.

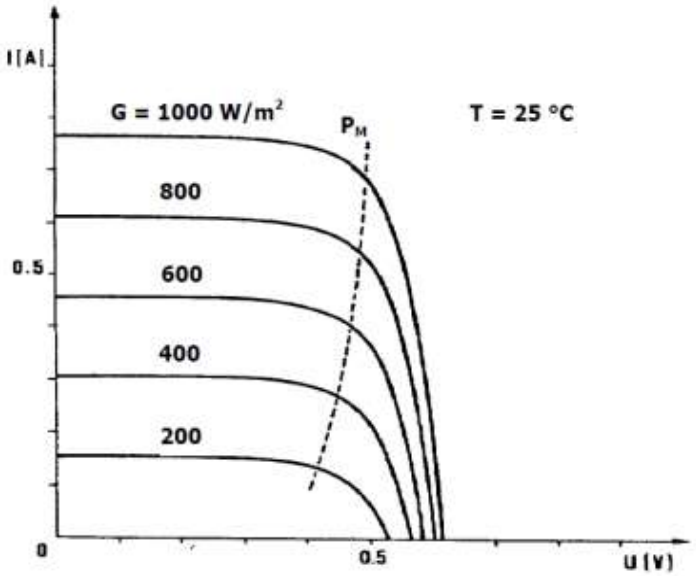

Fig. 2.25 – *Variation of the I-V curve at different value of the incident radiation G.*

Considering a system made by some modules in series and in parallel connected as in the scheme below, the shadowing can change the behavior of the module from generation to load mode.

To avoid this behavior some by-pass diodes are introduced to let the current pass to another module by-passing the shadowed one.

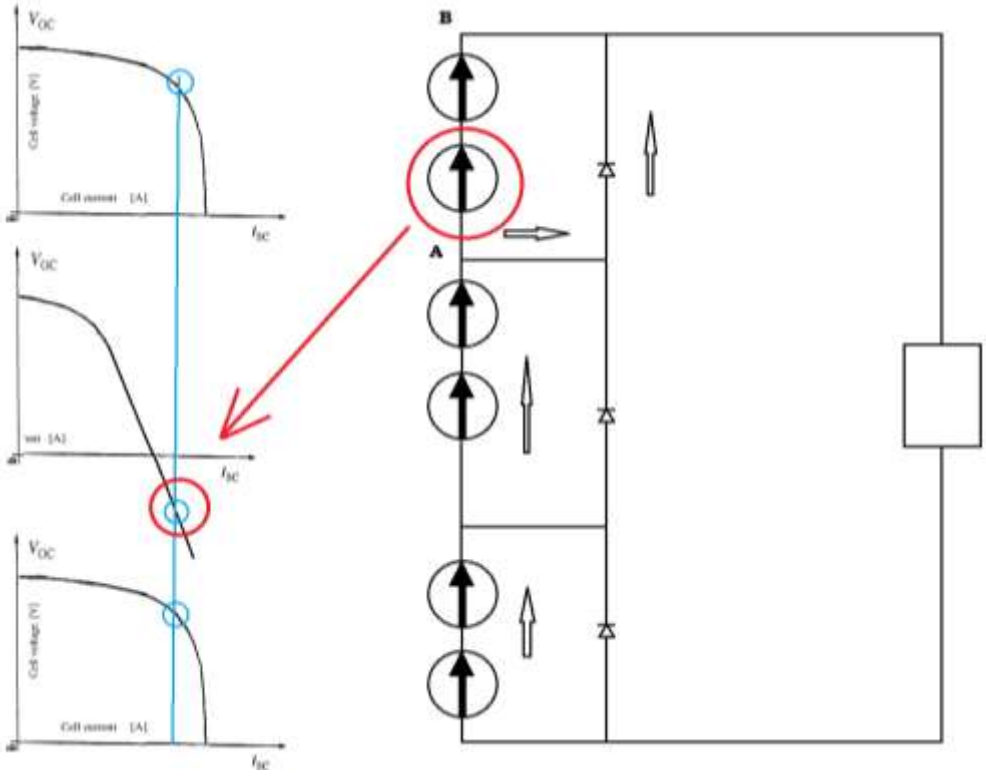

Fig. 2.26 – *PV cell behavior at shadowed conditions*

In each module there are by-pass diodes to avoid the breaking reverse tension (about 15÷30 V for silicon cells), due to the sum of the tension of the following cells. The diodes are inserted each 30÷60 cells (each cell reaches a tension of about 0,5 V).

The ideal condition would be a by-pass diode each cell to optimize the module against the shadowing, but the costs are too high to create a system like this. To avoid the "hot spot" condition there are some by-pass diodes each module to bypass the shadowed cells, and in the system to bypass the shadowed/malfunctioning module.

The use of microinverter systems is a way to avoid shadowing problems and the need of having a minimum number of series modules to reach the activation tension of the string inverter for starting the conversion.

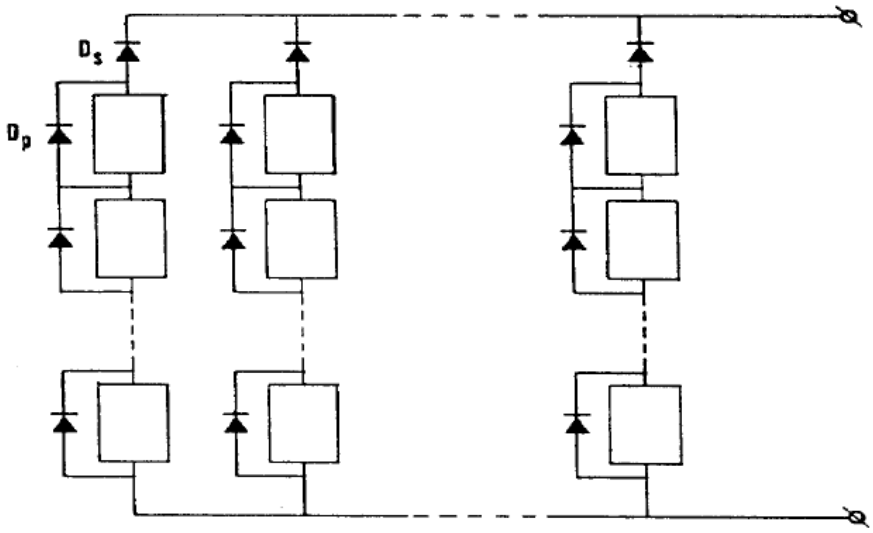

Fig. 2.27 – *Bypass diodes on PV modules and strings*

2.4.4.3 SOILING

It is almost the same effect of the shadowing: the radiation cannot reach the cell, so that there is part of the module that doesn't produce but works as a load for the system. The shadowing permits to use the diffusive radiation (obviously not for the concentrating systems that uses only the direct irradiation); the soiling can block totally the radiation received until the next module cleaning. Not only dust or sand, but also snowing can be considered as a source of soiling for the module.

Soiling losses are usually about 5% of the total efficiency.

2.4.4.4 CONDENSATION

The imperfect production of the module can cause the water condensation inside between the cell and the cover glass of the module. It has an effect similar at the shadowing or the soiling, but it is more serious because of the impossibility to operate inside the module.

Some modules are built with anti-condensation valves to balance the pressure between the inner part of the cell and the atmosphere.

2.4.4.5 SUN-TRACKING

Some PV systems are not roof fixed, but are fixed on mono o bi axial sun trackers in order to follow the sun during the day. For concentrating PV systems it's necessary to have biaxial sun tracker in order to receive the direct irradiation on the concentrating lenses of the optical system to give a multiplied radiation to the cell surface.

The sun-tracking losses are due to the malfunctioning of the tracking systems. Each concentrating optics has a tolerance angle that should be not exceeded in order to have the correct focus of the radiation on the cell.

2.4.4.6 DC WIRES

For the Ohm law there is a tension loss due to the resistance of the wires. For the Joule effect there is also a temperature raise. To avoid these losses it's necessary to have wires as short as possible (DC wires more than AC ones).Wires losses are about 2% of the total.

2.4.4.7 AGING

A feature of PV systems (crystalline silicon built) is a life time longer than 20 years. During the years there is a loss of efficiency of the system due to many factors that can affect the components of the system.

Thermal cycles, hard weather condition, radiation, humidity are for example some of the causes of deterioration of the PV modules.

One of the elements more exposed to ageing phenomenon is the polymeric cover of the module that can be affected by molecular breaks due to the UV radiation, physical breaks due to hard weather condition, etc. All this affects the optical transmission of the radiation to the cell.

The cell itself can be affected by molecular recombination of the doping inside the cell, displacement of the contacts due to thermal cycles during the years.

The Fill Factor and the short circuit current are the most affected by the ageing.

2.4.5 *Efficiency of the system AC* η_{sist_AC}

2.4.5.1 INVERTER AND TRANSFORMATION LOSSES

A photovoltaic power conditioner is a conversion system as in scheme below:

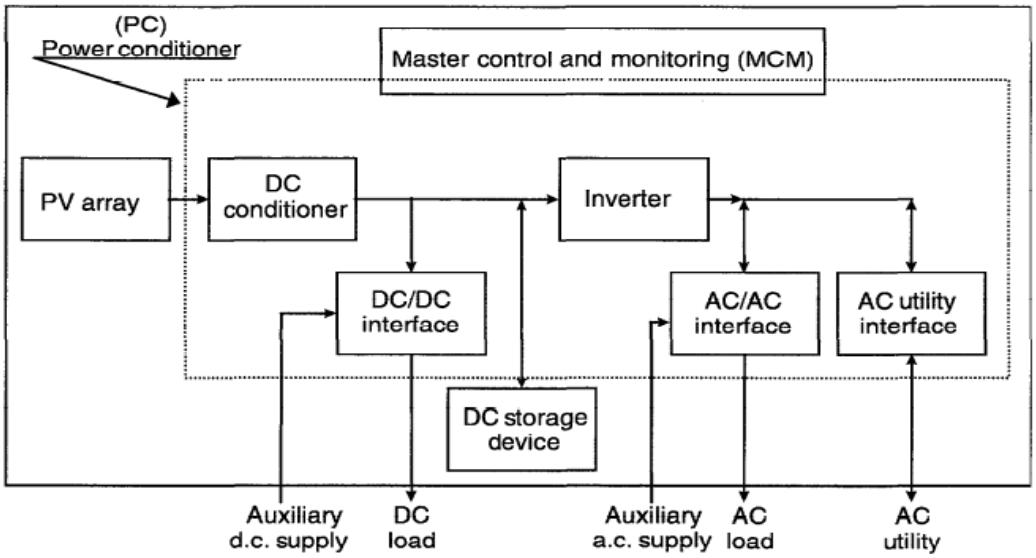

Fig. 2.28 – *Power conditioner scheme.*

There efficiency of the conversion can be calculated on the Power or on the Energy:

$$\eta_P = (P_{AC}/P_{aDC})$$

where P_{AC} is the outing power, and P_{DC} is the entering power.

The MPPT optimizes the tension to maximize the outside power.

The efficiency changes during the lifetime of the system. In order to evaluate the correct behavior of the PV system there is the need to create a weighted efficiency η_{WT}:

$$\eta_{WT} = \frac{\sum P_{Oi} \cdot T_i}{\sum P_{Ii} \cdot T_i} = \frac{P_{I1} \cdot \eta_1 \cdot T_1 + \cdots + P_{In} \cdot \eta_n \cdot T_n}{P_{I1} \cdot T_1 + \cdots + P_{In} \cdot T_n}$$
$$= K_1 \ \eta_1 + K_2 \ \eta_2 + \cdots + K_n \ \eta_n$$

with K_i:

$$K_i = P_{Ii} \cdot T_i / \sum P_{Ii} \cdot T_i \qquad \sum K_i = 1 \quad \text{and} \quad i = 1, 2, 3.....$$

;

As shown in the graph below:

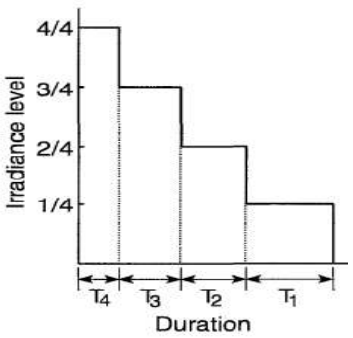

it is:

$$\eta_{WT} = \frac{1T_1}{T_{WT}}\eta_{1/4} + \frac{2T_2}{T_{WT}}\eta_{2/4} + \frac{3T_3}{T_{WT}}\eta_{3/4} + \frac{4T_4}{T_{WT}}\eta_{4/4} \geq \eta_{ER}$$

$$T_{WT} = 1T_1 + 2T_2 + 3T_3 + 4T_4$$

where:

- η_{ER} is the specific energy efficiency;
- $\eta_{1/4}$, … , are the efficiency at different power levels.

Losses are about 4÷8% of the total amount.

2.4.5.2 *AC WIRES, DIODES AND CONNECTIONS*

As for the DC wires, also the AC wires cause losses due to Joule effect or Kirchhoff law.

2.4.6 *Final efficiency*

Different level losses are summed to evaluate the final efficiency of the system starting from the cell, to the module, to the array and after the conversion to the final system efficiency.

The conversion system is usually after the array, but the use of micro-inverter can reduce some of the losses and raise up the energy production.

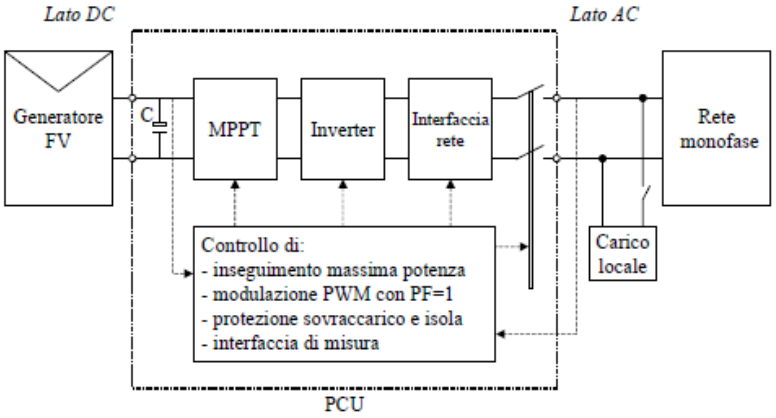

Fig. 2.30 – *Scheme of the components between the PV generator and the load.*

The efficiency of the systems depends on many factors.

It is so fundamental to analyze every single loss factors to enhance the performances and raise the energy production.

2.4.6.1 SYSTEM AVAILABILITY

The availability of the system is also as important as the efficiency: the occurrence of fails that blocks the production of the system affects the performances in the confrontation with other systems.

Bi-axial tracked or roof fixed systems, micro-inverter or string inverter, monocrystalline or multi-junction or amorphous systems have many differences and many fails occurrence prospects.

The optimum is obviously to find the best balance among costs, efficiency and availability with all the different technologies available.

CHAPTER 3

EVOLUTION OF PHOTOVOLTAIC

3.1 DIFFERENT KIND OF CELLS AND MANUFACTURING

During the last 40 years the researches have shown how many different paths can be followed to generate electricity from the sun beams through the photovoltaic effect.

Many kind of PV cells have been developed and an enormous enhance in efficiency has been reached.

There are some main categories in which PV cells can be divided:

- Silicon (mono-crystalline, multi-crystalline)
- Thin-film (a-Si – amorphous silicon, CdTe – cadmium telluride, CdS, CIS, CIGS – copper indium gallium selenide, CZTS, GaAs – gallium arsenide)
- Multi-junction
- Emerging PV (dye-sensitized or Grätzel, quantum dot, organic, plasmonic)

It is of fundamental importance to understand which is the right placement for every kind of technology developed, which are the main aims and the cost limits.

The first PV cells developed had the aim to give power to the first satellites sent on orbit in order not to carry fuels for giving power to the systems. In a political contest in which conquer of the space had no match with economical views, it was of no importance how much high was the cost per kW of the single PV cell.

In time political contests changed and also the economy was delivered to other paths.

Surely the space conquer had the enormous role to start the necessity of finding a way to generate energy from the sun beams; nowadays the environmental and economic necessities due to pollution and raising costs of electricity generation by the use of traditional power plants, have given a new "market pull" and a "technology push" to the photovoltaic research and development.

As shown in the graph below there are a lot of different kinds of PV cells. The highest efficiency reached in 2014 is about 44,4%.

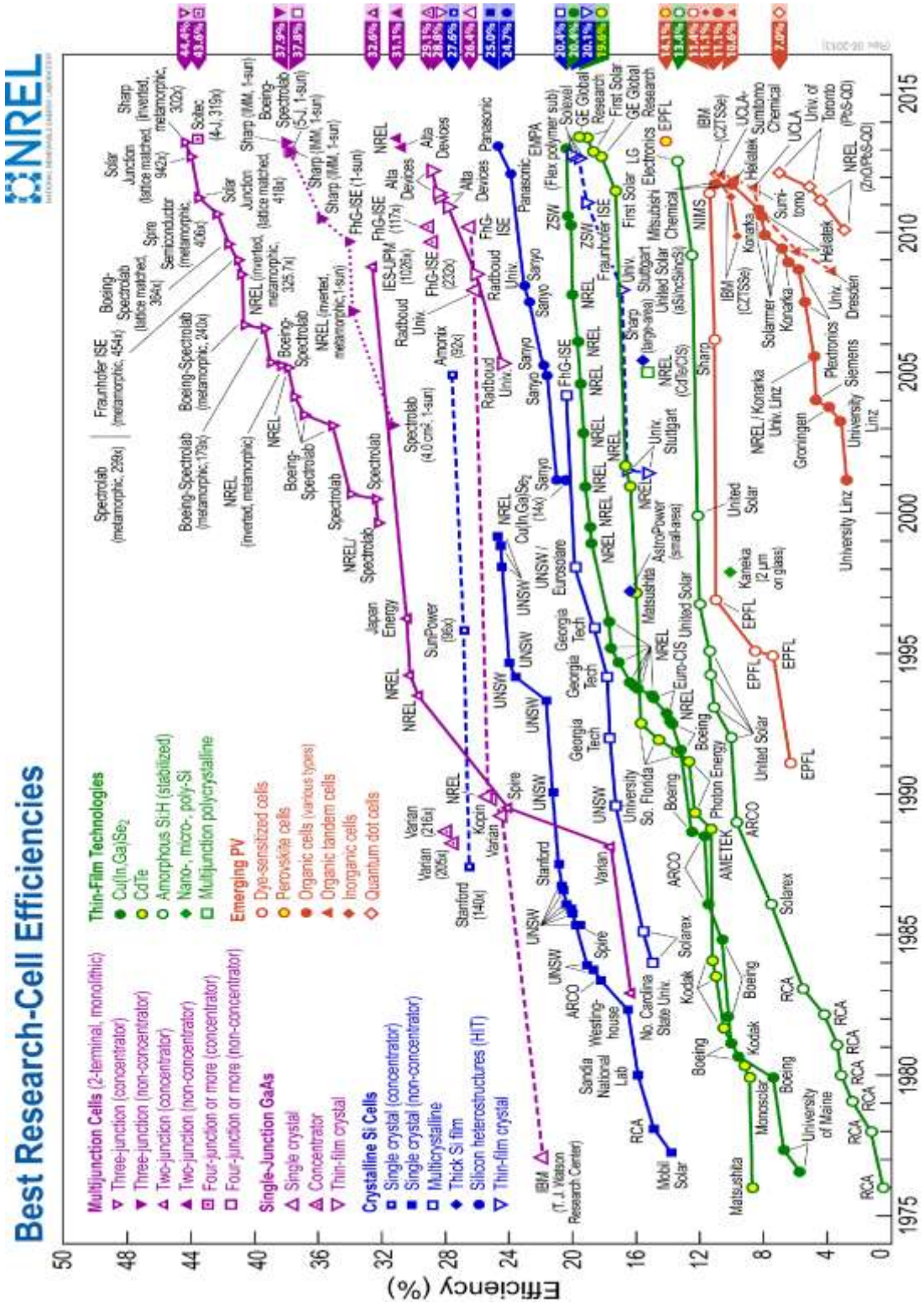

Fig. 3.1 – *Photovoltaic research cell efficiencies since 1975*

These are results obtained in laboratory. Commercial solutions have much lower efficiencies, but also lower costs.

An analysis of the different cells can show where the costs and the efficiencies come from.

	Efficiency (%)
Crystalline: single junction	
c-Si	24.7
GaAs	25.1
InP	21.9
Crystalline: multijunction	
GaInP/GaAs/Ge tandem	31.0
Thin-film: single junction	
CdTe	16.5
CIGS	18.9
Thin-film: multijunction	
a-Si/a-SiGe tandem	13.5
Photoelectrochemical	
Dye-sensitised TiO_2	11.0

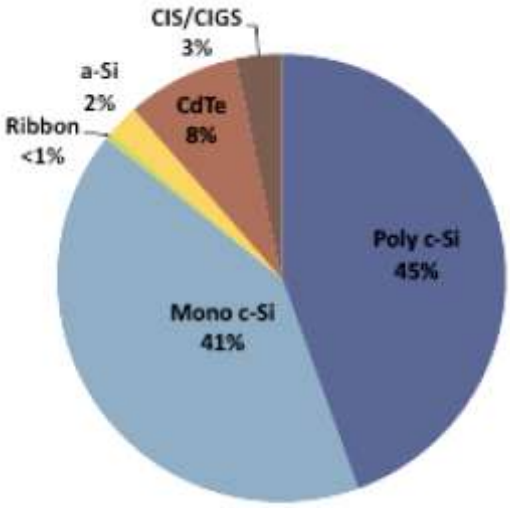

Fig. 3.2 – *Photovoltaic cells and modules lab efficiencies, market diffusion in 2013*

3.1.1 *Silicon cells*

The silicon cells are the most common kind of PV technology commercialized all over the world as shown in the graph above.

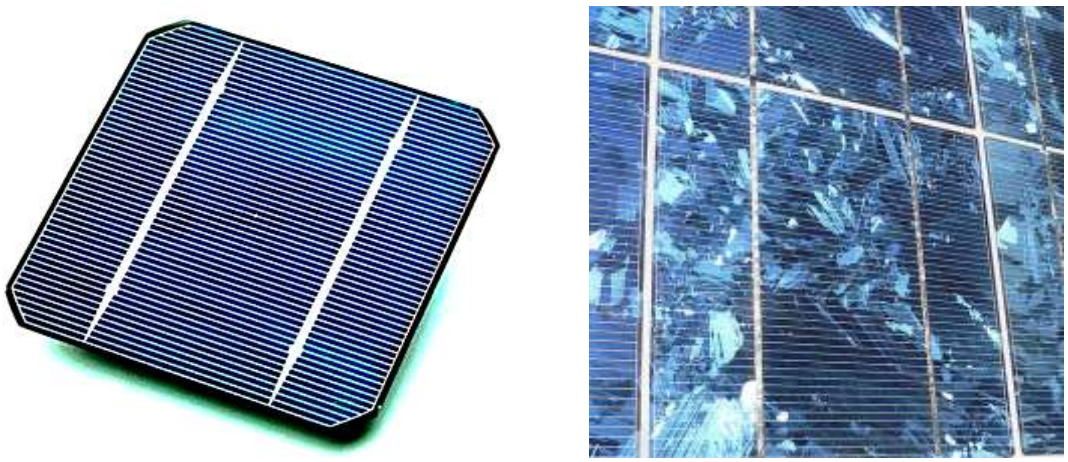

Fig. 3.3 – *Monocrystalline and polycrystalline silicon solar cells*

Silicon is a common element on earth as SiO_2 is one the major component in the sand. The different processes to obtain pure Si raise the cost production of the PV cells and so the final costs of the systems.

Metallurgical grade silicon is generated in electric arc furnaces at temperatures of about 1.800 °C. Through the following reaction it is possible to obtain 95% pure silicon.

- $SiO_2 + 2C = Si_{\_95\%} + 2CO$

(cost of the silicon obtained is about 2,30 $/kg)

The Siemens process helps to obtain much pure silicon through reactions with HCl:

- $Si_{\_95\%} + 3HCl = SiHCl_{3\_98,9\%\ (liq)} + H_{2\ (gas)} + (SiH_4)$ (must be avoid)

by distillation it is obtained $SiHCl_{3\_2\ ppm}$ (T~350°C)

- $SiHCl_{3\_2\ ppm\ (gas)} + H_{2\ (gas)} = Si_{\_2\ ppm\ (solid)} + 3HCl_{\ (liq)}$ (T~1100°C)

deposing pure microcrystalline Si

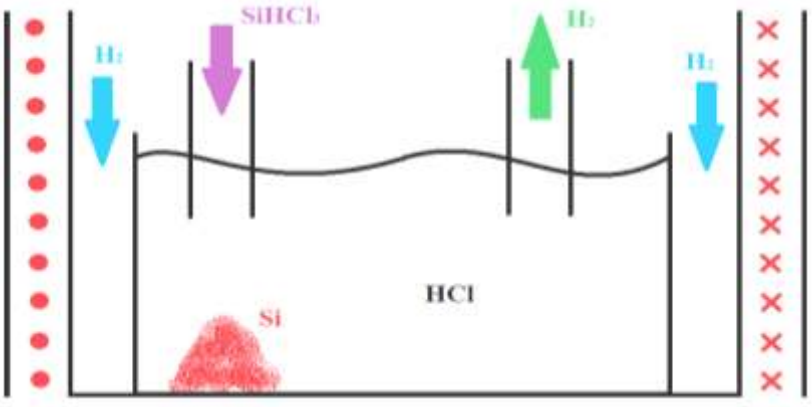

Fig. 3.4 – *Siemens process: generation of metallurgical grade Si powder in electric arc furnaces*

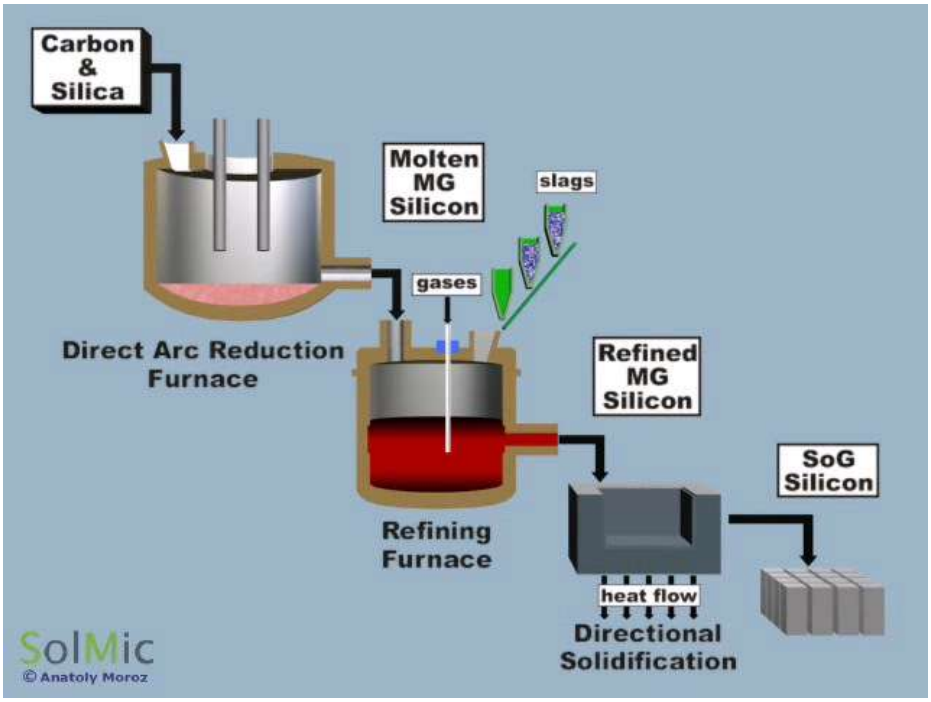

Fig. 3.5 – *Siemens process stages*

The positive doping process with Boron is made in the Silicon liquid during the refinement process.

The n doping is made through Electron Vapor Deposition, in a process in which the Phosphorus sublimates and is deposited on the Silicon surface by intermolecular diffusion.

The electronic grade silicon is even more refined than the metallurgic. It is commonly obtained through the Czochralski process.

By inserting a rotating bulk of silicon in the furnace, a cylinder of monocrystalline silicon is fused. The crystals created are 0,1÷1 ppm pure.

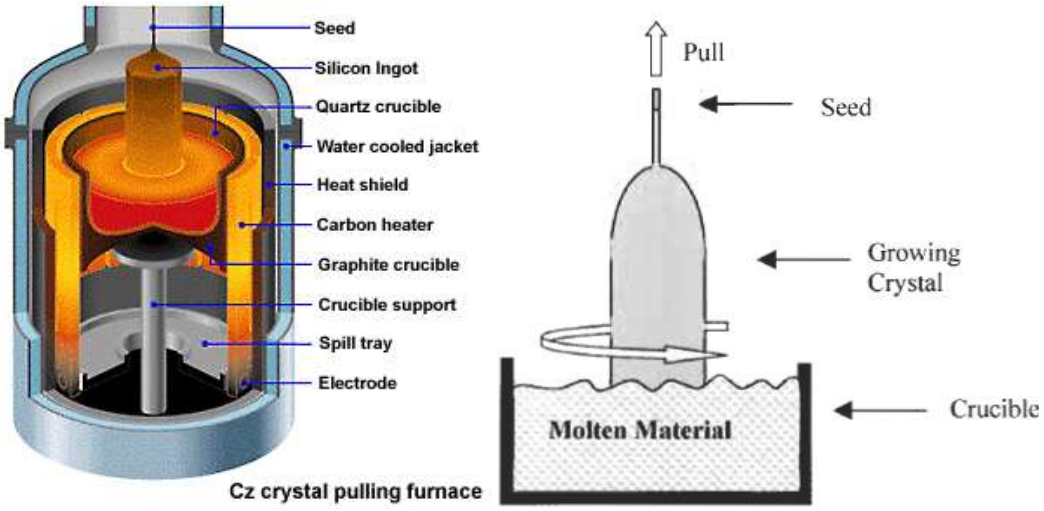

Fig. 3.6 – *Czochralski process stages*

Another way to create a crystal is through the floating zone process: by using the recovered silicon sands, a magnetized spire molts the sand and fuse the crystal in a specific direction. The crystals are less oriented than the Czochralski process, but this process is cheaper, faster and permits the use of recycled material.

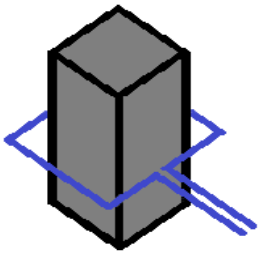

Fig. 3.7 – *Floating zone process*

The edge growth process works with the capillarity of a silicon solution to create the disk (that grows as multi crystal silicon).

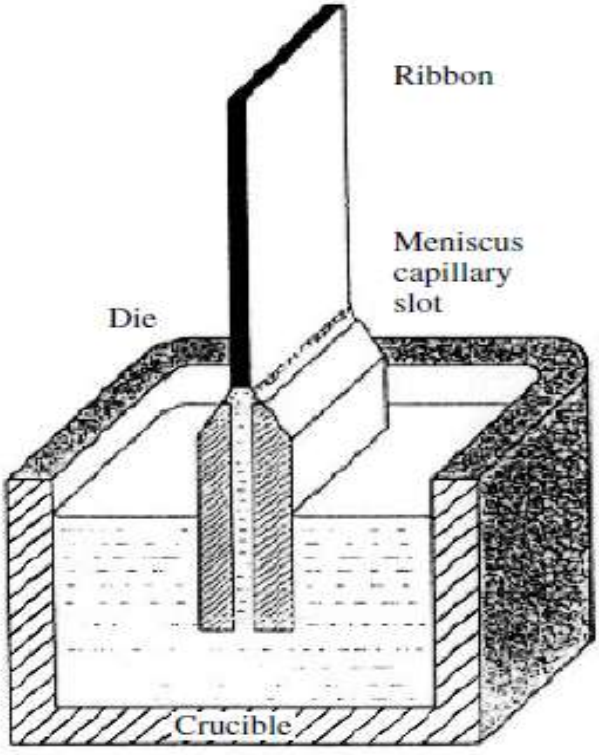

Fig. 3.8 – *Edge growth process*

The cutting of the silicon disks are one of the major causes of material losses during the processes. About the 50% of the silicon has to be reinserted in the crystallization process after the cut, due to the small width of the cells (about 200÷300 □m for standard cells).

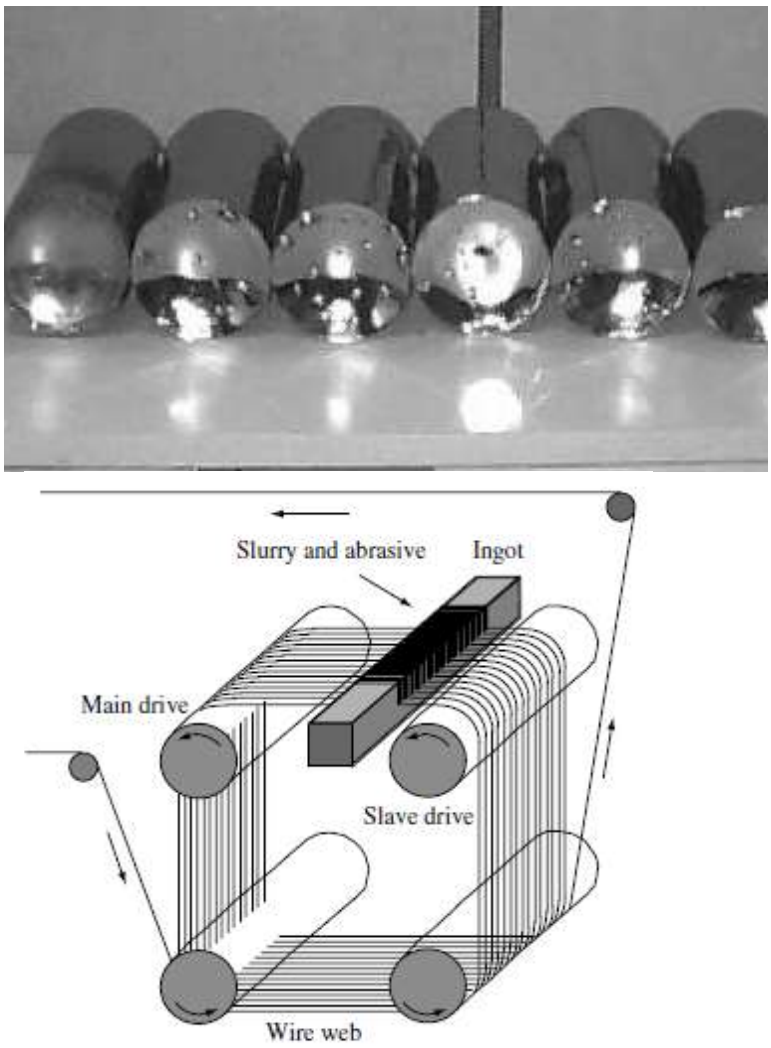

Fig. 3.9 – *Cutting techniques with wire saws*

Considering so the production process of a silicon module, the costs can be charged with the following percentages:

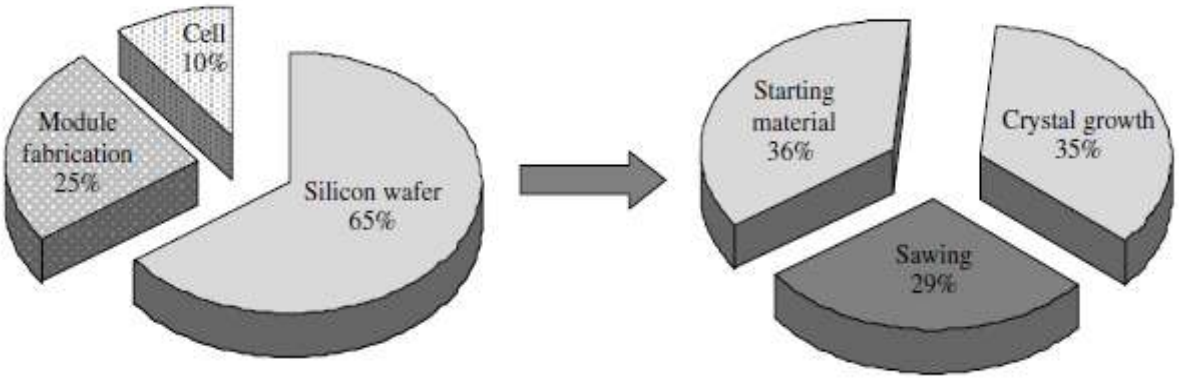

Fig. 3.10 – *Cost production percentages*

3.1.2 *Thin film cells*

The greatest advantages of using thin film cells are a reduction of material needed due to the very small thickness of the cells, a reduction of the costs and the enormous opportunities given by a flexible material that can change the view of how to utilize solar cells, giving surely an enormous numbers of new fields of utilization for the PV generation.

Fig. 3.11 – *Thin film modules*

On the other hand there are some issues to deal with and to overcome to gain more space in the PV market. More than the others we remember the reduced efficiencies and the materials used (some toxic, some not as common as the silicon).

One of the first thin film technology developed is the *amorphous silicon cell*.

The a-Si is a not crystallized silicon, much cheaper than the crystalline one but with worse efficiency. It has the benefit of a direct band gap and a higher absorption coefficient in the short wavelength range.

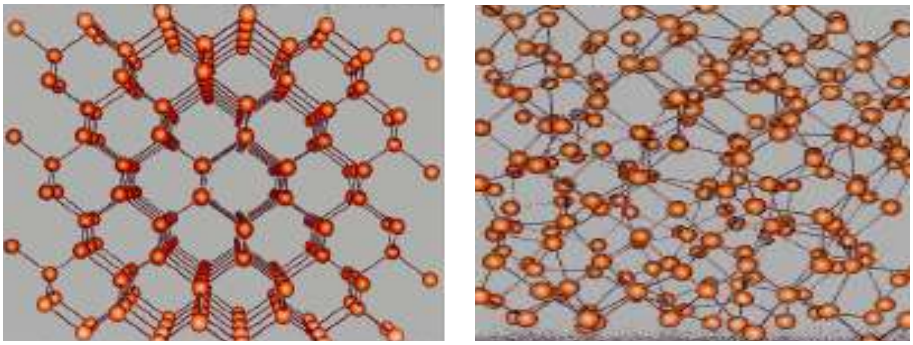

Fig. 3.12 – *Crystalline versus amorphous atoms distribution*

The a-Si has some dangling bonds that can be "filled" with hydrogen atoms to enhance the diffusion length and the mobility (that is lower than the crystalline silicon).

The energy adsorbed by the light during the first period of the lifetime can break the H-bonds and create again the defects avoided with the hydrogenation: the efficiency can reduce of about 30% during the first months.

The low efficiency is due to the defects that reduces the diffusion length of the generated charges.

To avoid this loss the use of an intrinsic layer among the p and the n layers can help to increase the diffusion length.

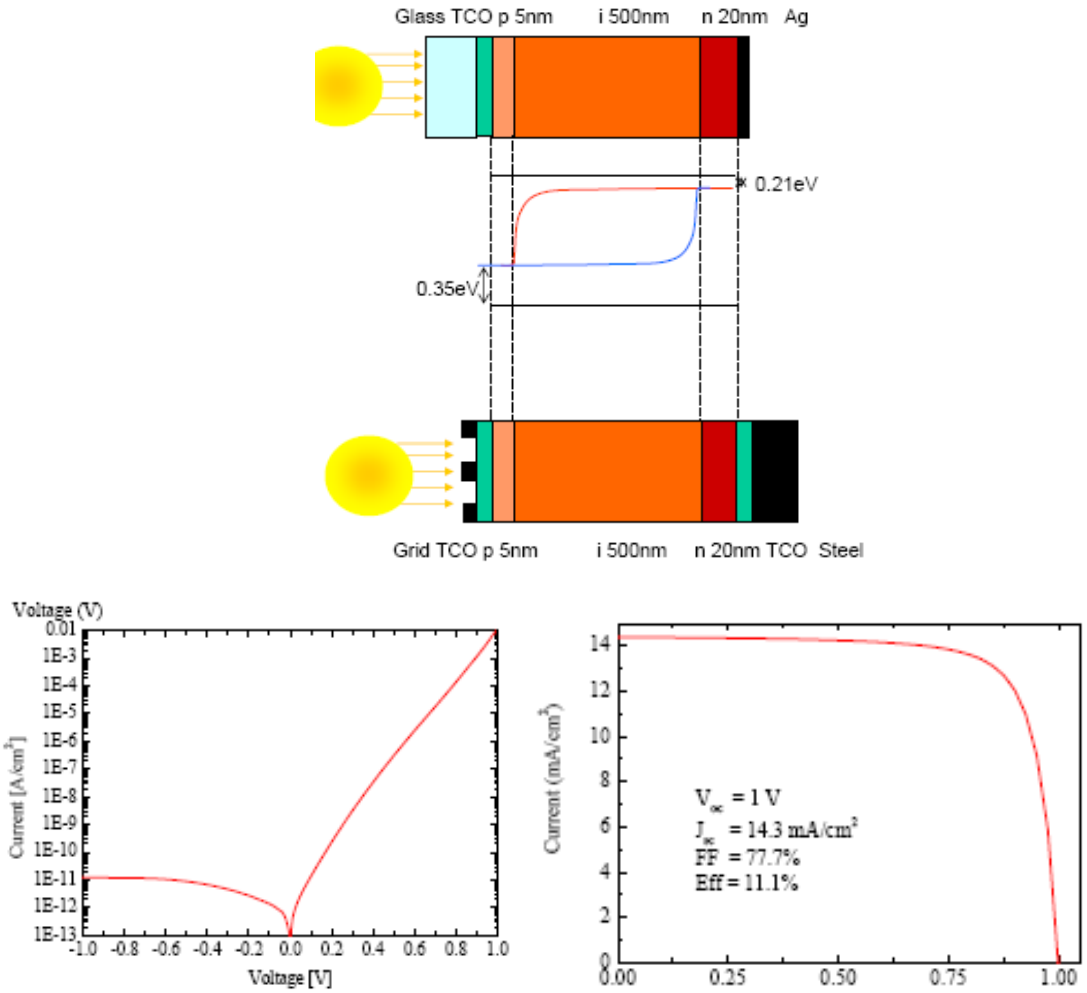

Fig. 3.13 – *Amorphous cell characteristics*

Even if efficiency reaches no more than 9%, the layer thickness of only 250 nm , against the 250 μm of standard c-Si cells: this means a reduction in quantity of silicon used of 10^3, and a reduction of costs (even the manufacturing process is cheaper) that can justify this technology in the comparison.

Another thin film technology is the *CdTe cells*. The very low cost per W of about 0,6 $/W, the direct band gap (an energy gap of about 1,5 eV with a maximum wavelength of 825 nm) , the easy deposition methods (sputtering, vapor deposition, bath deposition) are the main advantages of this kind of PV cells, on the other hand the

Also the *CdS cells* have similar proprieties, with the advantage of low temperatures for the manufacturing of the cells, and the spray-coating system for the deposition on the support layer.

Cadmium can be toxic and the efficiencies are about 10% (with a theoretical limit of 29%).

The *CIS* ($CuInSe_2$) or the *CIGS* ($Cu[In, Ga]Se_2$ *cells* have the advantage that the intrinsic defects of the materials have the effect of a p doping, and that an impure material has not great difference in energy performances from the pure ones. The indium shortage could be a problem in the future, but nowadays these kinds of modules are not so diffused. The price of the module is much higher than the CdTe cells, but the efficiency can reach values around 16%. The band gap goes between 1,04 2,7 eV, giving the chance to use a very large wavelength range.

To eliminate the Indium dependence the cells can be made differently: *CZTS cells* (Cu_2ZnSnS_4), but the efficiency is still around only 7%.

The *GaAs cells* can assure very high efficiencies, but the cost of the cell is expensive due to the material uses. It is mostly used on space PV cells.

Cell	Efficiency [%]
GaAs	25.1 ± 0.8
GaAs (thin film)	23.3 ± 0.7
GaAs(poly)	18.2 ± 0.5
InP	21.9 ± 0.7
GaInP/GaAs	30.3
GaInP/GaAs/Ge	28.7 ± 1.4
Si	24.7 ± 0.5
GaAs	27.6 ± 1.0
GaInAsP	27.5 ± 1.4
InP	24.3 ± 1.2
GaInP/GaAs/Ge	32.4 ± 2.0
GaAs/GaSb	32.6 ± 1.7
InP/GaInAs	31.8 ± 1.6
GaInP/GaAs	30.2 ± 1.4
Si	26.8 ± 0.8

Tab. 3.1 – *Cells efficiencies in laboratory*

3.1.3 *Multi junction cells*

The multiple junction cells can separate on different materials the adsorption of the radiation, so that each part of the cell is optimized for the right wavelength radiation.

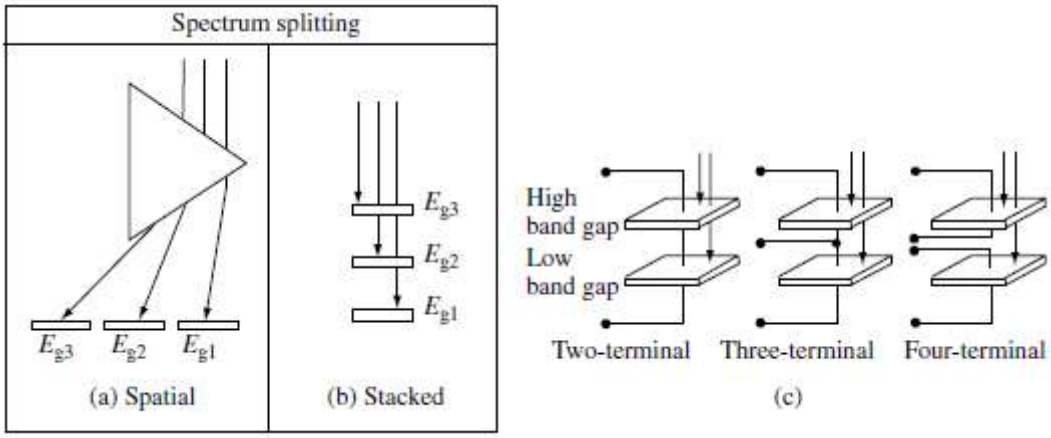

Fig. 3.14 – *Multi-junction cells: a) Prismatic beam splitting and spatial division; b) and c) Stacked mj-cell*

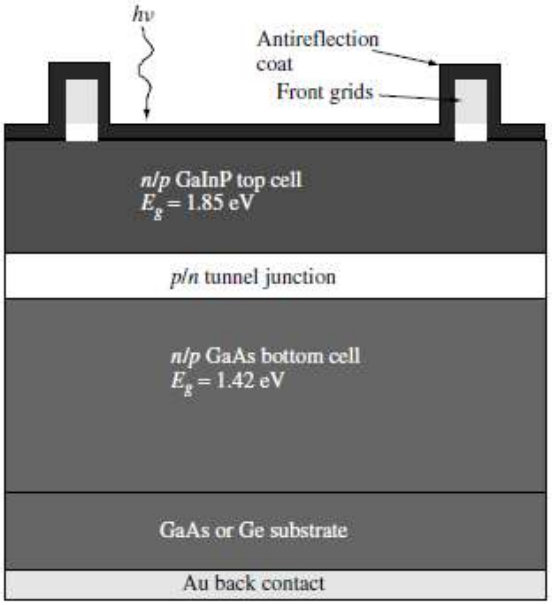

Fig. 3.15 – *Stacked mj-cell*

Concentration ratio	Number of cells in the stack	Maximum efficiency (%)
1	1	31.0
	2	49.9
	3	49.3
	...	
	∞	68.2
46.300	1	40.8
	2	55.7
	3	63.9
	...	
	∞	86.8

Tab. 3.2 – *Theoretical maximum efficiencies*

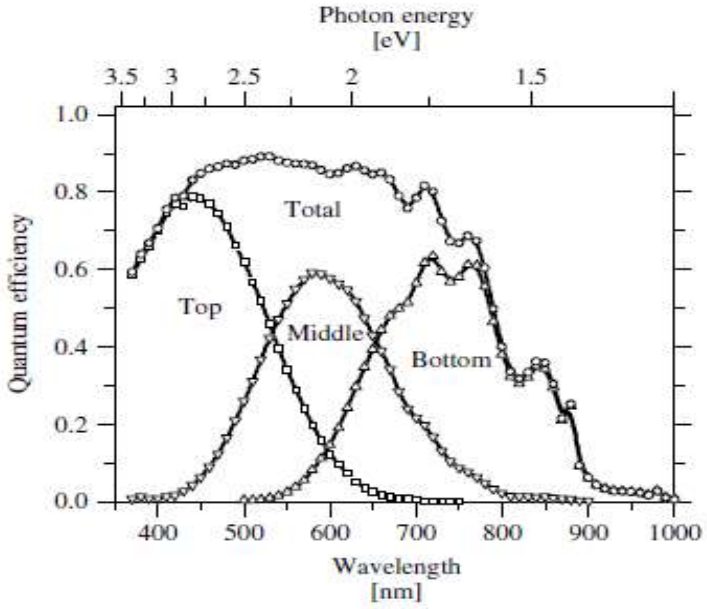

Fig. 3.16 – *The quantum efficiency is the ratio (at the specific photon energy considered) between the current per square centimeter generated and the incident photon flux* ***QE = j / ef*** *. The three different junctions are optimized for the different wavelengths, so that the total efficiency increases.*

3.1.4 *Emerging PV cells*

The *"Dye Sensitized Solar Cell" or "Grätzel cell"* are electrochemical photovoltaic generators. Two transparent electrodes contain a porous layer of TiO_2 covered with a molecular dye that absorbs the sunlight: the photons excite the electrons of the organic dye that through the TiO_2 are conducted to the electrodes. The main issue is the liquid electrolyte that causes instability outside a strict range of temperature.

The efficiency can reach about 15%, thanks to a great quantum efficiency that permits the conversion in electrons of about 90% of the photons. Although the temperature instability, the degradation caused by high energy radiation and so the short lifetime of the systems can be an enormous limit to this technology, the cheap production costs, the high QE and the theoretically feasibility of the cell production are very attractive for these systems.

Fig. 3.17 – *DSSC scheme.*

There are some other ways to raise the efficiency of the solar cells: the use of middle energy levels between the two bands to reduce the energy needed by the electrons to jump the gap is the idea behind *multi quantum well*, *quantum dot* solar cells.

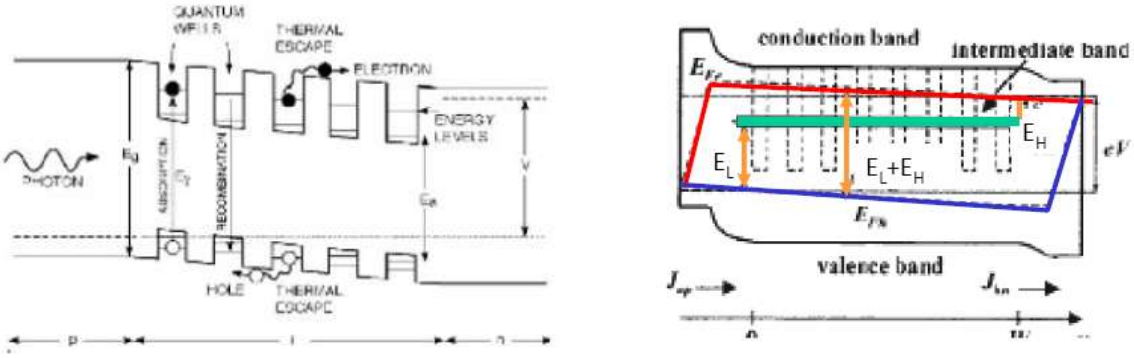

Fig. 3.18 – *Examples of multi quantum well (on the left) and quantum dot (on the right) solar cells: both the generators have been made with the aim of creating an intermediate band or by the use of interposed material, or by the use of nanocrystals with spatial dimension near to the wavelength of the radiation received.*

The creation (through doping, through nanocrystals rightly positioned, through the interposition of a layer of a specific material) of an intermediate band enhances the quantum efficiency of the cell and permits the generation of many more couples electron-hole improving the performances in terms of quantum efficiency and energy efficiency.

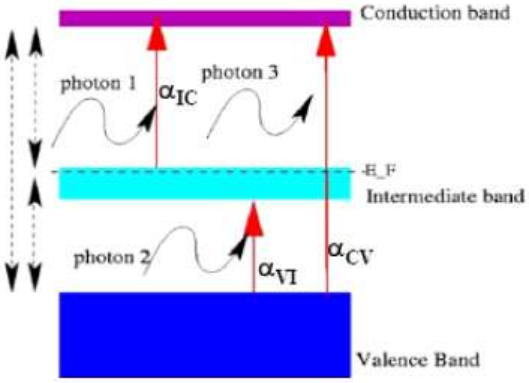

Fig. 3.19 – *Intermediate band sample.*

The idea of improving the quantum efficiency is also behind the *up converters* and *down converters* solar cells.

Instead of reflecting or being transparent to the photons too less with or too much energy, there is the chance to combine together two low energy photons (**2** photons with $h\nu < E_{gap}$ **= 1** photon with $h\nu > E_{gap}$) or to split a high energy photon (**1** photons with $h\nu >> E_{gap}$ **= 2** photon

with $h\nu > E_{gap}$) in order to generate photons with the needed energy to create the charge carriers needed for the generation of electricity.

Combining two photons not enough energetic to permit the jump (i.e. $h\nu < E_{gap}$) by the use of "mirrors" behind the cells, permits to recover lost photons and to enhance the efficiency of the cell.

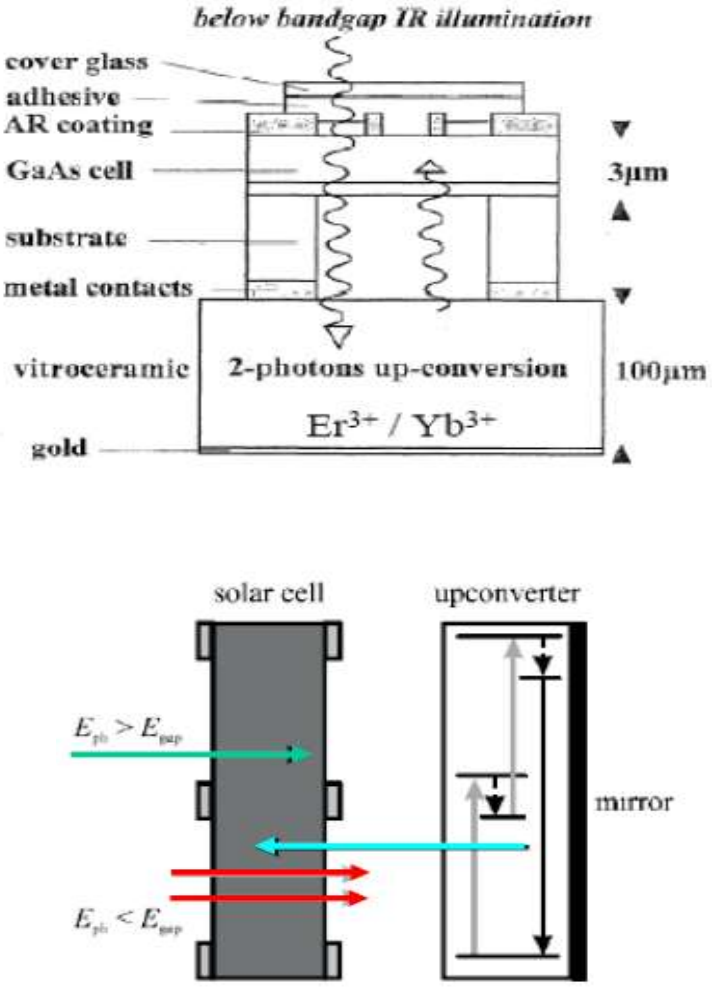

Fig. 3.20 – *Up converters systems aim to combine together all the photons less energetic than the band gap value to raise the quantum efficiency.*

Splitting a too much energetic photon (i.e. $h\nu > E_{gap}$) to avoid the thermalization caused by the excess of energy is the way of the down-converters cells. Reducing the thermalization, the cell temperature gets lower and so the efficiency raises.

As for the "up converters", the idea is to have a cell transparent to high energy photons that will reach a surface behind the cell.

This surface would thermalize and re-emit the radiation at the right wavelength for the cell (ThermoPhotovoltaic TPV).

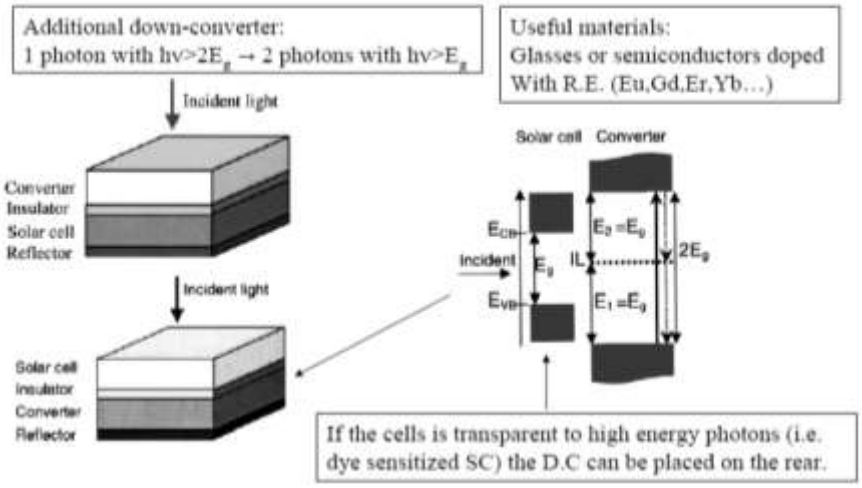

Fig. 3.21 – *Down converters systems aim to split all the photons more energetic than the band gap value to raise the quantum efficiency.*

3.2 CONCENTRATED PV SYSTEMS

A way to reduce the cost of the system is using less active material. The idea is to concentrate the radiation on smaller surfaces by the use of optical systems; doing so it is possible to use a small quantity of the best efficiency cells (that are usually the most expensive).

The other side of the coin is that the use of concentrated radiation needs a bi-axial tracking system in order to have the beam always focused on the solar cells, losing so the diffuse part of the global radiation.

This is the theory behind the concentrated PV systems.

The more complicated systems (mostly due to the trackers) pushes this technology to an industrial production more than a residential one.

3.2.1 *Optic systems*

The *"geometric concentrating ratio"* is the ratio between the area of incidence of the beam and the area of the PV cell. The *"number of suns"* is the ratio between the radiation on the PV cell and the mean value of the global radiation (0,1 W/cm^2).

Concentrating 10 W on a cell area of 2 cm^2 gives a concentration of 50 suns of geometric concentration. Considering that the radiation used is the direct one, equal to 0,085 W/cm^2, the optics efficiency is about 85%, the concentration becomes:

(10/0,2) * (0,085/0,1) * 85% = *36 suns*

The active area of a 1 cm^2 cell is about [0.8 cm × 0.8 cm = 0.64 cm^2]: making a geometric concentration of 100X we can consider 64 cm^2 active area for a cell [1 cm x 1 cm].

From a 10 cm^2 wafer (that means 52 cells of [1 cm x 1 cm], with an optics efficiency of 85% it would be: [85%$_{\_transmission}$ × 0,085$_{_direct\ rad}$ × 0,64$_{active\ area}$ × 100X$_{_gemoetric\ conc}$ x 52$_{n_celle}$ = 240 W].

If the receiving area was of 78 cm^2 (considering the global radiation of 0,1 W/cm^2) there would be a power of 7,8 W: concentrating with a 100X optics on the 10 cm^2 cell means an increment from 7,8 W to power of 240 W. With a normal PV cell, without optics, 31 times the surface would be needed to obtain the same power.

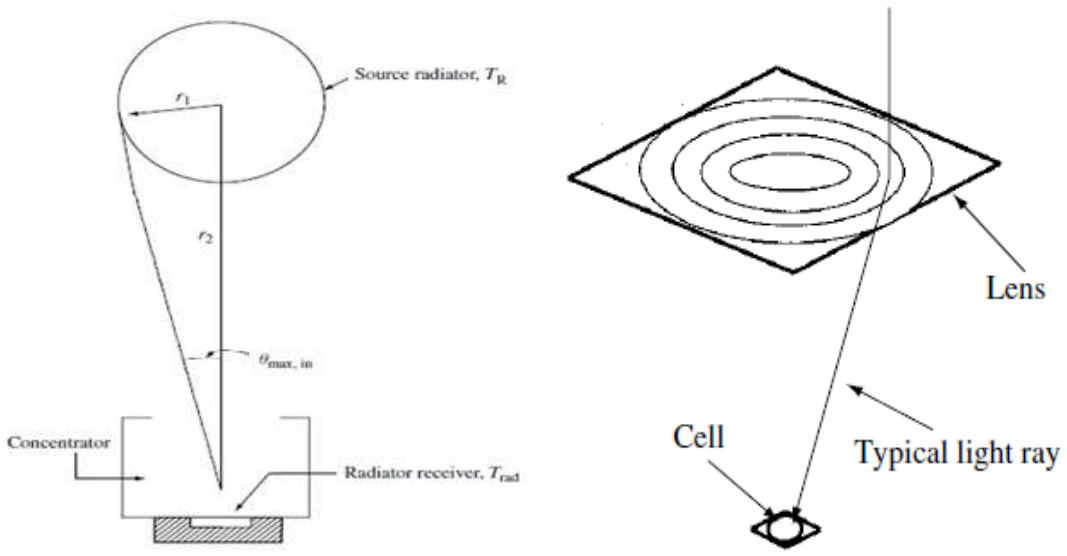

Fig 3.22 – *Concentrating system scheme*

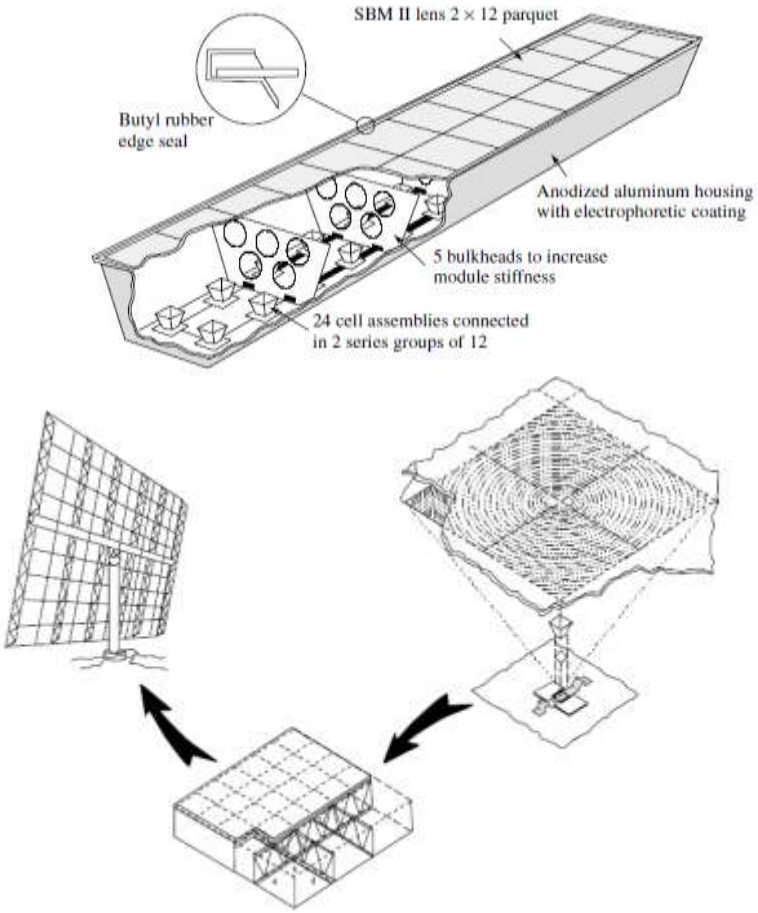

Fig 3.22 – *Concentrating system with Fresnel lenses.*

As seen in the figure above, there are usually also secondary optics systems to give a wider angle of tolerance of the received beam and make a "pre-concentration" of the radiation.

These are usually the "compound parabolic concentrators" that have a tolerance angle of about 30° and reflect the radiation to the bottom of the module where the Fresnel lens are, just in front of the PV cell.

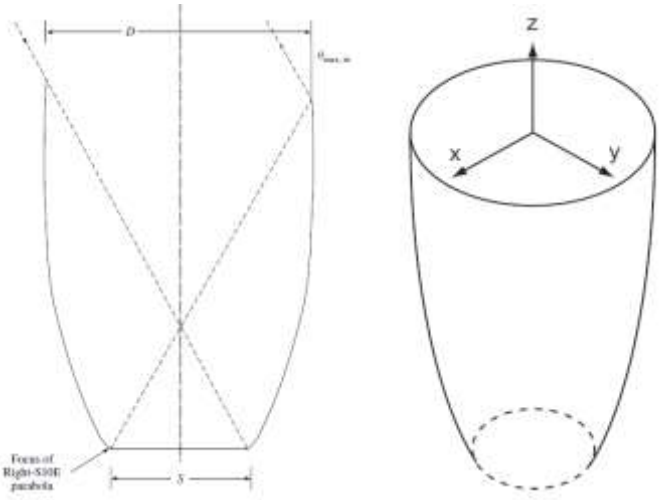

Fig 3.23 – *Compound parabolic concentrator (CPC) with* $\vartheta_{max} = 30°$.

3.2.2 *Tracking systems*

The sun tracker is the fundamental component to have always the direct radiation focused on the PV cell. Most of them are biaxial.

The most used is the pedestal sun-tracker: a plane surface tilted on a pole. An electric engine permits the vertical and horizontal rotations. The wind can create problems, so that all these systems should be positioned in protection position for high wind values.

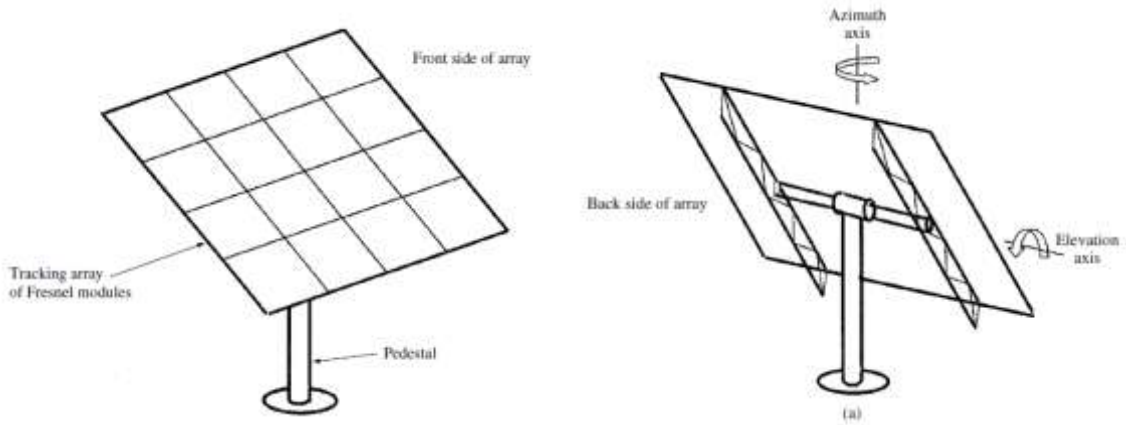

Fig 3.24 – *Pedestal biaxial sun--tracker.*

3.3 CONVERSION SYSTEMS

The energy produced by a photovoltaic cell is in direct current; the need of the loads is usually in alternate current. The inverters provide to solve the need of current conversion.

Usually the conversion is made after a string of a certain number of modules (as many to reach the activation tension of the inverter, but not too much to overload the conversion system).

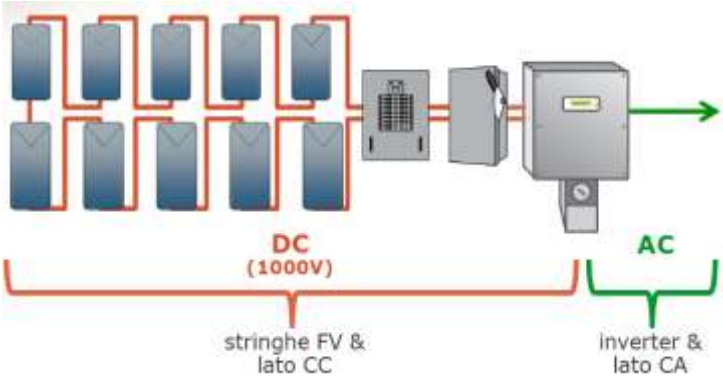

Fig 3.25 – *Traditional inverter conversion.*

In this thesis the research focuses on the new frontier of energy conversion: the micro-inverter.

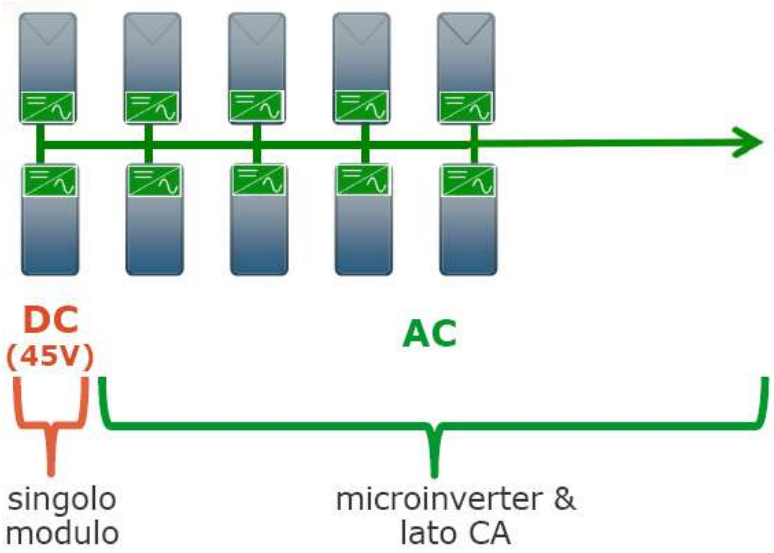

Fig 3.26 – *Micro-inverter conversion.*

Differently from the string inverter, the micro-inverters convert the current right after every single module, in order to have "alternate current PV modules".

There could be many advantages of using micro-inverters before talking of energy production:

- simplified system design;
- simplified installation procedures (no CC components, reduced cables quantity);
- reduced electric risks (low working tension, reduced voltaic arcs in CC);
- single module monitoring;
- reduced production stops (the failure of a module doesn't stop the production of the entire string);

The aim of this work is to analyze the compared production of installed PV systems with micro-inverter and string inverter in order to demonstrate/verify the main advantage of using micro-inverter systems: incremented performances and energy production (and so reduction of the payback time of the systems).

The two major reasons of incremented energy production are shown in the next two figures:

- reduced shading losses;
- flexibility of the design and use of small area roofs (not permitted by the minimal number of module per string needed by traditional inverters).

Fig 3.27-a – *Micro-inverter advantages against shadowing.*

Fig 3.27-b – *Micro-inverter advantages against minimal number of modules per string.*

3.4 THE PHOTOVOLTAIC MARKET

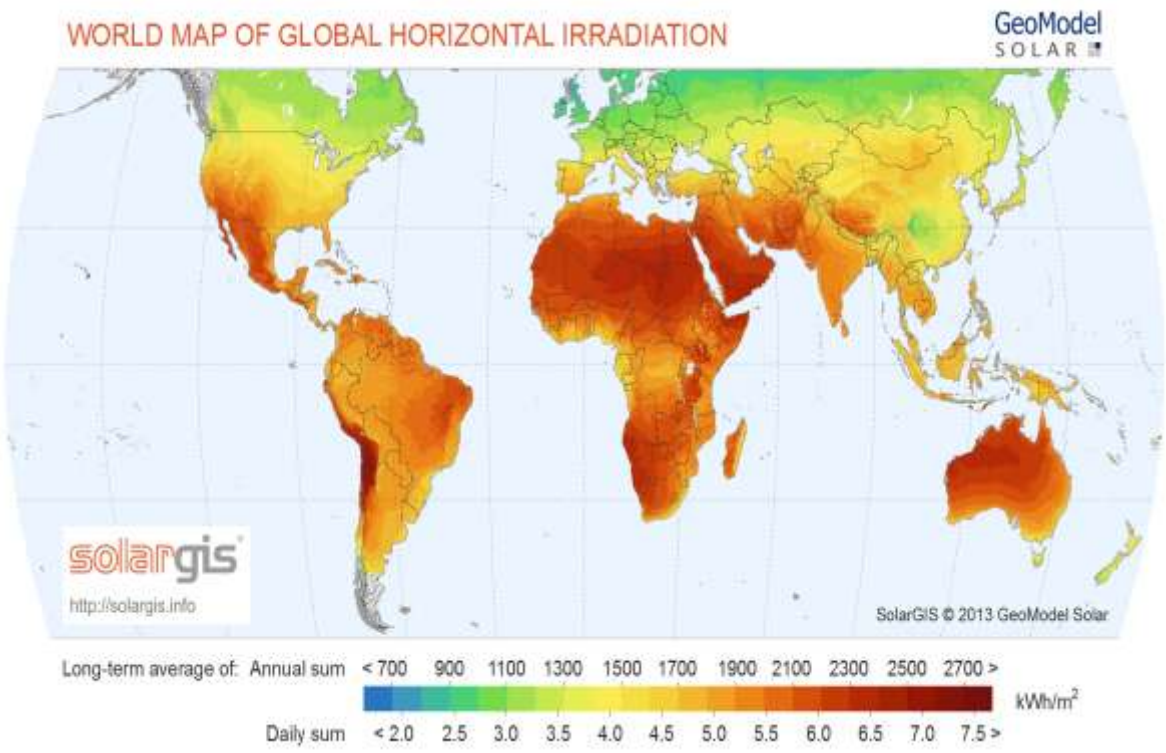

Fig 3.28 – *World solar irradiation.*

The photovoltaic business is one of the most emerging market nowadays, thanks also to the periodical crisis of oil market and the diffusion of environmental policies that pushes forward the renewable energy generation market.

The enormous potential of the solar irradiation all over the world helps the photovoltaic technology to be a worldwide diffused product.

During the years the production costs of the photovoltaic modules reduced so many that the "grid parity" is almost a reachable goal in many countries.

Every different PV technology has different efficiencies and costs (but even different possible applications: flexible modules, high efficiency modules for concentrating systems, standard modules). Each kind of module so may have a specific market segment.

A brief analysis has been made in order to understand the market of each kind of module. The costs analyzed are module costs, the final cost of the installation raises due to the system design, authorization, other materials and practical installation costs.

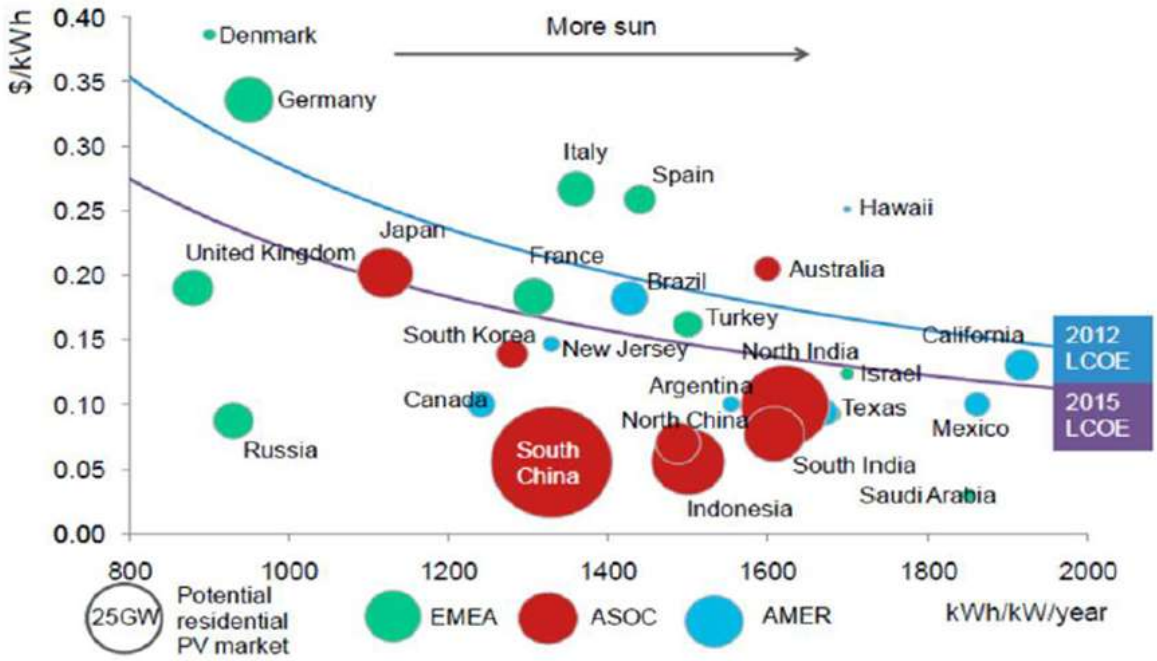

Fig. 3.29 – *Grid parity prediction. The higher is the electricity price and the Sun Irradiation, the closer is the goal line of grid parity.*

PV module	Efficiency %	2008 €/W_p	2009 €/W_p	2013 €/W_p
Monocrystalline Silicon	15,60	3,02	1,83	0,54
Polycrystalline Silicon	14, 94	2,8	1,97	0,46
CdTe	13,92	1,85	1,7	0,9
Amorphous Silicon	6,93	1,7	1,6	0,44

Tab. 3.4 – *Cost and efficiencies for different PV technologies [enfsolar.com]*

The efficiency is evaluated by the ratio between produced energy and received irradiation; to have the same energy production so different sizes and surfaces are needed for the different kinds of cell.

As seen the major system loss factors are due to the efficiency of the cell (quantum efficiency, cell transmission, couples recombination, band gap) and irradiation received (tilt angle, azimuth angle, weather condition, latitude, shadowing, soiling).

The estimated lifetime is about 80 years, but the ageing of the system cause is the cause of other losses in energy production during the years; the warranty is usually of 90% of the nominal power for the first 10 years, 80% for the first 25 years.

The disposal of the systems is so considered about 35-40 years after the first date of production.

Considering this it is possible to evaluate the value of the investment and so the payback time of the system not only "economical payback time", but also the "energy payback time" that is the time in which cumulated energy production of the system reaches the energy needed to produce the PV system.

For the different technologies is shown below the energy payback time in the city of Catania, whose site is characterized by a G of almost 1925 *kWh / m^2_{year}* and a DNI of 1794 *kWh / m^2_{year}*.

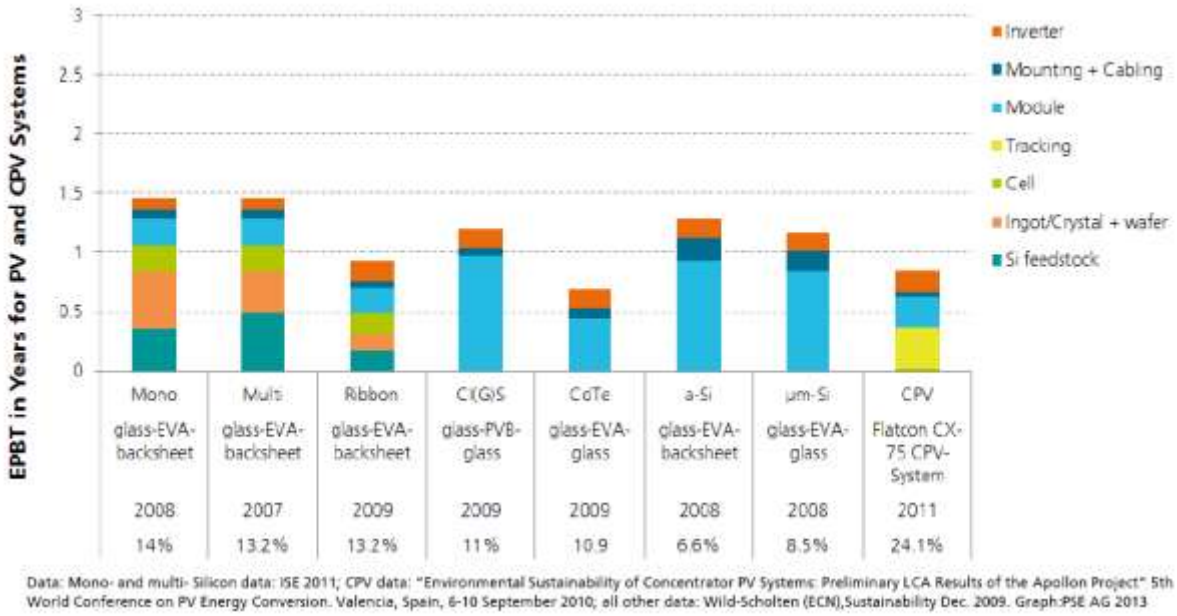

Fig. 3.30 – *Energy Payback Time in Catania for different PV technologies [Fraunhofer institute – Photovoltaic report 2013].*

3.4.1 *World market*

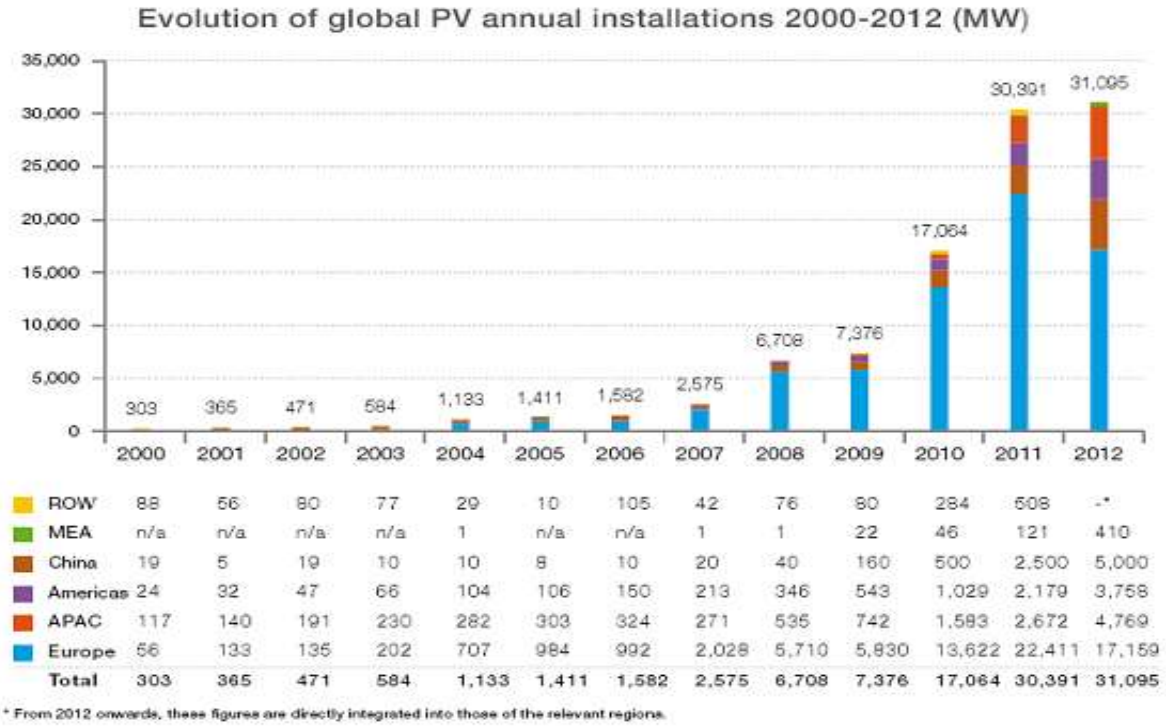

Fig. 3.31 –*European Photovoltaic Industry Association [Global Market Outlook for PV 2013/2017]*

The growth of the PV market in the last years shows clearly how Europe leads the cumulative installation and still leads also the annual installations.

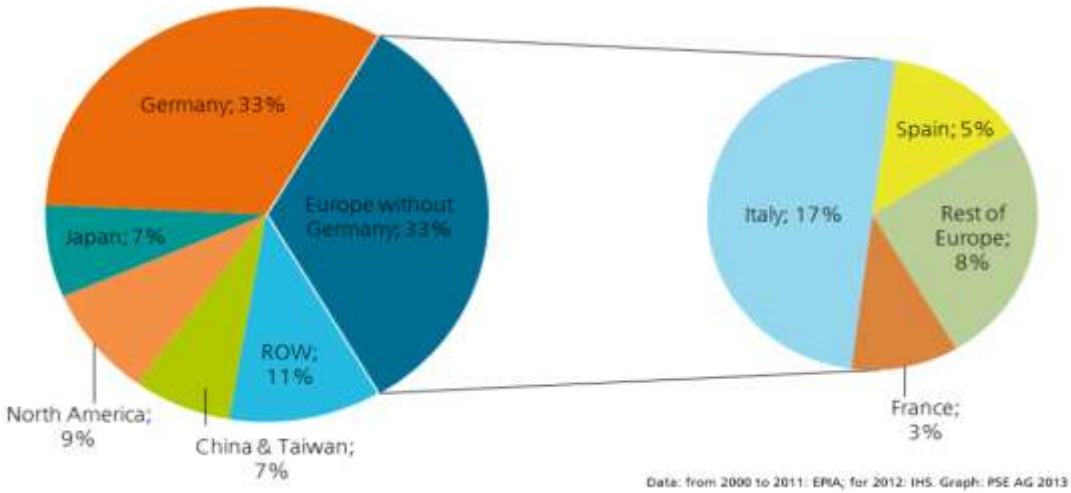

Fig. 3.32 – *European Photovoltaic Market [Global Market Outlook for PV 2013/2017]*

The "technology push" policies helped the Germany to be the market and production leader until now. While the policies in Italy have been "market pull", i.e. to help the consumers to buy the PV systems by paying for the PV energy generated sold to grid, the "technology push" is

the path followed in China, where the photovoltaic factories are "helped" by the government in production (doping the PV production market and letting the China modules to be during the last year the most sold all over the world).

The forecasts show comprehensible scenarios for the next years: the Australian, American (USA and South America) and Asian market (Japan, China and India) are the most suitable markets and is where the most of the installation will take place for the next future.

Undoubtedly China is going to be the next leader in PV market (modules production and installation) thanks to the enormous need of energy, the future need to avoid the pollution that is actually a real issue for Chinese population.

3.4.2 *Italian market*

In Italy the values of Global Irradiation are the highest in Europe similar to Spain and Greece. This helps Italy to be one of the most attractive nations to invest on PV technology.

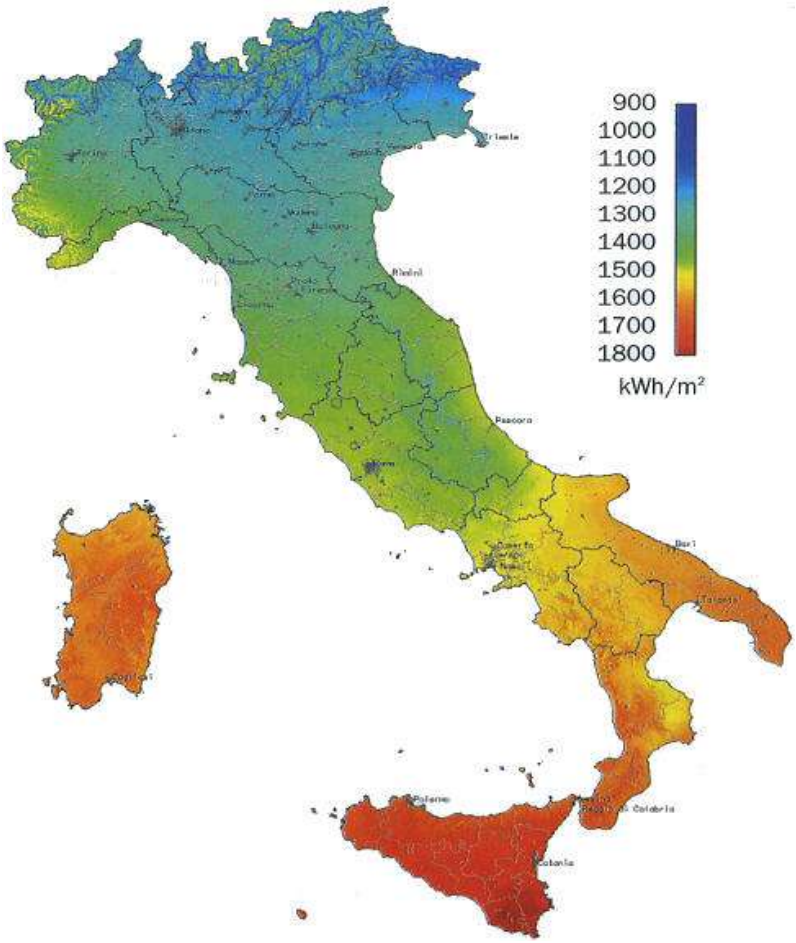

Fig. 3.33 – *Global Irradiation in Italy.*

At the end of 2012 in Italy there were 478.331 photovoltaic systems installed, for a cumulative power of 16,4 GW.

The production by PV systems reached the 23% of the renewable production (50% is still Hydroelectric power) with 18,8 TWh, for an amount equal to the 6,5% of the total production. This number is incredible considering that in 2010 this value was of only 1,9 TWh.

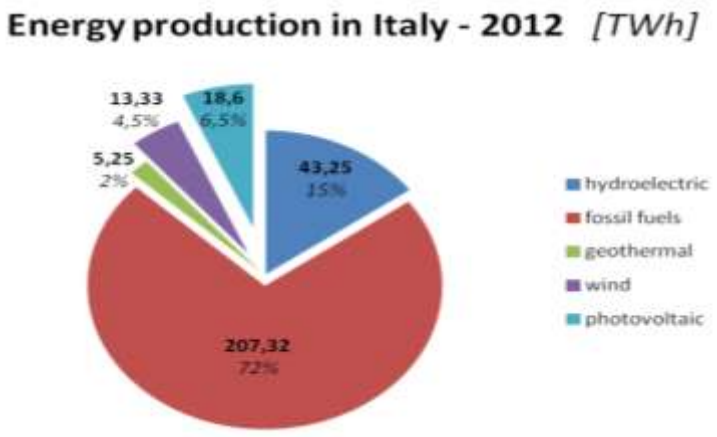

Fig. 3.34– *Italian energy production in 2012 [Terna report]*

In Italy the growth of the last years has been enormous thanks to the market pull policies that helped the diffusion of PV systems.

PV Energy Production in Italy	*2005*	*2006*	*2007*	*2008*	*2009*	*2010*	*2011*	*2012*
GWh	4	2,3	39	193	676,5	1.905	10.795	18.861

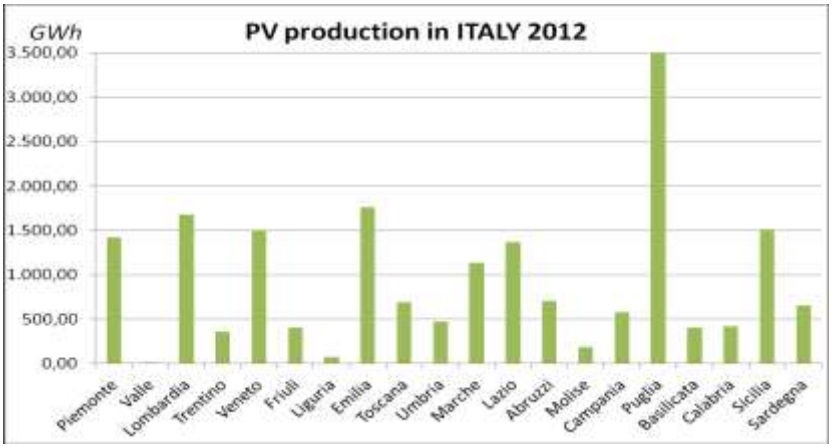

Fig. 3.35 – *Italian photovoltaic energy production in 2012*

In Puglia there is the highest concentration of systems, so that it is the region that leads the production. Surely Sicilia, Calabria and all the south regions are the most insulated and the most attractive for the PV market.

CHAPTER 4
EXPERIMENTAL EVALUATION OF THE TESTED PV SYSTEMS

4.1 SYSTEMS DESCRIPTIONS

A Data Acquisition Systems is provided for each system analyzed thanks to the "on board" technology that permits to measure the performance of the PV modules.

The string-inverter systems are provided with sensors of AC energy production and Instantaneous Power.

The micro-inverter systems have single module energy and power monitoring, so that is possible to evaluate the energy production of each module and so connect directly to the shading of the systems by analyzing the Energy Production connected to the layout of the systems and the position of the modules.

The radiation received is evaluated thanks to the PVgis software.

The data analyzed are so:

- the temperature of the sites: estimated by the UNI 8477-1 and simulated on the PVgis software;
- the GNI of the sites simulated on the PVgis software;
- the Energy Production of the systems: estimated during the design process of the systems; evaluated on the PVgis software; measured on site
- the shading percentage estimated during the design process and simulated on the Solergo software;
- the energy losses: evaluated on the PVgis software; estimated during the design process;
- the instantaneous power measured on site.

All the systems analyzed are installed in Sicily – Italy.

The medium GNI is about 1900 [kWh/m^2]$_{year}$. All of them are building integrated systems installed on roofs, so the tilt and azimuth angles are fixed.

The difference in Irradiation Received is not that high, as it is possible to notice by comparing the values of the Reference Yield of the system analyzed (in a range from 4,9 to 5,6 [h]); so the comparison among the system could have been done just by using the Array Yield values.

However by using the Reference Yield values it is possible to compare the best azimuth/tilt/location conditions (that are quite dissimilar in the different installations); in order to evaluate at best the performances so the PR has been used.

4.2 CENTRAL INVERTER SYSTEMS

4.2.1 CENTRAL INVERTER SYSTEM -1

The first Central inverter system analyzed is placed in "Fiumefreddo di Sicilia" on a roof with a tilt angle of 25° and an azimuth angle of 7°; it has a peak power of about 2,86 kW.

Fig.4.1-a – *Central inverter System 1*

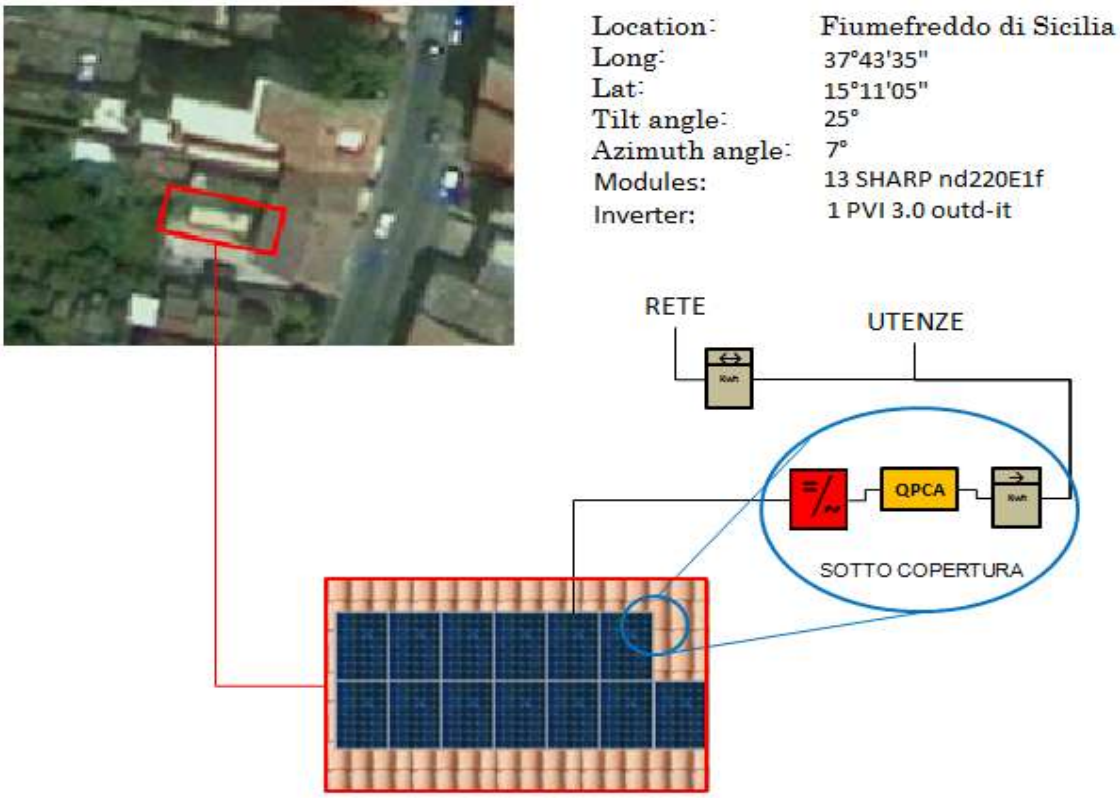

Fig.4.1-b – *Central inverter System 1*

Fig.4.1-c – *Central inverter System 1*

It is made with 13 polycrystalline Silicon modules with a mean efficiency of 13,4%.

There are not any obstacles that can shadow the area.

The electric scheme of the system is showed in the graph below: it is possible to notice the inverter on which the two strings of the systems converge for the current modulation.

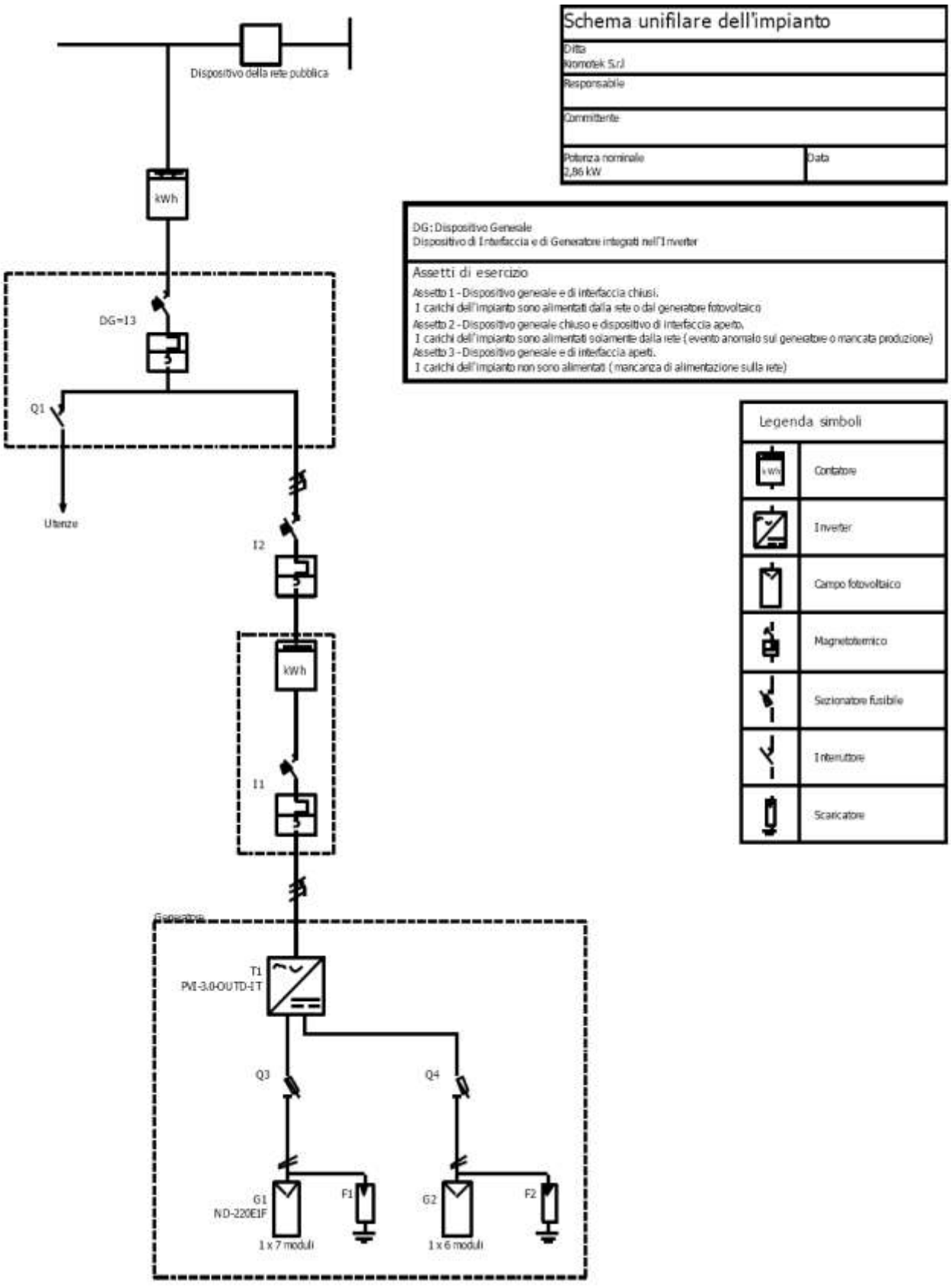

Fig.4.2 – *Central inverter System 1- Electric scheme*

The system has the following characteristics:

SYSTEM 1 *(GIUSA)*		**INVERTER**	
Peak power of the system	2860 W	***Number of inverters***	1 (PowerOne PVI outd)
Azimuth angle	7° (South – West)	P_o	3 kW
Tilt angle	25°	P_{max}	3,43 kW
Shadowing percentage	0 %	$P_{MPPTmax}$	2 kW
Location	Fiumefreddo (CT) *Long.* 37°43'35'' *Lat.* 15°11'05''	V_o	360 V
		V_{max}	600 V
MODULES		$V_{MPPTmin}$	90 V
Material	Poly-Si *(SHARP ND-220e)*	$V_{MPPTmax}$	580 V
Efficiency	13,4 %	V_1	231 V
P_{max}	220 W	I_o	20 A
V_n	29,2 V	I_{max}	20 A
V_o	36,5 V	$I_{MPPTmax}$	10 A
I_n	7,5 A	***Efficiency***	96 %
I_o	8,2 A	V_{MPP} **(STC)**	379,6 V
Number of modules	13	***Total modules Area***	20,8 m²

4.2.2 CENTRAL INVERTER SYSTEM-2

The second Central inverter system analyzed has a peak power of about 5,98 kW.

Fig.4.3-a – *Central inverter System 2*

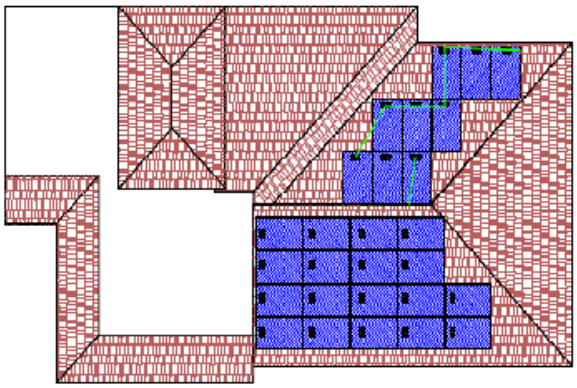

Location:	Modica (Sr)
Long:	36°51'47"
Lat:	14°45'37"
Tilt angle:	22
Azimuth angle:	-90° / +90°
Modules:	20 P LDK 220-P20
Inverter:	PV 6000 outd-it

Fig.4.3-b – *Central inverter System 2*

The system has the following characteristics:

SYSTEM 2 *(CANNATA)*		**INVERTER**	
Peak power of the system	5940 W	***Number of inverters***	1 (PowerOne 6000 outd-it)
Azimuth angle	-90° / +90° (East - West)	P_o	6 kW
Tilt angle	22°	P_{max}	6,2 kW
Shadowing percentage	0 %	$P_{MPPTmax}$	4 kW
Location	Modica (SR) *Long.* 36°51'47'' *Lat.* 14°45'37''	V_o	360 V
		V_{max}	600 V
MODULES		$V_{MPPTmin}$	84 V
Material	Poly-Si (Idk p20)	$V_{MPPTmax}$	580 V
Efficiency	13,5 %	V_1	231 V
P_{max}	220 W	I_o	36 A
V_n	29,8 V	I_{max}	36 A
V_o	36,5 V	$I_{MPPTmax}$	18 A
I_n	7,4 A	***Efficiency***	96 %
I_o	8,1 A	V_{MPP} ***(STC)***	387.4 V
Number of modules	27	***Total modules Area***	43,2 m²

The system is orientated East and West (two different orientations for the two strings) with a tilt angle of 22 degrees. There are not any obstacles that can shadow the area.

4.3 MICRO INVERTER SYSTEMS

4.3.1 MICRO-INVERTER SYSTEM - 1

The first micro inverter system analyzed has a peak power of about 3,00 kW.

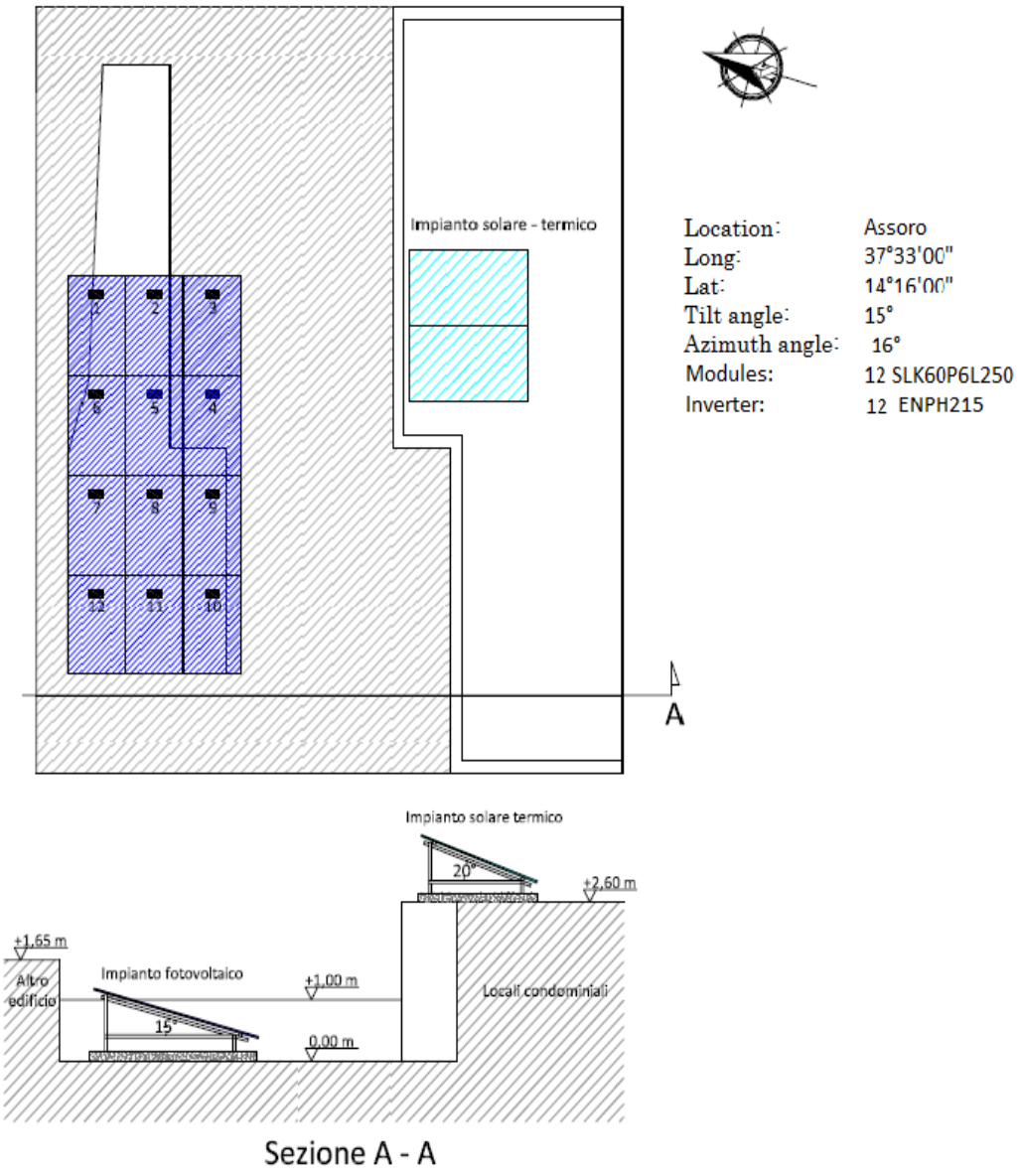

Fig.4.4-a – *Micro inverter System 1*

Fig.4.4-b – *Micro inverter System 1*

The system is orientated South-East with a tilt angle of 15 degrees. There are some obstacles that can shadow the area. An evaluation of the average shadow percentage during the year has given a value of 9,4 %.

The system has the following characteristics:

SYSTEM 3 *(BELINTENDE)*		**INVERTER**	
Peak power of the system	3000 W	***Number of inverters***	12 (Enphase 215)
Azimuth angle	-16° (South – East)	P_o	0,2 kW
Tilt angle	15° (supports)	P_{max}	0,3 kW
Shadowing percentage	9,4 %	$P_{MPPTmax}$	0,3 kW
Location	Assoro (EN) *Long.* 37°33'00'' *Lat.* 14°16'00''	V_o	29 V
		V_{max}	45 V
MODULES		$V_{MPPTmin}$	22 V
Material	Poly-Si (Siliken 250 6op)	$V_{MPPTmax}$	36 V
Efficiency	14,8 %	V_1	231 V
P_{max}	250 W	I_o	10,5 A
V_n	29,8 V	I_{max}	15 A
V_o	37,1 V	$I_{MPPTmax}$	15 A
I_n	8,4 V	***Efficiency***	95 %
I_o	8,9 V	V_{MPP} ***(STC)***	30,7 V
Number of modules	12	***Total modules Area***	19,48 m²

Fig.4.4-c – *Micro inverter System 1*

4.3.2 MICRO-INVERTER SYSTEM - 2

The second micro inverter system analyzed has a peak power of about 3,00 kW.

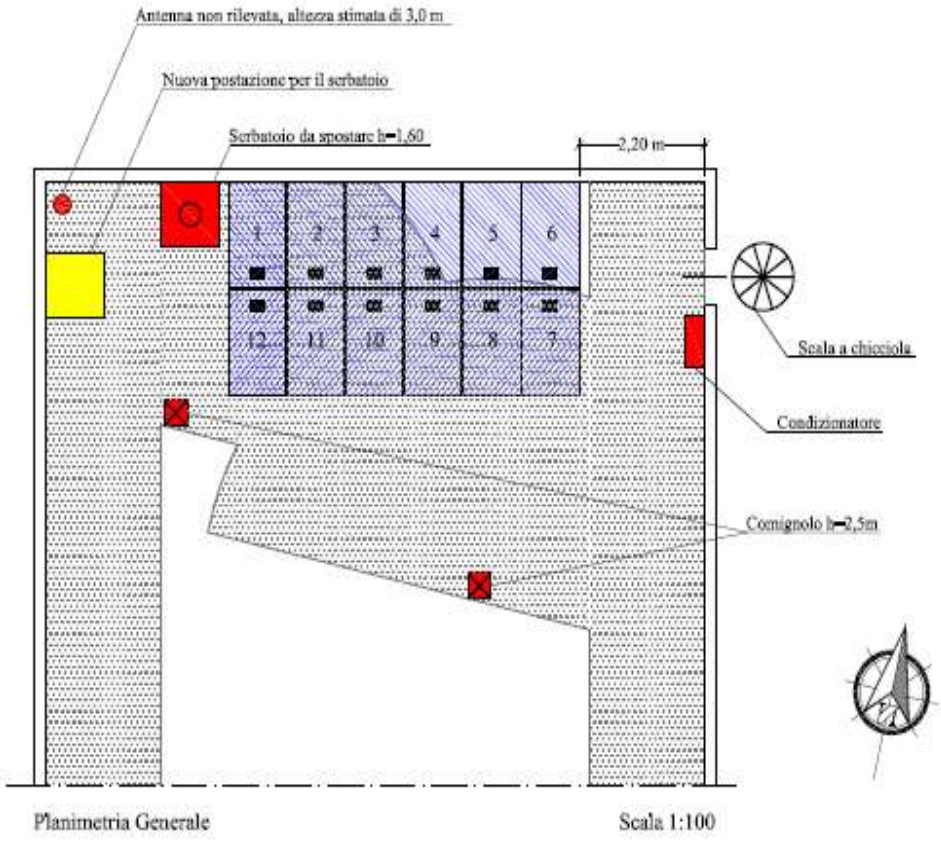

Fig.4.5-a – *Micro inverter System 2*

Fig.4.5-b – *Micro inverter System 2*

Fig.4.5-c – *Micro inverter System 2*

Fig.4.5-d – *Micro inverter System 2*

The system is orientated South-East with a tilt angle of 17 degrees. There are some obstacles that can shadow the area. An evaluation of the average shadow percentage during the year has given a value of 12%.

The system has the following characteristics:

SYSTEM 4 *(CORDESCHI)*		**INVERTER**	
Peak power of the system	3000 W	***Number of inverters***	12 (Enphase 215)
Azimuth angle	-13° (South – East)	P_o	0,2 kW
Tilt angle	17°	P_{max}	0,3 kW
Shadowing percentage	12 %	$P_{MPPTmax}$	0,3 kW
Location	Noto (SR) *Long.* 36°53'32'' *Lat.* 15°03'54''	V_o	29 V
		V_{max}	45 V
MODULES		$V_{MPPTmin}$	22 V
Material	Poly-Si (Siliken 250 6op)	$V_{MPPTmax}$	36 V
Efficiency	14,8 %	V_1	231 V
P_{max}	250 W	I_o	10,5 A
V_n	29,8 V	I_{max}	15 A
V_o	37,1 V	$I_{MPPTmax}$	15 A
I_n	8,4 V	***Efficiency***	95 %
I_o	8,9 V	V_{MPP} ***(STC)***	30,7 V
Number of modules	12	***Total modules Area***	19,48 m²

4.3.3 MICRO-INVERTER SYSTEM - 3

The third micro inverter system analyzed has a peak power of about 2,88 kW.

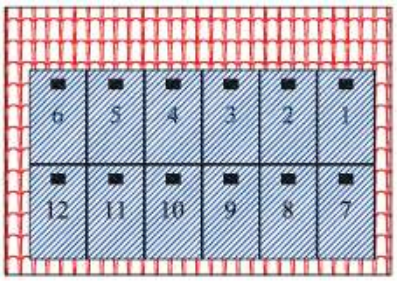

Fig.4.6-a – *Micro inverter System 3*

Fig.4.6-b – *Micro inverter System 3*

The system is orientated South-East with a tilt angle of 51 degrees. There are not obstacles that can shadow the area.

The system has the following characteristics:

SYSTEM 5 *(DI FRANCO)*		**INVERTER**	
Peak power of the system	2880 W	***Number of inverters***	12 (Enphase 215)
Azimuth angle	-51° (South – East)	P_o	0,2 kW
Tilt angle	12°	P_{max}	0,3 kW
Shadowing percentage	0 %	$P_{MPPTmax}$	0,3 kW
Location	Calascibetta (EN) *Long.* 37°35'22'' N *Lat.* 14°16'13'' E	V_o	29 V
		V_{max}	45 V
MODULES		$V_{MPPTmin}$	22 V
Material	Poly-Si (Siliken 240 R1J)	$V_{MPPTmax}$	36 V
Efficiency	14,0 %	V_1	231 V
P_{max}	240 W	I_o	10,5 A
V_n	30,7 V	I_{max}	15 A
V_o	37,4 V	$I_{MPPTmax}$	15 A
I_n	7,9 V	***Efficiency***	95 %
I_o	8,6 V	V_{MPP} ***(STC)***	30,7 V
Number of modules	12	***Total modules Area***	19,48 m²

Fig.4.6-c – *Micro inverter System 3*

4.3.4 MICRO-INVERTER SYSTEM - 4

The fourth micro inverter system analyzed has a peak power of about 2,94 kW.

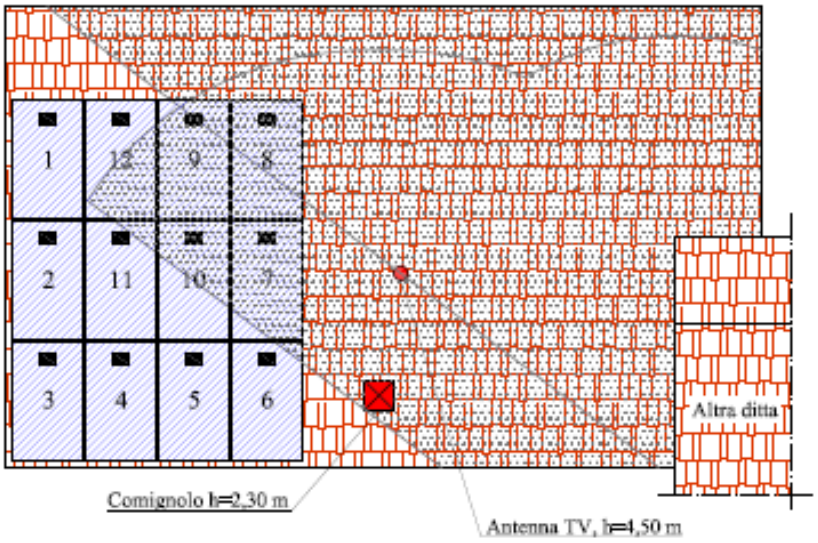

Fig.4.7-a – *Micro inverter System 4*

Fig.4.7-b – *Micro inverter System 4*

The system is orientated South-East with a tilt angle of 37 degrees. There are some obstacles that can shadow the area. An evaluation of the average shadow percentage during the year has given a value of 5,4 %.

The system has the following characteristics:

SYSTEM 6 *(MAGAGNINI)*		**INVERTER**	
Peak power of the system	2940 W	***Number of inverters***	12 (Enphase 215)
Azimuth angle	-37° (South – East)	P_o	0,2 kW
Tilt angle	17°	P_{max}	0,3 kW
Shadowing percentage	5,4 %	$P_{MPPTmax}$	0,3 kW
Location	Valverde (CT) *Long.* 37°34'49'' N *Lat.* 15°05'40'' E	V_o	29 V
		V_{max}	45 V
MODULES		$V_{MPPTmin}$	22 V
Material	Poly-Si (Sharp ND-R245)	$V_{MPPTmax}$	36 V
Efficiency	14,9 %	V_1	231 V
P_{max}	245 W	I_o	10,5 A
V_n	30,7 V	I_{max}	15 A
V_o	37,4 V	$I_{MPPTmax}$	15 A
I_n	8 V	***Efficiency***	95 %
I_o	8,6 V	V_{MPP} ***(STC)***	30,7 V
Number of modules	12	***Total modules Area***	19,48 m²

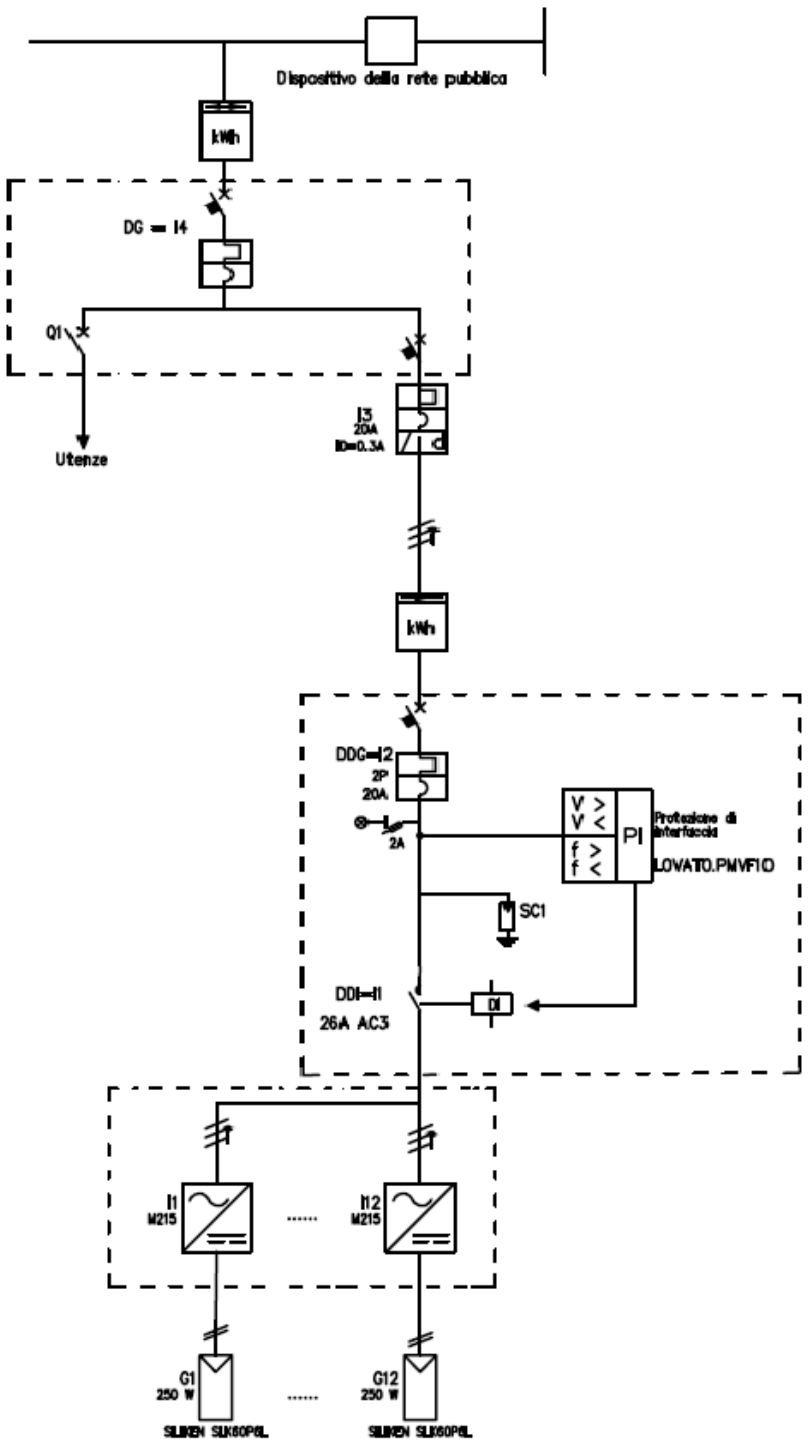

Legenda simboli	
	Contatore bidirezionale
	Contattore unidirezionale
	Inverter
	Campo fotovoltaico
	Magnetotermico
	Magnetotermico–Differenziale
	Sezionatore fusibile
	Interruttore
	Scaricatore
	Contattore

DG: Dispositivo Generale
DDI: Dispositivo di Interfaccia

Assetti di esercizio

Assetto 1 – Dispositivo generale e di interfaccia chiusi.
I carichi dell'impianto sono alimentati dalla rete o dal generatore fotovoltaico

Assetto 2 – Dispositivo generale chiuso e dispositivo di interfaccia aperto.
I carichi dell'impianto sono alimentati solamente dalla rete (evento anomalo sul generatore o mancata produzione)

Assetto 3 – Dispositivo generale e di interfaccia aperti.
I carichi dell'impianto non sono alimentati (mancanza di alimentazione sulla rete)

Schema unifilare dell'impianto

Ditta
KROMOTEK S.R.L.

Responsabile

Committente

Potenza nominale
3kW

Data

CHAPTER 5

DATA ANALYSIS

A whole year analysis has been conducted for all the six systems.

To analyze the performances the indexes showed in chapter 2.4 have been used.

In order to have comparable values of measured and calculated energy production, by the simulation with the PVgis software the following energy conversion losses from the sun beams have been estimated for each system:

- Losses due to temperature and low irradiance (using local ambient temperature)
- Losses due to angular reflectance effects
- Other losses (cables, inverter etc.)
- Combined PV system losses

The thermal losses are related with the cell temperature or the ambient temperature as follows:

$$P_{tpv} = \{T_{cell} - 25\} * \gamma / 100$$

where:

- **γ**: power temperature coefficient (for silicon modules is 0,4÷0,5 %/°C).
- **NOCT**: Nominal operating cell temperature (usually 40÷50°C).
- **T_{atm}**: atmospheric temperature
- **T_{cell}**: is the temperature of the PV module = $[T_{atm} + (NOCT - 20) * I / 800]$

The energy production of the system is given by the relation from the UNI 8477-1:

$$E = P \times Irr / 1000 \times (1\text{-}Disp) \quad [kWh/year]$$

where:

- **P** is the peak power of the system [kW];
- **Irr** is the average year global irradiation per square meter received by the modules [kWh / m^2]
- **Disp** is the percentage of energy losses

The energy E has been evaluated in four different ways:

- Using the value of ***Disp_estimated*** during the design of the systems and the value of ***Irr from the UNI 10349***;
- Using the value of ***Disp_estimated*** during the design and the ***Irr_real***.
- Using the value of ***Disp_evaluated*** through the PVgis software and the ***Irr_real***.
- Using the value of ***measured Energy Production***;

where:

- *H = Irr* is taken from the UNI
- *H_real = Irr_real* is taken from the PVgis
- *Disp* are the power losses estimated during project:
    - Shading
    - Temperature
    - Mismatching
    - Direct current
    - Soiling, Cables, Misc.
    - Conversion

The values of irradiation received by the systems have been evaluated by using the PVgis software at the different latitudes of the sites (*H_real*).

Each micro-inverter has a peak power of 215 W: this means that connected to a 250 W module, the maximum power cannot overcome the value of 215 W.

To avoid this limitation in evaluating the performances an "enhanced" approach for the micro-inverter systems has been used: the evaluation of the Energy Yield *Yf* has been made on a maximum power of 2,58 kW, that is the maximum power reachable by the micro-inverters.

So three different values have been found for the calculation of the PR:

- **PR_estimated** by using the values of energy production estimated by the PVgis software;
- **PR_real** by using the real values of energy production from the systems measured on site;
- **PR_enhanced** by using for the micro-inverter systems an enhanced value of energy yield *Yf* by using a peak power of 2,58 kW, the maximum that can be used by the 12 micro-inverter of the systems.

The values of **losses evaluated** from the PVgis for the 6 different systems are:

LOSSES	*Central 1*	*Central 2*	*Micro 1*	*Micro 2*	*Micro 3*	*Micro 4*
Temperature Low Irradiance	15,5 %	14,4 %	14,8 %	15,5 %	15,6 %	10,0 %
Angular Reflectance Effects	2,6 %	3,3 %	2,7 %	2,8 %	2,0 %	3,0 %
Cables, Inverter, Misc.	5,4 %	0 %	9,5 %	5,3 %	6,0 %	6,6 %
TOTAL	**23,5 %**	**17,7 %**	**27,0 %**	**23,6 %**	**23,6 %**	**19,6 %**

A little difference has been found with the **losses estimated** with the designing software Solergo:

LOSSES	*Central 1*	*Central 2*	*Micro 1*	*Micro 2*	*Micro 3*	*Micro 4*
Shading	0,00 %	0,00 %	9,70 %	12,10 %	0,00 %	5,20 %
Temperature	9,46 %	7,74 %	6,30 %	7,70 %	7,20 %	8,90 %
Mismatching	5,00 %	5,00 %	5,00 %	5,00 %	5,00 %	5,00 %
Direct current	1,50 %	1,50 %	1,50 %	1,50 %	1,50 %	1,50 %
Other losses (soiling, cables,..)	2,77 %	3,10 %	1,10 %	0,30 %	3,00 %	1,50 %
Conversion losses	4,00 %	3,60 %	4,60 %	4,60 %	4,60 %	4,60 %
TOTAL	**22,73 %**	**20,94 %**	**28,20 %**	**31,20 %**	**21,30 %**	**26,70 %**

The Energy values found have been so:

ENERGY PRODUCED *[kWh / year]*	*Central 1*	*Central 2*	*Micro 1*	*Micro 2*	*Micro 3*	*Micro 4*
E1 $Irr_{\_UNI}$ kWh/m² $Disp_{\_estimated}$	4367,3 *1976,2* *22,73 %*	9370 *1995,2* *20,94 %*	4280,6 *1988,08* *28,20 %*	4089,3 *1981,7* *31,20 %*	4351,1 *1981,91* *21,20 %*	4178,8 *1940,4* *21,20 %*
E2 $Irr_{\_real}$ kWh/m² $Disp_{\_estimated}$	4324,84 *1957,00* *22,73 %*	8413,37 *1791,5* *20,94 %*	4181,33 *1941,20* *28,20 %*	4230,12 *2049,5* *31,20 %*	4218,99 *1853,9* *21,20 %*	4268,98 *1980,79* *21,20 %*
E3 $Irr_{\_real}$ kWh/m² $Disp_{\_evaluated\text{-}PVgis}$	4281,74 *1957,00* *23,50 %*	8758,16 *1791,5* *17,70 %*	4251,21 *1988,08* *27,00 %*	4697,39 *2049,5* *23,60 %*	4090,50 *1853,9* *23,60 %*	4681,98 *1980,79* *23,60 %*
E4 *measured*	4263,81	8713,49	4231,87	4673,83	4291,73	4452,17

The values of the PR are showed in the tab and the graphs below:

	PR estimated *H_real* *Yf_ PVgis*	**PR real** *H _real* *Yf_measured*	**PR enhanced** *H_real* *Yf_measured (string)* *Yf_enhanced (micro)*
GIUSA *fiumefreddo (CT)*	**0,770**	**0,700**	**0,700**
CANNATA *modica (SR)*	**0,830**	**0,840**	**0,840**
BELINTENDE *assoro (EN)*	**0,736**	**0,731**	**0,850**
CORDESCHI *noto (SR)*	**0,769**	**0,770**	**0,899**
DI FRANCO *calascibetta (EN)*	**0,810**	**0,775**	**0,865**
MAGAGNINI *valverde (CT)*	**0,772**	**0,786**	**0,904**

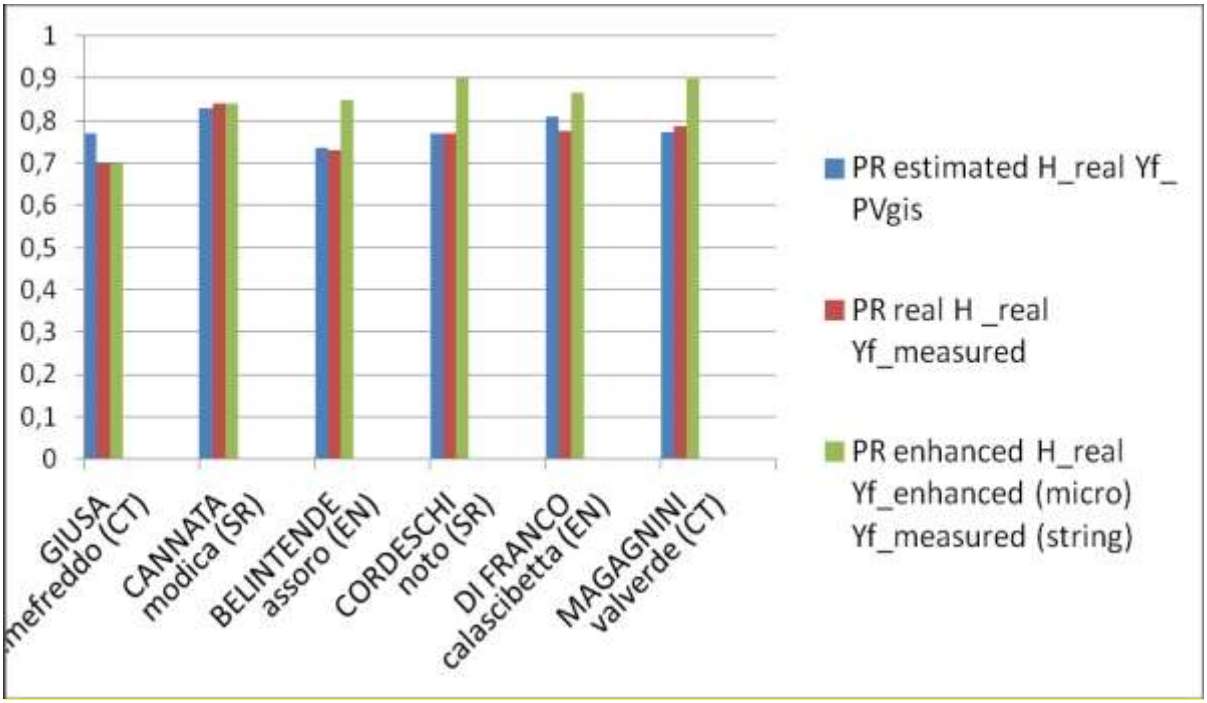

Fig.5.1 – *PR confrontation*

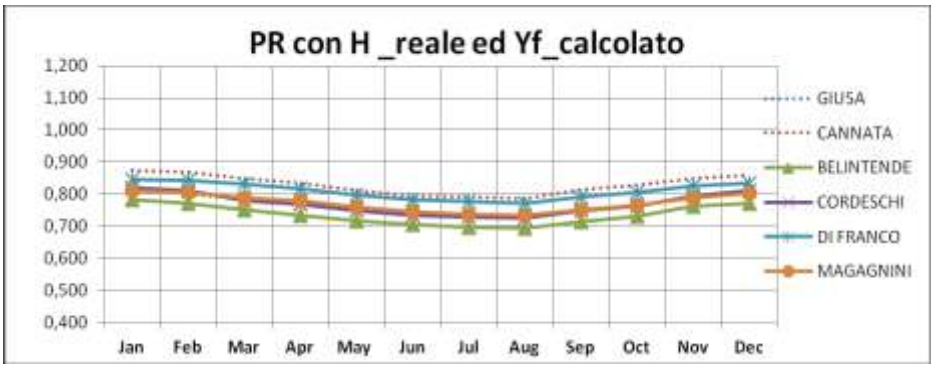

Fig.5.2-a – *PR_estimated with the PVgis values of Irradiation H and the predicted Energy Production in the Yf_calculated*

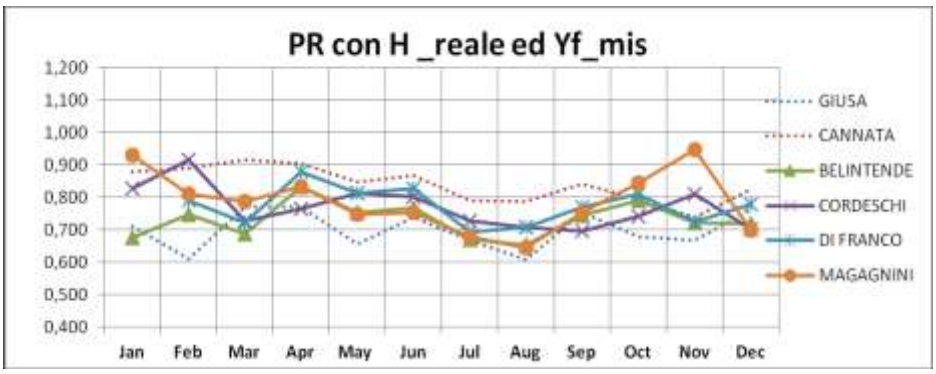

Fig.5.2-b – *PR_real with the real PVgis values of Irradiation H and the measured Energy Production in the Yf_measured*

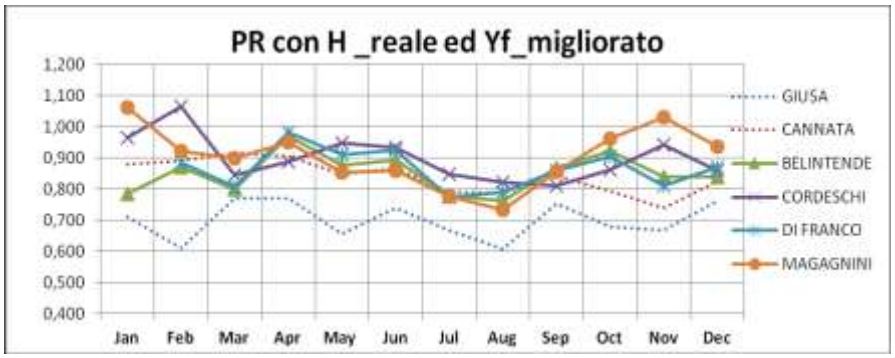

Fig.5.2-c – *PR_enhanced with the real PVgis values of Irradiation H and the enhanced values of Energy Production in the Yf_enhanced by the ratio with the maximum microinverter peak power*

The *PR_estimated* have been evaluated by using the project data in the PVgis software and were a prediction of how the systems should have worked.

The *PR_real* have been evaluated by using the measured data from the systems.

The *PR_enhanced* have been evaluated by using a different value of peak power of the micro-inverter systems: the maximum output power that every single microinverter can give is 215 W. By evaluating the energy yields with a "reduced" peak power of 2,58 kW instead that 3 kW it has been calculated the value of the maximum performance ratio of the micro-inverter systems.

CHAPTER 6

CONCLUSIONS

A whole year analysis has been conducted for all the six systems.

By taking a *mean* between the two string inverter systems as the *reference*, a comparison has been made among all the systems to understand the performances showed during the evaluation time.

By watching the *enhanced* performances of the micro-inverter systems it is clear that the energy produced per peak power has been higher than the string inverter.

Studying the *real* production only one micro inverter worked worse than the second string inverter (even if more than 9% of the surface was shadowed during the year).

	Energy produced *kWh/year*	**Yf comparison with the reference value = 3.925** (mean between the string systems)
GIUSA *fiumefreddo (CT)*	*4263,81*	*no shadow*
Yf_real	**3,73**	**95%** (-5% than the reference)
Yf_enhanced	**-**	
CANNATA *modica (SR)*	*8713,49*	*no shadow*
Yf_real	**4,12**	**105%** (+5% than the reference)
Yf_enhanced	**-**	
BELINTENDE *assoro (EN)*	*4231,87*	*9.4% shadow*
Yf_real	**3,88**	**98,8%** (-1,2% than the reference)
Yf_enhanced	**4,52**	**115%** (+15% than the reference)
CORDESCHI *noto (SR)*	*4673,83*	*12% shadow*
Yf_real	**4,30**	**109,5%** (+9.5% than the reference)
Yf_enhanced	**5,01**	**127,6%** (+27,6% than the reference)
DI FRANCO *calascibetta (EN)*	*4291,73*	*no shadow*
Yf_real	**4,11**	**104,7%** (+4,7% than the reference)
Yf_enhanced	**4,58**	**116,6%** (+16,6% than the reference)
MAGAGNINI *valverde (CT)*	*4452,17*	*5.4% shadow*
Yf_real	**4,17**	**106,2%** (+6,2% than the reference)
Yf_enhanced	**4,77**	**121,5%** (+21,5% than the reference)

With a mean shading percentage on micro-inverter systems of 6,7%, the energy production per peak power *Yf* have been higher than 4,8% on real analysis, than 20,17% on enhanced analysis.

The enhanced analysis showed a failure by the evaluation of values of PR > 1 for 3 over 48 evaluation points.

Nevertheless it is a way to consider that in a system correctly sized, just for purely technical reasons and not for economical evaluations, in which the peak power of the microinverter and of the PV modules matches perfectly, the power production will be higher than the one measured with the unmatched systems analyzed, enhancing the +4,8% evaluated in the real production analysis to an higher value for sure closer to the 20,17% founded by this method.

An economic analysis of the microinverter investment has also been realized.

Cost in Euros €	*String inverter*	*Micro inverter*
Modules	2100	2100
Inverter	*850*	*1950*
Electric material CC+CA	*350*	*240*
Installation costs	1200	1200
Project designing	800	800
Marketing, taxes, sales crew, etc…	700	700
TOTAL €	**6000**	**6990**
	+ Euro €	*990*
	+ %	*16.50%*
generated kWh price (in Italy) *€/kWh*	0.20	
mean ***shading*** percentage	0%	6.7%
mean **Yf *[h]***	3.925	3.925 **+ 4.8%** = 4.113
mean Energy for 3 kWp ***[kWh]***	11775	12340.200
Energy surplus ***[kWh/year]***	-	565.200
economic surplus ***€/year***	-	113.04
payback time surplus ***(years)***	-	**8.75**
mean value of **enhanced Yf *[h]***	3.925	3.925 **+ 20.17%** = 4.72
mean Energy for 3 kWp ***[kWh]***	11775	14150.017
Energy surplus ***[kWh/year]***		2375.017
economic surplus ***€/year***		475.00
payback time surplus ***(years)***		**2.08**

The analysis shows that the microinverter system mean cost is higher up to 16.5% over the total string inverter system cost, due to the multiple number of inverters.

Though the cost is higher, the energy production is higher too: up to 4,8% for the real analysis, up to 20,17% on the enhanced one.

At the end it means from 2 to 8 years to recover the higher investment cost for the microinverter systems.

If we consider a lifetime up to 25 years it means that for at least 17 years the microinverter systems will have an higher refund than the central inverter ones.

A different scenario has been created by the comparison among different kind of roofs.

The string inverter systems need a roof of a certain area that can contain at least 5 or 6 modules (990 mm * 1640 mm * 6 modules is almost 10 m^2) (in order to reach the V_0 of the inverter to start converting from DC to AC).

The micro-inverter systems can be installed module by module, giving so much more options on utilizable roofs and size of the systems.

A percentage of contracts rejected due to massive shading or inappropriate roofs has been made during a 3 years study by the Kromotek S.r.l. before the introduction of micro-inverter systems on the PV market.

About 57% of possible contracts for a peak power from 3 to 6 kW have been refused due to these causes.

This means that the possible energy produced could have been at least 57% higher than the energy produced during these 3 years.

Making a world energy production analysis, it is possible to fill the tables with these numbers and compare the energy production of string and micro inverter systems.

Making a reference to the mean energy production of the string inverter systems analyzed during the study it is possible to say that by using a micro-inverter system the energy production would raise from:

- +4,8% to +20,17% not considering the shadows;
- +61,8 to +77,17% considering also the roofs that could have been used for the production.

These results show the enormous potential of micro-inverter systems for raising the energy production by having an higher energy production using the same area, or much more than this by having the opportunity of using many other areas not utilizable with the traditional systems.

NOMENCLATURE

E	*kWh*	Energy
m	*kg*	Mass
c	*m/s*	Speed of light
e^-		Positron
γ		Photon
ν_e		Neutrino
H		Hydrogen
He		Helium
ΔV	*V*	Voltage delta
ΔT	*°C*	Temperature delta
N		Number of thermocouples
α		Coefficient
I_{diff}	*kWh/m²*	Scattered Irradiation
I_{glob}	*kWh/m²*	Global Irradiation
I_{norm}	*kWh/m²*	Normal Irradiation
θ_z	°	Incidence angle
υ	*m/s*	Wind speed
ω	*°/s*	Angular velocity
υ_o	*m/s*	Initial threshold
V_u	*V*	Voltage output
a		Angular coefficient
V	*V*	Voltage
R	*Ω*	Resistance
R_o	*Ω*	Threshold resistance
A,B,C		Constants of Callendar-van Dusen
t	*°C*	Temperature
$E_$	*J*	Photon energy
	m	Wavelength
h		Plank's constant
I_{ph}	*A*	Current generated by the photons
k		Constant of the kind of cell
A	*m^2*	Cell's surface
G		Irradiance
I_j	*A*	Recombination current
I_o	*A*	Junction reverse current
U_j	*V*	Junction voltage
V_j	*V*	Junction voltage
q	*eV*	Electron charge
K		Boltzmann's constant
T	*K*	Junction temperature
m		Junction coefficient

R_{sh}	Ω	Shunt resistance
R_s	Ω	Series resistance
I_{sh}	A	Shunt current
R_s	Ω	Emitter resistance
R_b	Ω	Resistance of the base
R_{fc}	Ω	Front contact resistance
R_{bc}	Ω	Back contact resistance
R_f	Ω	Finger contact resistance
R_{bb}	Ω	Collecting busbar resistance
U_{oc}	V	Open circuit Voltage
I_{sc}	A	Short circuit current
P_{id}	kW	Ideal Power
P_{max}	kW	Max Power
I_m	A	Max Current
V_m	V	Max Voltage
FF	%	Fill Factor
R_s	m	Sun dimension
R_{SE}	m	Earth-Sun distance
η	%	Cell efficiency
MPPT		Maximum Power Point Tracker
NOCT		Nominal Operating Cell Temperature
T_a	°C	Temperature atmosphere
T_c	°C	Temperature cell
η_{glob}	%	Panel efficiency
P_{sun}	kW	Sun Irradiation Power
η_{riemp}	%	Efficiency filling
η_{incap}	%	Efficiency encapsulation
η_{irr}	%	Efficiency disuniform irradiance
η_C	%	Efficiency conversion
η_{TR}	%	Efficiency optical transmission
η_{MIS}	%	Efficiency mismatch
C		Geometrical concentration ratio
A_{conc}	m^2	Area concentrator
A_{ric}	m^2	Area receiver
η_{max_in}	°	Max in angle concentrator
η_{max_out}	°	Max out angle concentrator
N		Refraction index
r_1	m	Emitter radius
r_2	m	Emittiter – receiver distance
P_{rad}	kW	Irradiation Power
σ		Stefan-Boltzmann ' constant
T_s	°C	Temperature source
T_r	°C	Temperature receiver
AHA	°	Max acceptance angle
TPV		ThermoPhotoVoltaic
CPC		Compound Parabolic Concentrator
E_{DNI}	kWh/m^2	Normal solar Irradiation Direct

DNI	*W/m²*	Direct Normal Irradiance
Y_R	*hour*	Reference Yield
Y_f	*hour*	Array Yield
P_o	*kW*	Power
E_{DC}	*kWh*	Energy generated in Direct Current
E_{AC}	*kWh*	Energy generated in Alternate Current
PR		Performance Ratio
L_c	*hour*	Losses in DC
L_s	*hour*	System losses
E_G		Energy Gap
AM		Air Mass
J		Current density
s		Cell spectrum response
η_P	*%*	Power efficiency
η_C	*%*	Conversion factor
P_{aAC}	*kW*	Active Power in AC
P_{aDC}	*kW*	Active Power in DC
P_{fAC}	*kW*	Power 1st harmonic
P_{fDC}	*kW*	Medium power
η_R	*%*	Output efficiency
P_o	*kW*	Output power
P_i	*kW*	Input power
η_E	*%*	Energy efficiency
W_o	*kWh*	Output energy
W_i	*kWh*	Input energy
P_a	*kW*	Active Power
v(t)	*V*	Variable voltage
P(t)	*kW*	Variable power
i(t)	*A*	Variable current
T		Time period
PF	*%*	Power Factor
η_{WT}	*%*	Medium efficiency
K_i		Weight factor
CSTC		Standard Test Conditions (STC)
Vmpp	*V*	Maximum power voltage
Impp	*A*	Maximum power current
NOCT		Nominal Operative Cell Temperature
MOCVD		Metal Organic Chemical Vapour Deposition
PMMA		Poli Metyl Metacrylate
DTIRC		Dielectric filled Total Internal Reflecting Concentrator
γ		Temperature coefficient

BIBLIOGRAPHY

[1] S.Mauro, M.Messina, R.Lanzafame - Wind turbine CFD modeling using a correlation-based transitional model – Renewable energy, 2013 - Elsevier

[2] Aliakbar Akbarzadeh, Abhijit Date, ... - Monitoring and maintaining the water clarity of salinity gradient solar ponds – Solar energy, 2011 - Elsevier

[3] SF Maenza - Analisi e sviluppo di impianti fotovoltaici a concentrazione – 2010 – Politecnico di Milano

[4] M.Zimbone, M.G.Grimaldi, ... - An enhanced photocatalytic response of nanometric TiO_2 wrapping of Au nanoparticles for eco-friendly water applications – Nanoscale, 2014

[5] I.Crupi, S.Boscarino, ... - Optimization of ZnO:Al/Ag/ZnO:Al structures for ultra-thin high-performance transparent conductive electrodes – Thin Solid Films, 2012 - Elsevier

[6] P.M.Sberna, ... - Competition between uncatalyzed and catalyzed growth during the plasma synthesis of Si nanowires and its role on their optical properties – Journal of Applied Physics, 2013

[7] A.Gentile, F.Ruffino, ... - Structural and optical properties of solid-state synthesized Au dendritic structures – Applied Surface Science, 2014 - Elsevier

[8] Antonio Luque, Steven Hegedus – Handbook of Photovoltaic Science and Engineering – Wiley 2003.

[9] Tom Markvart, Luis Castaner – Practical Handbook of Photovoltaics (Fundamentals and Applications) – Elsevier 2003.

[10] Andrea Abete, Filippo Spertino - Generatori e impianti fotovoltaici – PoliTo 2001-02.

[11] Simone Maenza – La progettazione fluidodinamica di una microturbina eolica – Tesi Università di Catania 2007.

[12] Daniela Fasanaro – Misura delle grandezze radiometriche fondamentali per la caratterizzazione dei sistemi fotovoltaici a concentrazione presso il sito Enel di Passo Martino – Tesi Università di Catania.

[13] Johan Nilsson – Optical Design and Characterization of Solar Concentrators for Photovoltaics – Lund University 2005.

[14] Normative: CEI EN 61724, CEI 11-20, CEI EN 61683, CEI-82_081028, CENELEC_82_494, CEI 61646, CEI 60904-7, CEI EN 60904-1, CEI EN 61215, CENELEC 82_488, CENELEC 60891.

[15] G.Almonacid – The CPV Challenge: Achieving Grid Parity – Universidad de Jaèn.

[16] Tina G., Scrofani S. – Electrical and Thermal Model for PV Module: Temperature Evaluation – University of Catania.

[17] Ward Bower, Chuck Whitaker, William Erdamn, Michael Behnke, Mark Fitzgerald – Performance Test Protocol for Evaluating Inverters Used in Grid-Connected PV Systems.

[18] Tina G., Abate R. – Experimental Verification of Thermal Behavoiur of Photovoltaic Modules – University of Catania.

[19] Carl Osterwald – NREL LAB – Thermal Model Development For Energy Rating of Photovoltaic Module.

[20] Alsema E.A. – The real environmental impact of crystalline silicon PV modules: *an analysis based on up-to-date manufacturer's data* - European PV Solar Energy Conference.

[21] Coiante D. – Le nuove fonti di energia rinnovabile

[22] Enel – Divisione Ingegneria ed Innovazione – Rapporti Tecnici.

[23] www.terna.it (Dati Terna sulla Produzione).

[24] www.GSE.it (Statistiche sulle fonti rinnovabili in Italia; Il Solare – Dati sulla produzione).

[25] www.IEA.com (Annual Report; Trends in Photovoltaic Applications).

[26] Photon Consulting – Resoconti annuali.

SPECIAL THANKS

A special thank goes to my brother Giampiero: you gave me the spark to start this experience in Australia that changed my current path.

Another special thank sure goes to Paolo Sberna, which has been the first among us to take the flight off: if it wasn't for you, I would have never been brave enough to do it as well.

I want to thank Stefano Mauro as my best co-worker and friend in the uni office.

Stefano, Antonella and Lina who are my PhD crew with whom I have shared this experience, and the Lanzy team that was the other arm of the university body.

I want to thank all my fellows at Kromotek (whose data were used for this project): best working experience ever where I found true friends that will last for all my life!

Many thanks to the professors that followed me during this period: among them Massimo Zimbone, Isodiana Crupi, my abroad tutors Aliakbar Akbarzadeh and Abhijit Date; with them all the staff that helped me solving all the bureaucracy papers to permit me to live this experience.

At the end of a project that lasts three years you realize what happened during this period long enough to change all your life. Some persons were with me from the beginning to the end of this PhD (I'll never thank enough my classmates, friends since forever), some others of them I found and lost along the path. One thing that helps me to deal with all these changes is one of the capoeira song I learnt years ago:

"Embora a vida tenha encontro e desencontro,

eu vou plantando com meu canto com axe que me ensinó"

(Although in life there are meeting and partings,
I'm planting with my song with the energy that I have been taught)

I know I'm not an easy fellow and never will I be,

but somehow you were always there for me.

Thank you all!!!

Simon F. Maenza

RINGRAZIAMENTI

Un ringraziamento particolare va a mio fratello Giampiero: hai acceso la scintilla per farmi iniziare questa esperienza in Australia che ha cambiato il mio percorso attuale.

Un altro ringraziamento va sicuramente a Paolo Sberna, che é stato il primo tra noi a partire: se non fosse stato per te non avrei mai avuto il coraggio di farlo anche io.

Voglio ringraziare Stefano Mauro, il mio miglior collega ed amico nell'ufficio in universitá.

Stefano, Antonella e Lina che compongono il mio gruppo di Dottorato con cui ho condiviso questa esperienza, ed il Lanzy Team che é stato l'altro braccio del corpo universitario.

Voglio ringraziare i miei amici della Kromotek (i cui dati sono stati usati per questo progetto): la migliore esperienza lavorativa dove ho trovato vere amicizie che dureranno per sempre!

Grazie ancora ai professori che mi hanno seguito: tra questi Massimo Zimbone, Isodiana Crupi, i miei tutor australiani Akbarzadeh e Date; con loro ringrazio anche lo staff amministrativo che mi ha aiutato nel risolvere la burocrazia necessaria per vivere questa esperienza.

Alla fine di un progetto che dura tre anni realizzi quanto é successo durante questo periodo lungo abbastanza da cambiarti la vita. Alcune persone erano con me sin dal principio (non ringrazieró mai abbastanza i miei compagni di classe, amici da sempre), altre le ho trovate e perse lungo il percorso. Una cosa che mi aiuta a capire come affrontare tutti questi cambiamenti é una canzone di capoeira che ho imparato anni fa:

"Embora a vida tenha encontro e desencontro,

eu vou plantando com meu canto com axe que me ensinó"

(Sebbene nella vita ci siano incontri ed addi,
io condivido con il mio canto quella energia che mi é stata data)

Non sono una persona facile e mai lo saró,

ma comunque voi siete rimasti qui con me.

Grazie a tutti!!!

Simon F. Maenza

UNIVERSITY OF CATANIA
FACULTY OF MATH AND PHYSICS

PhD –MATERIAL SCIENCE AND TECHNOLOGY – XXVII C.

SIMONE MAENZA

Integration and optimization of new technology for building integrated PV systems

PhD thesis

Supervisor:
Prof. Ing. Rosario Lanzafame
Faculty of Engineering

YEAR 2011 – 2014

UNIVERSITÀ DEGLI STUDI DI CATANIA
FACOLTÀ DI MATEMATICA E FISICA

DOTTORATO in SCIENZA E TECNOLOGIA DEI MATERIALI

SIMONE MAENZA

Integrazione ed ottimizzazione delle tecnologie innovative per il fotovoltaico integrato nell'edilizia

TESI DI DOTTORATO

Relatore:
Prof. Ing. Rosario Lanzafame
Facoltà di Ingegneria

PERIODO ACCADEMICO 2011 – 2014